An enhanced CRISPR repressor for targeted mammalian gene regulation

Citation: Yeo, Nan Cher, et al. “An Enhanced CRISPR Repressor for Targeted Mammalian Gene Regulation.” Nature Methods, vol. 15, no. 8, Aug. 2018, pp. 611–16.

Published Version: https://doi.org/10.1038/s41592-018-0048-5

Publisher: Nature Publishing Group

Permanent Link: http://hdl.handle.net/1721.1/120355

Version: Author's final manuscript: final author’s manuscript post peer review, without publisher’s formatting or copy editing

An enhanced CRISPR repressor for targeted mammalian gene regulation

Nan Cher Yeo[1,2,†], Alejandro Chavez[3,†,*], Alissa Lance-Byrne[1], Yingleong Chan[1,2,Φ], David Menn[4,Φ], Denitsa Milanova[1,2,Φ], Chih-Chung Kuo[5,6,Φ], Xiaoge Guo[1,2], Sumana Sharma[7], Angela Tung[1], Ryan J. Cecchi[1], Marcelle Tuttle[1], Swechchha Pradhan[4], Elaine T Lim[1,2], Noah Davidsohn[1,2], Mo R. Ebrahimkhani[4,8], James J. Collins[1,9,10,11,11], Nathan E. Lewis[5,6,13], Samira Kiani[4,*], and George M. Church[1,2,*]

[1]Wyss Institute for Biologically Inspired Engineering, Harvard University, Cambridge, Massachusetts, USA.
[2]Department of Genetics, Harvard Medical School, Boston, Massachusetts, USA.
[3]Department of Pathology and Cell Biology, Columbia University College of Physicians and Surgeons, New York, New York, USA
[4]School of Biological and Health Systems Engineering, Ira. A Fulton Schools of Engineering, Arizona State University, Tempe, Arizona, USA.
[5]Department of Bioengineering, University of California, San Diego, USA.
[6]Novo Nordisk Foundation Center for Biosustainability at the University of California, San Diego, USA.
[7]Cell Surface Signalling Laboratory, Wellcome Trust Sanger Institute, Cambridge CB101SA, United Kingdom.
[8]Division of Gastroenterology and Hematology, Mayo Clinic College of Medicine and Science, Phoenix, Arizona, USA.
[9]Institute for Medical Engineering & Science, Massachusetts Institute of Technology, Cambridge, Massachusetts, USA.
[10]Synthetic Biology Center, Massachusetts Institute of Technology, Cambridge, Massachusetts, USA.
[11]Department of Biological Engineering, Massachusetts Institute of Technology, Cambridge, Massachusetts, USA.
[12]Broad Institute of MIT and Harvard, Cambridge, Massachusetts, USA.
[13]Department of Pediatrics, University of California, San Diego, USA

[†]Co-first authors
[Φ]These authors contributed equally to the manuscript

[*]Correspondence can be addressed to:
Alejandro Chavez
E-mail: ac4304@cumc.columbia.edu

Samira Kiani
E-mail: samira.Kiani@asu.edu

George M. Church
E-mail: gchurch@genetics.med.harvard.edu

ABSTRACT

The RNA-guided endonuclease Cas9 can be converted into a programmable transcriptional repressor, yet inefficiencies in target gene silencing have limited its utility. Here we describe an improved Cas9 repressor based on the C-terminal fusion of a rationally designed bipartite repressor domain, KRAB-MeCP2, to nuclease-null Cas9. We demonstrate the system's superiority in silencing coding and non-coding genes, simultaneously repressing a series of target genes, improving the results of single and dual gRNA library screens, and enabling new architectures of synthetic genetic circuits.

INTRODUCTION

The Clustered Regularly Interspaced Short Palindromic Repeats (CRISPR)-Cas9 system, which mediates adaptive immunity within bacteria and archaea, has emerged as a powerful tool for genome engineering[1-7]. Cas9 is an RNA-guided endonuclease that can be directed to specific DNA sequences through complementarity between the Cas9-associated guide RNA (gRNA) and the target locus, provided that a protospacer-adjacent motif (PAM) is proximal to the target. Because changing the target locus only requires alteration of the delivered gRNA, Cas9 has been quickly adopted for selective gene ablation and for performing unbiased genome-wide screens[8–11]. However, Cas9 cutting can lead to cellular toxicity due to the formation of DNA double-strand breaks and Cas9-generated modifications are irreversible, which limit its applications[12].

Within Cas9, the amino acids critical for DNA catalysis can be mutated to generate a nuclease-dead Cas9 (dCas9), which remains competent for DNA binding but lacks endonuclease activity[13]. When directed towards the transcriptional start site (TSS) of a gene, dCas9 can physically block RNA polymerase passage, thereby leading to

gene silencing[13]. Further improvement in transcriptional inhibition can be achieved by addition of repression domains such as the Krüppel-associated box (KRAB) to dCas9, with the resultant dCas9-KRAB fusion protein being the current gold standard for dCas9-based repression studies[14-17]. While widely adopted, the dCas9-KRAB system suffers from inefficient knockdown and poor performance when compared to Cas9 nuclease-based methods[14,18-19].

Previous work has shown that by fusing several transcriptional regulators to dCas9 in tandem, a synergistic increase in activity can be achieved[20-23], with initial efforts focused on building more potent transcriptional activators. Here we assemble and screen combinations of potent repressor domains to engineer a highly effective dCas9-KRAB-MeCP2 transcriptional repressor.

RESULTS

Identification of dCas9-KRAB-MeCP2

To begin to design a more potent Cas9 repressor, we separately fused more than 20 different effector domains known to play a role in transcriptional regulation and gene silencing to the C-terminus of dCas9. The resulting dCas9 fusion proteins were then transfected into HEK293T cells along with a gRNA targeting the promoter of an enhanced yellow fluorescent protein (*EYFP*) reporter gene. The majority of dCas9 fusions were able to repress *EYFP* expression, with a few exhibiting greater repression (up to 8-fold) compared to dCas9 (**Supplementary Fig. 1**). Next we generated a library of dCas9 bipartite repressors consisting of the commonly used KRAB repressor and the six top-performing domains from our initial screen (MeCP2, SIN3A, HDT1, MBD2B, NIPP1, and HP1A). Our library contained all pairwise repeating and non-repeating

combinations of the seven selected domains. As expected, many bipartite fusion proteins showed stronger improvement, ranging from 5- to 60-fold greater repression of *EYFP* compared to dCas9 (**Supplementary Fig. 2**).

Having done our initial studies with a synthetic reporter, we next determined whether our most potent repressors could also downregulate endogenous target genes. We selected nine bipartite repressors for further characterization. Each of the dCas9 variants was co-transfected into HEK293T cells along with a set of gRNAs targeting four different endogenous genes. While varying degrees of gene repression were observed depending upon the target gene, the dCas9 repressor consisting of KRAB and the TRD domain of MeCP2, named dCas9-KRAB-MeCP2 (**Fig. 1a** and **Supplementary Table 1**), was the most potent across all targets (**Supplementary Fig. 3**). We also generated a series of tripartite fusion proteins to test whether further improvements in repression could be achieved by employing three different effector domains (**Supplementary Fig. 4**). No improvement in gene silencing was obtained using any of the designed tripartite repressors as compared to the dCas9-KRAB-MeCP2 protein (**Supplementary Fig. 5**). The lack of improved repression with the tripartite repressors could be due to the domains recruiting identical secondary effectors that have already been recruited. It is also possible that the extent to which the domains fold and function properly decreases as greater numbers of effectors are fused together.

To understand the contributions of KRAB and MeCP2 to the overall effect, we performed a side-by-side comparison of different dCas9 fusion proteins consisting KRAB or MeCP2 (**Supplementary Fig. 6)**. The dCas9-KRAB-MeCP2 fusion outperformed either KRAB or MeCP2 either as single or double fusions to dCas9,

suggesting that it is the combined effect of both domains leading to increased gene repression.

Improved repression of endogenous gene using dCas9-KRAB-MeCP2

We next systematically compared the activity of dCas9-KRAB-MeCP2 to that of the current gold-standard dCas9-KRAB repressor by targeting a wide range of endogenous loci in HEK293T cells. For the majority of single genes tested, dCas9-KRAB-MeCP2 showed improved repression (**Fig. 1b**). To test whether dCas9-KRAB-MeCP2 could downregulate the expression of multiple genes more effectively, we co-transfected four gRNAs each targeting a different locus into HEK293T cells (**Fig. 1c**). dCas9-KRAB-MeCP2 showed improved multiplexed repression for all genes tested except for two where it showed similar activity to dCas9-KRAB.

We next designed an array of gRNAs targeting both the template and non-template strands ranging from 1-kb upstream to 1-kb downstream of the TSS for two different genes (*CANX and SYVN1*). 15 out of 25 gRNAs tested showed improved repression with dCas9-KRAB-MeCP2 as compared to dCas9-KRAB. These results were independent of the DNA strand targeted and whether or not the gRNA was directed outside of the previously characterized optimal targeting window for repression[15] (**Fig. 2a-b**). Initial studies with CRISPR repressors suggested that using multiple gRNAs targeting the same locus led to marked improvement in gene knockdown[13]. In contrast to these results, neither dCas9-KRAB nor dCas9-KRAB-MeCP2 showed improved repression when multiple guides against the same target were used; rather, they exhibited an activity that appeared to be dictated by the most potent guide within the set tested, consistent with recent observations[24] (**Fig. 2b-c**).

The effect of dCas9-KRAB-MeCP2 is highly specific

Effector domains recruiting chromatin modifiers can cause widespread epigenetic changes over large regions of DNA[25-27]. We evaluated the targeting specificity of dCas9-KRAB-MeCP2 by probing the expression of neighboring genes when either *CXCR4 or SYVN1* was targeted (**Supplementary Fig. 7a-b**). No significant off-target effect was observed on the neighboring genes examined.

We next targeted the *CXCR4* gene and performed whole-transcriptome sequencing (RNA-seq) to evaluate the specificity of dCas9-KRAB-MeCP2 on a genome-wide scale. Results were compared to those obtained from cells transfected with either dCas9 or dCas9-KRAB. dCas9-KRAB-MeCP2 showed the strongest repression signal for the target gene, *CXCR4*. The global transcriptome profiles of all dCas9-repressors were highly correlated with that of the negative control, cells transfected with gRNA alone (**Fig. 3** and **Supplementary Fig. 7c**), although an overlapping set of differentially expressed (DE) genes was also observed (**Supplementary Fig. 8-9, Supplementary Table 2-3**, and **Supplementary Data 1)**. Of the few DE genes that showed downregulation, none exhibited a near-sequence match to the *CXCR*4-targeting gRNA, suggesting that these changes did not result from inappropriate targeting of repressors to the loci with altered expression.

dCas9-KRAB-MeCP2 efficiently suppresses genes when used at library scales

One of the most powerful uses of CRISPR-Cas9 technology is to enable facile genome-wide screens. To determine whether our tool was amenable to such screening, we generated heterogenous populations of human haploid (HAP1) cells stably expressing either dCas9, dCas9-KRAB, or dCas9-KRAB-MeCP2. RNA expression

levels of the dCas9-KRAB and dCas9-KRAB-MeCP2 repressors were similar in these haploid lines but were significantly lower than that of dCas9 alone (**Supplementary Fig. 10a**). When endogenous genes were targeted, cells containing dCas9-KRAB-MeCP2 showed a stronger repression compared to cells with other dCas9 constructs (**Supplementary Fig. 10b**).

Genes that are essential for cellular function serve as a useful set of targets for comparing the relative performance of different screening platforms[19]. Consequently, we infected each of our dCas9-expressing lines, as well as wild-type HAP1 cells, with a lentiviral single-gRNA (sgRNA) library targeting an assortment of essential and non-essential genes. We then passaged the cells over a period of 14 days and quantified the extent to which the various sgRNAs were depleted over time. In the screen, cells-expressing dCas9-KRAB-MeCP2 showed the strongest depletion for guides targeting essential genes relative to non-essential genes ($p= 3.52 \times 10^{-80}$ using dCas9-KRAB-MeCP2 vs. 5.41×10^{-19} using dCas9-KRAB at day 14) (**Fig. 4a**, **Supplementary Table 4**, and **Supplementary Data 2**). In addition, strong depletion signals (up to 256-fold depletion) were observed with dCas9-KRAB-MeCP2 as early as day 7, compared to the mostly weak signals exhibited by dCas9-KRAB (up to 2-fold depletion). No depletion in sgRNAs targeting essential genes was observed for wild-type cells, indicating that our results were not due to technical artifacts (**Supplementary Fig. 10c**).

To test the generality of our system, we repeated the above screen in SH-SY5Y, a near-diploid human neuroblastoma cell line (**Fig. 4b** and **Supplementary Data 3**), and HEK293T (**Fig. 4c** and **Supplementary Data 4**). While the overall depletion signal was not as strong as that observed in HAP1 cells, cell lines containing dCas9-KRAB-

MeCP2 showed a greater degree of depletion for sgRNAs targeting essential genes at all times of measurement compared to previous technologies (**Supplementary Table 5-6**).

We plotted sgRNA depletion as a function of position from the TSS for the several hundred essential gene-targeting sgRNAs used (**Supplementary Fig. 11a** and **Supplementary Table 7**). As expected, sgRNAs positioned within the previously identified optimal targeting window (-50bp to +200bp from TSS) showed a higher likelihood of being depleted compared to sgRNAs positioned outside of the window (**Supplementary Fig. 11b**). Regardless of targeting position, dCas9-KRAB-MeCP2 outperformed dCas9-KRAB (**Supplementary Fig. 11c**).

In the dCas9-KRAB-MECP2 screen, a few of the sgRNAs designed to target non-essential genes also showed marked depletion. We found that a subset of these sgRNAs also showed depletion when combined with either dCas9-KRAB or dCas9 alone (**Supplementary Fig. 12** and **Supplementary Data 5**), indicating that the observed off-target binding is not only a property of our improved repressor. Furthermore, a few sgRNAs that showed unexpected depletion within the HAP1 screen also showed depletion within the SH-SY5Y screen for either dCas9-KRAB-MeCP2 or dCas9-KRAB (**Supplementary Data 5**). These data suggest that there are consistent off-target sites that these unique sgRNAs are binding to which affect growth. We hypothesize that because dCas9-KRAB-MeCP2 is a more potent repressor, signals from these off-target binding events are more readily observed.

To assess the overall performance of dCas9-KRAB-MeCP2 within screening environments, we used the conventional MAGeCK analysis pipeline[28]. MAGeCK takes

into account the behavior of all sgRNAs against a given gene when determining whether it is subject to selection during the screen. In HAP1 cells, dCas9-KRAB-MeCP2 correctly identified 21 essential genes compared to only 3 identified by dCas9-KRAB at day 14. Similarly in HEK293T cells, dCas9-KRAB-MeCP2 identified 11 essential genes compared to 5 identified by dCas9-KRAB. In SH-SY5Y cells, dCas9-KRAB-MeCP2 showed similar performance by identifying 11 essential genes compared to 10 identified by dCas9-KRAB. No non-essential genes were deemed significant in any of the experimental groups, (**Supplementary Fig. 13** and **Supplementary Data 6**). These results support that dCas9-KRAB-MeCP2 is a more potent tool for screening gene essentiality compared to dCas9-KRAB.

dCas9-KRAB-MeCP2 improves genetic interaction mapping

To further assess the capabilities of dCas9-KRAB-MeCP2, we performed a combinatorial repression screen. Our screening library consisted of dual guides against genes involved in DNA repair along with a set of positive and negative controls. Within our library each construct contained two gRNAs, with the majority of gRNA pairs targeted to two different genes (**Supplementary Table 8**). Similar to the single gene targeting screens, samples for the dual guide screen that contained dCas9-KRAB-MeCP2 showed improved selection for or against specific gRNA pairs over time compared to samples containing dCas9-KRAB (**Fig. 5a**).

We next estimated the fitness effects for each individual gRNA and quantified genetic interactions (indicated by pi-scores) between gene pairs[29] (See **Supplementary Note 1** for interpretation of pi-scores). Specifically, we tested whether distant gene pairs tend to engage more in negative genetic interactions, while gene pairs that form protein

complexes tend to have positive pi-scores[30,31]. For the negative control and dCas9-KRAB screens, no clear correlation was observed between gene distance in the protein complex network and pi-scores. In contrast, the expected effect was observed in dCas9-KRAB-MeCP2 screens (**Supplementary Fig. 14a-b**).

Clustering of genetic interaction profiles provides a quantitative measure of functional similarity[32]. Among the samples, only dCas9-KRAB-MeCP2-containing cells showed a discernible clustering structure (**Fig. 5b**, **Supplementary Fig. 14c-d**, and **Supplementary Data 7**). We subsequently looked at the gene pairs with the strongest interactions within the dCas9-KRAB-MeCP2 dataset. One of the most significant negative interactions was between *BLM* and *SOD1,* in line with previous data showing this to be a synthetically lethal interaction[33]. We also detected a negative genetic interaction between *BLM* and *DNA2*, consistent with results from yeast showing that the *BLM* homologue, *SGS1*, could rescue *DNA2* deficiency, and absence of both genes cause enhanced DNA damage sensitivity[34,35]. Analyses of the positive genetic interactions revealed a strong interaction between *CHEK1* and *RECQL1.* This result is consistent with previous knowledge that a loss of RECQL1 led to activation of CHEK1 signaling, which causes cell cycle arrest. Thus in cells lacking RECQL1, the growth arrest caused by CHEK1 activation should be alleviated upon its removal, enabling the double mutants to grow better[36]. When the same interactions are examined within cells expressing dCas9-KRAB, either no interaction is observed (*BLM-DNA2*) or the interaction is the opposite of what is expected (*BLM-SOD1* and *CHEK1-RECQL1*).

Superiority of dCas9-KRAB-MeCP2 in synthetic gene circuits

We next performed five separate experiments highlighting the benefit of dCas9-

KRAB-MeCP2 in the context of synthetic gene circuits. First, we constructed a simple repressor circuit in which *EYFP* was repressed by a U6-driven gRNA in combination with different dCas9 repressors. Approximately 400-fold repression was observed using dCas9-KRAB-MeCP2, while earlier dCas9 variants repressed <60-fold (**Supplementary Figure 15a)**.

Next, these U6-driven gRNAs were added to a two-layer repressor circuit. Here, an sgRNA/dCas9 pair repressed the expression of a TALE repressor, which in turn repressed expression of *EYFP*. *EYFP* should be repressed in the absence of sgRNA, but should be derepressed upon addition of sgRNA to the circuit, depending on the strength of the dCas9 repressor. As expected, dCas9-Krab-MeCP2 led to higher levels of derepression of *EYFP*, to the extent that it was indistinguishable from *EYFP* expressed in the absence of TALE repressors (**Supplementary Fig. 15b**).

Because inducible circuits are desirable within many synthetic gene networks, we reconstructed two previously described circuits in which gRNA expression was driven by a doxycycline-inducible RNA polymerase II (Pol II) promoter[37]. While similar constructs have previously been shown to be functional, their activity has been inferior to that of constructs in which gRNA expression is under the control of Pol III promoters[37]. In the context of a simple repressor circuit, dCas9-KRAB-MeCP2 significantly increased the efficiency of Pol II-driven gRNA repression (**Fig. 6a**). We next employed it within a Pol II-driven two-layer cascade. Unlike previous dCas9 tools, we observed, for the first time, a clear transfer of information using dCas9-KRAB-MeCP2, which showed the expected changes in *EYFP* expression between induced and uninduced states (**Fig. 6b**).

We next sought to determine whether dCas9-KRAB-MeCP2 could be used to create a functional three-layer cascade with an output being expression of an endogenous gene. We constructed a circuit in which a U6-driven gRNA/dCas9 complex represses a TALE repressor (layer1). The TALE repressor suppresses another gRNA (layer 2), which targets the endogenous *CXCR4* locus and mediates repression of this gene when combined with dCas9 repressors (layer 3). We tested the different repressors in circuits containing either all three layers, layers 2 and 3, or layer 3 alone, and we measured the surface expression of CXCR4. Our results demonstrate that only dCas9-KRAB-MeCP2 can facilitate transfer of information in all settings, with CXCR4 levels showing the expected expression patterns (**Fig. 6c**).

DISCUSSION

Here we identify the multimeric fusion protein dCas9-KRAB-MeCP2 as a highly potent transcriptional repressor. Using this tool we observed improved knockdown of both reporter and endogenous genes. Furthermore, our data show that dCas9-KRAB-MeCP2 outperforms previous dCas9 repressors in identifying genes essential for cell survival, detecting genetic interactions between genes, and actuating complex regulatory activity within various synthetic gene circuits. These data demonstrate the power of our tool to assist in the interrogation and selective regulation of the mammalian genome.

Similar to our work with transcriptional activators, the improved performance of dCas9-KRAB-MeCP2 repressor is likely due to the distinct mechanisms by which each of the fused domains function. The KRAB domain represses transcription via interaction with KAP1, which functions as a scaffold to recruit co-repressors including

heterochromatin protein 1 (HP1), histone deacetylases, and SETDB1[38-40]. The transcription repression domain (TRD) of MeCP2 binds to a different set of transcriptional regulators including the DNA methyltransferase DNMT1 and the SIN3A-histone deacetylase corepressor complex[41-44].

RNA-seq data suggest that dCas9-KRAB-MeCP2 is not inducing additional gross differences in the cellular transcriptome outside of those already produced by current methods. It is worth pointing out that in our screen targeting essential genes, the dCas9-KRAB-MECP2-expressing cells exhibited a much more robust depletion, but a few of the guides designed to target non-essential genes also showed marked depletion. Further investigations are needed to clarify the source of these effects. Although not utilized in these studies, various methods to improve Cas9 specificity have been reported in the literature such as using a “high-fidelity” Cas9 protein or truncated sgRNAs, each of which have been shown to help mitigate off-target activity[45,46].

For the majority of loci tested, dCas9-KRAB-MeCP2 achieved greater degrees of gene repression than dCas9-KRAB. Yet, there were a few loci for which we observed only modest repression from either tool. Potential causes for variations in gene silencing include poorly functional guides, insufficient time between targeting and measurement of gene expression, local chromatin effects, competition for binding between Cas9 and endogenous transcriptional regulators, and interference from already present epigenetic marks preventing further modification by our tools[47–49]. For the most part, these inefficiencies in repression can be overcome by simply targeting the same gene with an array of different sgRNAs. The utility of this strategy is shown in our essential gene screen. For most essential genes tested, at least one of the targeting guides exhibited

the expected levels of depletion, with the most robust effects observed in samples expressing dCas9-KRAB-MeCP2.

ACKNOWLEDGEMENTS

G.M.C was supported by NIH grants RM1 HG008525 and P50 HG005550. A.C. was funded by the National Cancer Institute grant no. 5T32CA009216-34 and the Burroughs Wellcome Fund Career Award for Medical Scientists. S.K was supported by the DARPA Young Faculty Award D16AP00047 and Arizona State University, Fulton Schools of Engineering startup fund. J.J.C. was supported by the Paul G. Allen Frontiers Group.

AUTHOR CONTRIBUTIONS

A.C. and N.C.Y. conceived the study. N.C.Y. and A.C. designed experiments. A.C. and A.T. designed, built, and tested the initial set of dCas9 repressor fusions. N.C.Y. performed the majority of endogenous gene targeting experiments with assistance from A.L.B. along with additional technical contributions from Ryan C., M.T., and A.C. Library screens and next generation sequencing were performed by N.C.Y. with analysis of the essential gene library data performed by Y.C. with contributions from N.C.Y. and A.C. S.S. performed MAGeCK analysis. RNA-seq analysis was led by Denitsa M. with assistance in library preparation from N.C.Y. and data interpretation by N.C.Y and A.C. C.C.K. with oversight from N.E.L. analyzed the dual guide epistasis experiment and interpreted data with assistance from N.C.Y. and A.C. X.G. aided in next generation sequencing and performed preliminary analysis of the sequencing data. N.D. provided technical experience and insight. E.L. helped analyze a portion of the library screening data. David M. and S.P. performed the synthetic circuit experiments under the guidance of M.R.E. and S.K. S.K. designed all synthetic circuits used in the study. Research was

performed within the laboratory of G.M.C with oversight from both J.J.C and G.M.C. N.C.Y. and A.C. wrote the manuscript with contributions from all authors.

COMPETING FINANCIAL INTERESTS STATEMENT

G.M.C. is a founder and advisor for Editas Medicine. G.M.C. has equity in Editas and Caribou Biosciences (for full disclosure list, please see: http://arep.med.harvard.edu/gmc/tech.html).

REFERENCES

1. Cho, S. W., Kim, S., Kim, J. M. & Kim, J.-S. Targeted genome engineering in human cells with the Cas9 RNA-guided endonuclease. *Nat. Biotechnol.* **31,** 230–232 (2013).
2. Cong, L. *et al.* Multiplex genome engineering using CRISPR/Cas systems. *Science* **339,** 819–823 (2013).
3. Mali, P. *et al.* RNA-guided human genome engineering via Cas9. *Science* **339,** 823–826 (2013).
4. Jinek, M. *et al.* A programmable dual-RNA-guided DNA endonuclease in adaptive bacterial immunity. *Science* **337,** 816–821 (2012).
5. DiCarlo, J. E. *et al.* Genome engineering in Saccharomyces cerevisiae using CRISPR-Cas systems. *Nucleic Acids Res.* **41,** 4336–4343 (2013).
6. Hwang, W. Y. *et al.* Efficient genome editing in zebrafish using a CRISPR-Cas system. *Nat. Biotechnol.* **31,** 227–229 (2013).
7. Wang, H. *et al.* One-step generation of mice carrying mutations in multiple genes by CRISPR/Cas-mediated genome engineering. *Cell* **153,** 910–918 (2013).
8. Zhou, Y. *et al.* High-throughput screening of a CRISPR/Cas9 library for functional genomics in human cells. *Nature* **509,** 487–491 (2014).

9. Shalem, O. *et al.* Genome-scale CRISPR-Cas9 knockout screening in human cells. *Science* **343,** 84–87 (2014).
10. Wang, T., Wei, J. J., Sabatini, D. M. & Lander, E. S. Genetic screens in human cells using the CRISPR-Cas9 system. *Science* **343,** 80–84 (2014).
11. Koike-Yusa, H., Li, Y., Tan, E.-P., Velasco-Herrera, M. D. C. & Yusa, K. Genome-wide recessive genetic screening in mammalian cells with a lentiviral CRISPR-guide RNA library. *Nat. Biotechnol.* **32,** 267–273 (2014).
12. Mandegar, M. A. *et al.* CRISPR Interference Efficiently Induces Specific and Reversible Gene Silencing in Human iPSCs. *Cell Stem Cell* **18,** 541–553 (2016).
13. Qi, L. S. *et al.* Repurposing CRISPR as an RNA-guided platform for sequence-specific control of gene expression. *Cell* **152,** 1173–1183 (2013).
14. Gilbert, L. A. *et al.* CRISPR-mediated modular RNA-guided regulation of transcription in eukaryotes. *Cell* **154,** 442–451 (2013).
15. Gilbert, L. A. *et al.* Genome-Scale CRISPR-Mediated Control of Gene Repression and Activation. *Cell* **159,** 647–661 (2014).
16. Thakore, P. I., Black, J. B., Hilton, I. B. & Gersbach, C. A. Editing the epigenome: technologies for programmable transcription and epigenetic modulation. *Nat. Methods* **13,** 127–137 (2016).
17. Konermann, S. *et al.* Optical control of mammalian endogenous transcription and epigenetic states. *Nature* **500**, 472-476 (2013).
18. La Russa, M. F. & Qi, L. S. The New State of the Art: Cas9 for Gene Activation and Repression. *Mol. Cell. Biol.* **35,** 3800–3809 (2015).
19. Evers, B. *et al.* CRISPR knockout screening outperforms shRNA and CRISPRi in

identifying essential genes. *Nat. Biotechnol.* **34,** 631–633 (2016).

20. Chavez, A. *et al.* Highly efficient Cas9-mediated transcriptional programming. *Nat. Methods* **12,** 326–328 (2015).
21. Konermann, S. *et al.* Genome-scale transcriptional activation by an engineered CRISPR-Cas9 complex. *Nature* **517,** 583–588 (2015).
22. Zalatan, J. G. *et al.* Engineering complex synthetic transcriptional programs with CRISPR RNA scaffolds. *Cell* **160,** 339–350 (2015).
23. Tanenbaum, M. E., Gilbert, L. A., Qi, L. S., Weissman, J. S. & Vale, R. D. A protein-tagging system for signal amplification in gene expression and fluorescence imaging. *Cell* **159,** 635–646 (2014).
24. Shao, S. *et al.* Multiplexed sgRNA Expression Allows Versatile Single Non-repetitive DNA Labeling and Endogenous Gene Regulation. (2017). doi:10.1101/121905
25. Stolzenburg, S. *et al.* Stable oncogenic silencing in vivo by programmable and targeted de novo DNA methylation in breast cancer. *Oncogene* **34,** 5427–5435 (2015).
26. Li, F. *et al.* Chimeric DNA methyltransferases target DNA methylation to specific DNA sequences and repress expression of target genes. *Nucleic Acids Res.* **35,** 100–112 (2007).
27. Stepper, P. *et al.* Efficient targeted DNA methylation with chimeric dCas9-Dnmt3a-Dnmt3L methyltransferase. *Nucleic Acids Res.* **45,** 1703–1713 (2017).
28. Li, W. *et al.* MAGeCK enables robust identification of essential genes from genome-scale CRISPR/Cas9 knockout screens. *Genome Biol.* **15**: 554 (2014).
29. Shen, J. P. *et al.* Combinatorial CRISPR-Cas9 screens for de novo mapping of

genetic interactions. *Nat. Methods* **14,** 573–576 (2017).

30. Dixon, S. J., Costanzo, M., Baryshnikova, A., Andrews, B. & Boone, C. Systematic mapping of genetic interaction networks. *Annu. Rev. Genet.* **43,** 601–625 (2009).
31. Menche, J. *et al.* Disease networks. Uncovering disease-disease relationships through the incomplete interactome. *Science* **347,** 1257601 (2015).
32. Costanzo, M. *et al.* A global genetic interaction network maps a wiring diagram of cellular function. *Science* **353,** (2016).
33. Sajesh, B. V. & McManus, K. J. Targeting SOD1 induces synthetic lethal killing in BLM- and CHEK2-deficient colorectal cancer cells. *Oncotarget* **6,** 27907–27922 (2015).
34. Imamura, O. & Campbell, J. L. The human Bloom syndrome gene suppresses the DNA replication and repair defects of yeast dna2 mutants. *Proc. Natl. Acad. Sci. U. S. A.* **100,** 8193–8198 (2003).
35. Budd, M. E. & Campbell, J. L. The pattern of sensitivity of yeast dna2 mutants to DNA damaging agents suggests a role in DSB and postreplication repair pathways. *Mutat. Res.* **459,** 173–186 (2000).
36. Popuri, V., Croteau, D. L., Brosh, R. M. & Bohr, V. A. RECQ1 is required for cellular resistance to replication stress and catalyzes strand exchange on stalled replication fork structures. *Cell Cycle Georget. Tex* **11,** 4252–4265 (2012).
37. Kiani, S. *et al.* CRISPR transcriptional repression devices and layered circuits in mammalian cells. *Nat. Methods* **11,** 723–726 (2014).
38. Friedman, J. R. *et al.* KAP-1, a novel corepressor for the highly conserved KRAB repression domain. *Genes Dev.* **10**: 2067-78 (1996).

39. Kim, S. S. et al. A novel member of the RING finger family, KRIP-1, associates with the KRAB-A transcriptional repressor domain of zinc finger proteins. *PNAS* **93**, 15299-304 (1996).
40. Moosmann, P. *et al.* Transcriptional repression by RING finger protein TIF1 beta that interacts with the KRAB repressor domain of KOX1. *Nucleic Acids Res.* **24**, 4859-67 (1996).
41. Jones, P. L. *et al.* Methylated DNA and MeCP2 recruit histone deacetylase to repress transcription. *Nat Genet.* **19**, 187-91 (1998).
42. Nan, X. *et al.* Transcriptional repression by the methyl-CpG-binding protein MeCP2 involves a histone deacetylase complex. *Nature* **393**, 386-9 (1998).
43. Wade, P. A. *et al.* Histone deacetylase directs the dominant silencing of transcription in chromatin: association with MeCP2 and the Mi-2 chromodomain SWI/SNF ATPase. *Cold Spring Harb Symp Quant Biol.* **63**, 435-45 (1998).
44. Kimura, H. and Shiota, K. Methyl-CpG-binding protein, MeCP2, is a target molecule for maintenance DNA methyltransferase, Dnmt1. *JBC* **278**, 4806-12 (2003).
45. Kleinstiver, B. P. *et al.* High-fidelity CRISPR-Cas9 nucleases with no detectable genome-wide off-target effects. *Nature* **529,** 490–495 (2016).
46. Fu, Y., Sander, J. D., Reyon, D., Cascio, V. M. & Joung, J. K. Improving CRISPR-Cas nuclease specificity using truncated guide RNAs. *Nat. Biotechnol.* **32,** 279–284 (2014).
47. Polstein, L. R. *et al.* Genome-wide specificity of DNA binding, gene regulation, and chromatin remodeling by TALE- and CRISPR/Cas9-based transcriptional activators. *Genome Res.* **25,** 1158–1169 (2015).

48. Wu, X. *et al.* Genome-wide binding of the CRISPR endonuclease Cas9 in mammalian cells. *Nat. Biotechnol.* 32, 670–676 (2014).
49. Kuscu, C., Arslan, S., Singh, R., Thorpe, J. & Adli, M. Genome-wide analysis reveals characteristics of off-target sites bound by the Cas9 endonuclease. *Nat. Biotechnol.* **32,** 677–683 (2014).

FIGURE LEGENDS

Figure 1 Repression of endogenous genes using dCas9-KRAB-MeCP2. (a) Schematic of dCAS9-KRAB and dCas9-KRAB-MeCP2 repressors. NLS=nuclear localization signal. (b) RNA expression of targeted single gene. n=2 biologically independent samples (cell cultures). (c) RNA expression during three separate multiplex repression studies. In each study, four different genes were targeted simultaneously. Two non-coding (nc) genes, *XIST* and *TERC*, were studied. n=2 biologically independent samples (cell cultures).

Figure 2 dCas9-KRAB-MeCP paired with gRNA at various positions. (a) An array of gRNAs was design to target 1-kb upstream to 1-kb downstream of the TSS for *CANX*. Shown is RNA expression of *CANX* when different gRNA was used. T=template strand, NT=non-template strand. n=2 biologically independent samples (cell cultures). (b) Shown is RNA expression of *SYVN1* when individual or combinations of different gRNAs were used. n=2 biologically independent samples (cell cultures). (c) RNA expression of the indicated target genes using one or two gRNAs. n=2 biologically independent samples (cell cultures).

Figure 3 dCas9-KRAB-MeCP2-mediated repression is highly specific in human cells. RNA-seq analyses of HEK293T cells transfected with a gRNA targeting *CXCR4* along

with dCas9, dCas9-KRAB or dCas9-KRAB-MeCP2 repressors. Data are normalized and log_2-transformed counts per million (CPM) values are plotted for each repressor (y-axis) versus that of a negative control transfected with gRNA alone (x-axis). Pearson's and Spearman's correlation coefficients are provided for each repressor. n=2 biologically independent samples (cell cultures).

Figure 4 dCas9-KRAB-MeCP2 outperforms previous tools in screens of gene essentiality. (a) Shown are log_2 odd ratios of all sgRNA constructs as compared to the HAP1 wild-type cells at days 14. sgRNAs targeting essential genes are marked in orange and sgRNAs targeting non-essential genes are marked in blue. A similar experiment was repeated in (b) SH-SY5Y and (c) HEK293T cells. Shown are log_2 odd ratios of all sgRNA constructs as compared to the respective wild-type cells at days 14.

Figure 5 dCas9-KRAB-MeCP2 improves genetic interaction mapping. (a) A density plot showing negative and positive selection pressure against gRNA pairs over time. (b) Shown is the hierarchical clustered heatmap of genetic interactions for dCas9-KRAB and dCas9-KRAB-MeCP2. Only the screen using dCas9-KRAB-MeCP2 showed a discernible clustering structure.

Figure 6 Superiority of dCas9-Krab-MeCP2 in regulating complex synthetic circuits. (a) When expressed from a doxycycline inducible Pol II promoter and edited by Csy4, gRNA showed improved repression of EYFP when co-expressed with dCas9-KRAB-MeCP2, relative to dCas9 or dCas9-KRAB. n=4 biologically independent samples (cell cultures). (b) Inducible Pol II-expressed gRNA edited by Csy4 and complexed with dCas9-KRAB-MeCP2 showed improved performance in a two-tier repressor cascade. n=4 biologically independent samples (cell cultures). (c) With full circuit, dCas9-KRAB-

MeCP2 decreases CXCR4 protein level. In absence of layer 1, dCas9-KRAB-MeCP2 mediates derepression of CXCR4. In absence of layers 1 and 2, the repressor surpasses dCas9 and dCas9-KRAB in repressing CXCR4 levels. n=3 biologically independent samples (cell cultures). For a-c, data are presented as mean ± s.e.m. One-sided Student T-test was performed for all statistical comparison. # $p < 0.05$ vs. unrepressed or TALER only control, ¥ $p < 0.05$ v.s. dCas9, and *$p < 0.05$ v.s. dCas9-KRAB.

ONLINE METHODS

Repressor and gRNA plasmid construction

Repressor fusions were initially cloned into a modified Gateway-compatible dCas9 plasmid backbone[50]. The bipartite and tripartite dCas9 fusions were cloned into a modified Golden Gate-compatible version of the dCas9-m4 vector (Addgene plasmid #47316). DNA fragments containing the specific domains of interest were then PCR amplified and cloned into each of our vectors using either Gateway or Golden Gate assembly methods. For bipartite and tripartite repressors, a glycine-serine-rich linker was placed in between the different domains. The sequences, as well as species origin, of all protein domains used to construct the different repressors are listed in **Supplementary Data 8**. The sequences of dCas9-KRAB (Addgene plasmid #110820) dCas9-KRAB-MeCP2 (Addgene plasmid #110821) are provided in **Supplementary Table 1**. All other vectors are available upon request.

All gRNAs for endogenous gene repression were selected to bind within -50 to +200 bp around the gene TSS, unless the position was specified otherwise. Target genes were selected based on use in previous publications or because they were of particular

interest to our research group, such as DNA repair and cell motility genes[14,15]. To generate sgRNA expression plasmids, oligonucleotides containing gRNA sequence were cloned into a pSB700 vector (Addgene plasmid #64046) or variants with different selection markers downstream of a U6 promoter using Golden Gate assembly methods. Sequences for gRNAs are listed in **Supplementary Table 9**.

Cell culture and transfections

HEK293T cells (gift from P. Mali, University of California, San Diego) were maintained in Dulbecco's Modified Eagle's Medium (DMEM) (Life Technologies) with 10% heat-inactivated fetal bovine serum (FBS) (Life Technologies) and penicillin-streptomycin (Life Technologies) as previously described[50]. Approximately 50,000 cells were seeded per well in 24-well plates and next day transfected using lipofectamine 2000 (Life Technologies) as previously described[50]. 200 ng of dCas9 repressors, 50 ng of sgRNA, and 60 ng of EYFP reporter along with 50 ng of Gal4-VP16 (reporter assay only) were delivered to each well of cells. 50 ng of puromycin-resistant plasmids (endogenous gene study) or 25 ng EBFP-expressing plasmids (reporter assay) were co-transfected to select for transfected cells. 10 ng of each sgRNA per gene were used during multiplex repression. For the endogenous gene study, cells were treated with 3 ug/ml of puromycin at 24 hours post-transfection to enrich for transfected cells. 48 or 72 hours after transfection cells were collected to assay by flow cytometry or lysed for RNA purification, for reporter and endogenous experiments, respectively. Cells were tested every 3 months for mycoplasma contamination and consistently tested negative.

Flow cytometry for reporter assays

Reporter assays were performed by targeting dCas9 fusion proteins to a Gal4-VP16

regulated EYFP reporter gene. The reporter plasmid contains an sgRNA-binding sequence (tacctcatcaggaacatgt) followed by a PAM (tgg). HEK293T cells were transfected with the reporter, Gal4-VP16 activator, sgRNA, and the indicated dCas9 fusion proteins along with an EBFP-expressing plasmid to aide in analyzing only cells that were transfected. Cells were assayed using flow cytometry 48 hours after transfection. Analysis was performed on cells expressing > 10^3 arbitrary units of EBFP2 and the median of EYFP intensity within the gated population was quantified using FlowJo**.**

Quantitative real-time polymerase chain reaction (qPCR) to analyze endogenous gene expression

Total RNA was extracted using RNAeasy Plus mini kit (Qiagen). 500 ng of RNA was used to make cDNA using qScript cDNA synthesis kit (Quanta Bio). KAPA SYBR Fast universal 2x quantitative PCR master mix (KAPA Biosystems) with 0.5 ul of cDNA and 0.4 ul of each forward and reverse primers at 10 uM were used for qPCR, with cycling conditions: 95 ^{o}C for 3 min, and 40 cycles of 95 ^{o}C for 10 sec, 55 ^{o}C for 20 sec, and 72 ^{o}C for 30 sec. RNA expression was normalized to the housekeeping gene *ACTB* and relative gene expression was calculated using $2^{-\Delta\Delta CT}$ method[51]. Sequences for qPCR primers are listed in **Supplementary Table 10**.

Statistical analysis

For reporter and endogenous gene targeting studies, at least two biologically independent samples (independent transfections) per group were used. Statistical comparison was performed in experiments using sample sizes (n) of 3 or 4 biologically independent samples using one-tailed Student's T-test with a *p*-value < 0.05 as the

threshold for significance. The exact n values used to calculate statistics are described in the associated figure legends. Statistical analyses for RNA-seq, gRNA library screening, and circuit experiments are described in **Supplementary Note 2-5**.

Whole transcriptome RNA sequencing (RNA-seq) for analyzing repressor specificity

For each sample, total RNA was extracted using RNeasy mini kit (Qiagen) and treated with on-column RNase-free DNase I (Qiagen) following manufacturer's instructions. 1 ug of RNA from each sample was used for library preparation. RNA-seq libraries were constructed using TruSeq Stranded Total RNA Library Prep Kit with Ribo-Zero Gold (Illumina) designed for cytoplasmic and mitochondrial rRNA depletion. All coding RNA and certain forms of non-coding RNA were isolated using bead-based rRNA depletion, followed by cDNA synthesis, and PCR amplification as per the manufacturer's protocol. Final libraries were analyzed on TapeStation, quantified with qPCR, pooled together, and run on one lane of an Illumina HiSeq 2500 using 2 × 100-bp paired-end reads. The Illumina paired-end adapter sequences were removed from the raw reads using Cutadapt v1.8.1. The TruSeq adaptor sequence 5'-AGATCGGAAGAGCACACGTCTGAACTCCAGTCAC-3' was used for read 1, and its reverse complement, 3'-AGATCGGAAGAGCGTCGTGTAGGGAAAGAGTGTAGATCTCGGTGGTCGCCGTATCATT-5' was used for read 2.

Next, RNA libraries were processed using a pipeline that includes STAR-HtSeq-EdgeR for alignment, count generation, and gene expression. Briefly, STAR aligner (v. 2.4.0j) was used to map the reads to hg19, and HtSeq was used to generate gene expression

counts. For gene expression and differential expression (DE) analyses, edgeR, limma, and custom R scripts were used to filter out very lowly expressed genes (with a cutoff of 1 count in at least 2 samples), calculate normalization factors, and compute effective library sizes using Trimmed Mean of M Values (TMM) normalization. Gene count is then reported in counts per million (CPM) and correlations are calculated on $\log_2$-transformed data. Finally, to determine the most biologically significant differentially expressed genes, relative gene expression was performed by fold-change thresholding ($\log_2$ FC >1.5) and ranking by p-value. See **Supplementary Note 2** for details in DE analysis. A small set of genes in addition to the target gene *CXCR4* showed decreases ($\log_2$ FC < 1.5) in their transcript expression (**Supplementary Table 3**). These genes were further analyzed to assess whether the observed DE was caused by non-specific binding of our gRNA. Genomic sequences of 2 kb upstream and downstream from TSS of those genes were examined by searching for the presence of a full-length gRNA binding site (up to 6 mismatches for near matches) as well as searching for the seed region of the gRNA alone (8 bp in proximal to PAM).

Cell culture and generation repressor-expressing stable cell lines

HAP1 cells (Horizon Discovery) were maintained in Iscove's Modified Dulbecco's Medium (IMDM) with 10% FBS (Life Technologies) and penicillin-streptomycin (Life Technologies) following the manufacturer's instructions. SH-SY5Y (ATCC) was maintained in 1:1 mixture of Eagle's Minimum Essential Medium (EMEM) and F12 Medium (ATCC) with 10% FBS and penicillin-streptomycin following the manufacturer's instructions. To generate stable dCas9 repressor-expressing cell lines, approximately 30,000-50,000 cells were transfected in 24-well plates with 400 ng of dCas9 repressor-

containing PiggyBac expression plasmids (Addgene plasmid #110822, #110823, #110824) and 100 ng of transposase vector using lipofectamine 3000 (Life Technologies) as previously described[50]. Media was changed after 24 hours. Cells were allowed to recover for 2 days and then treated with 5 ug/ml of blasticidin. Cells were passaged regularly in drug media for more than 2 weeks to select for heterogeneous populations of dCas9 repressor integrant-containing cells.

Production of single gene-targeting gRNA lentivirus and cell transduction

HEK293T cells were seeded at 200,000 cells per well in 6-well plates a day prior to transfection. Cells were transfected with 450 ng of pSB700 sgRNA expression plasmid (with puromycin-resistant marker), 600 ng of psPAX2 (a gift from Didier Trono, Addgene plasmid # 12260), and 150 ng of pCMV-VSV-G (a gift from Bob Weinberg Addgene plasmid # 8454) using lipofectamine 2000 (Life Technologies). Viral supernatants were collected at 72 hours after transfection by centrifuging the medium at 400 g for 5 min to remove cell debris. HAP1 and SH-SY5Y repressor stable cell lines were seeded at ~15,000 and 35,000 cells, respectively, per well in 24-well plates. The following day each sample was infected with 100 ul of sgRNA-containing lentiviruses. Cells were treated with 0.5 ug/ml (HAP1) or 2.5 ug/ml (SH-SY5Y) of puromycin to select for transductants at 48 hours after transduction. Cells stably expressing sgRNA were passaged for 2 weeks and collected for RNA extraction and qPCR analysis. Sequences for qPCR primers are listed in **Supplementary Table 10**.

Production of lentiviral single and dual guide RNA (gRNA) libraries

The plasmid containing single guide RNA library targeting essential genes was a gift from Dr. Rene Bernards[19]. To generate the dual guide library a series of

oligonucleotides were designed such that the forward oligo created the first gRNA within the array and the reverse oligo was used to introduce the second gRNA into the array (list of oligos used for library construction are provided within **Supplementary Table 8**). A template containing a modified sgRNA tail sequence fused in cis to the 7SK pol III promoter was then used as a PCR template (sequence of sgRNA2-7SK template listed in **Supplementary Table 11**). To generate the dual guide library a PCR reaction was performed in which all forward and reverse primers were mixed together. The resulting ~475bp PCR product was run on a gel, extracted and inserted into the pSB700 gRNA expression backbone using Golden Gate cloning. To produce lentiviruses expressing each gRNA library, approximately 1 million HEK293T cells were plated on a 10 cm dish. The following day cells were transfected with each of the gRNA library plasmids mixed with psPAX2 and pCMV-VSV-G at 4:3:2 ratio using a total of 7-8 ug of DNA using the following protocol. Total plasmid DNA was diluted in 1 ml of serum-free media. Polyethylenimine or PEI (Polysciences) was added to the diluted DNA based on 3:1 ratio of PEI (ug): total DNA (ug). Mixtures were incubated for 15 min at room temperature and then added onto the cells. Viral supernatants were collected at 72 hours and concentrated using PEG Virus Precipitation Kit (BioVision) according to manufacturer's instructions.

CRISPR repressor screens

To compare the ability of different repressors in screening, a series of stable cell lines each containing a unique repressor along with a control cell line without a repressor integrated into the genome were seeded in 6-well plates and allowed to grow to 30-50% confluency to prepare for transduction the following day. Lentiviruses expressing each

guide RNA library were produced and used to infect experimental cells so the multiplicity of infection (MOI) was <0.5. Cells were treated with 0.5 ug/ml (HAP1, 293T) or 2.5 ug/ml (SH-SY5Y) of puromycin at 48 hours (HAP1) or 72 hours (SY-SH5Y, 293T) post virus transduction. After drug selection, 50% of the cells were collected immediately for DNA extraction using Epicentre Quick Extract Solution, and 50% of the cells were seeded into a set of 15 cm dishes for subsequent passaging. Cells were regularly passaged using standard protocols and collected again at 7, 14, and 22 days (SH-SY5Y screen only) post-drug selection for DNA extraction. The number of cells manipulated was kept sufficiently large such that we maintained a ~500 to 1000-fold coverage of the library at each stage of passaging. For PCR, 25 ug (lethality screen) or 60 ug (gene epistasis screen) of genomic DNA divided over 25 or 60 reactions, respectively, were amplified using KAPA2G Robust PCR kit (KAPA Biosystems) along with primer set, PCR 1 (**Supplementary Table 12**). The products of all first-round PCR reactions from the same sample were then pooled. 1 ul of the pooled product was used for a sample indexing in preparation for next generation sequencing using either Illumina Truseq or Nextera indexing primers. PCR cycling conditions are listed in **Supplementary Table 13**. See **Supplementary Note 3 and 4** for bioinformatics analyses of screen data**.**

Circuit experiments

HEK293FT cells were transfected as previously described[37] using PEI reagents. For inducible circuits, 2 ug/uL of doxycycline was added to samples and changed daily post-transfection until flow-cytometry. All samples were processed for flow-cytometry at 72 hours post-transfection and data were analyzed by FlowJo. **Supplementary Note 5**

provides detailed methods and materials used to perform circuit experiments.

Software

FlowJo (version 7) was used to analyze data generated from flow-cytometry experiments. MAGeCK (0.5.7) was used to analyze single gRNA library screens to determine gene essentiality.

Detailed information on experimental design and reagents is described in the Life Sciences Reporting Summary

DATA AVAILABILITY AND ACCESSION CODE AVAILABILITY STATEMENTS

All NGS data generated in this study are deposited with NCBI SRA (SRP142027) under BioProject (PRJNA451252). The authors declare that all other data supporting the findings of this study are available within the paper and supplementary files. All custom scripts are available upon request.

METHODS-ONLY REFERENCES

50. Chavez, A. *et al.* Comparison of Cas9 activators in multiple species. *Nat. Methods* **13,** 563–567 (2016).
51. Livak, K. J. & Schmittgen, T. D. Analysis of relative gene expression data using real-time quantitative PCR and the 2(-Delta Delta C(T)) Method. *Methods San Diego Calif* **25,** 402–408 (2001).

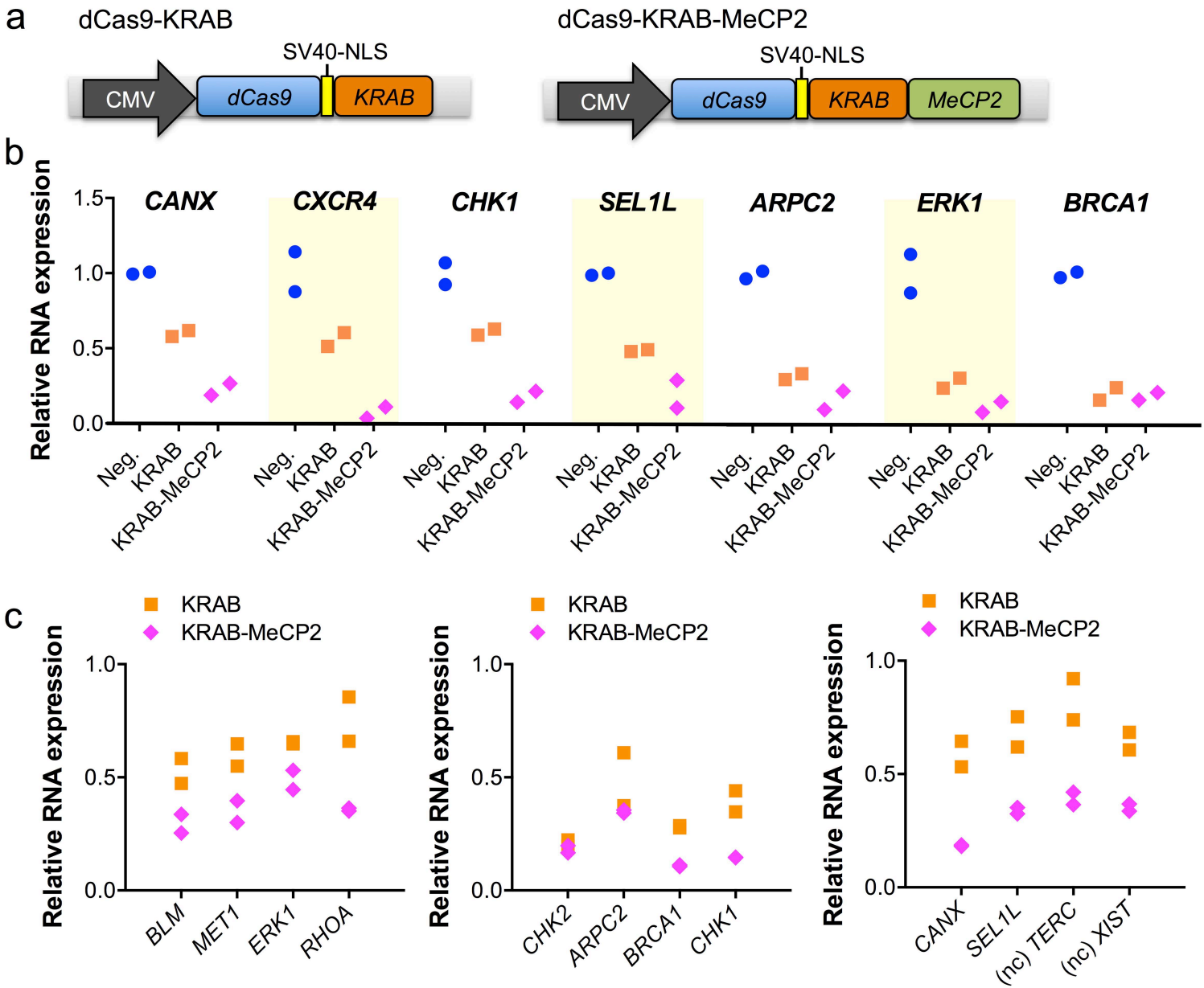
a
dCas9-KRAB
SV40-NLS
CMV
dCas9
KRAB
dCas9-KRAB-MeCP2
SV40-NLS
CMV
dCas9
KRAB
MeCP2
b
Relative RNA expression
1.5
1.0
0.5
0.0
CANX
CXCR4
CHK1
SEL1L
ARPC2
ERK1
BRCA1
Neg.
KRAB
KRAB-MeCP2
c
KRAB
KRAB-MeCP2
Relative RNA expression
1.0
0.5
0.0
BLM
MET1
ERK1
RHOA
CHK2
ARPC2
BRCA1
CHK1
CANX
SEL1L
(nc) TERC
(nc) XIST

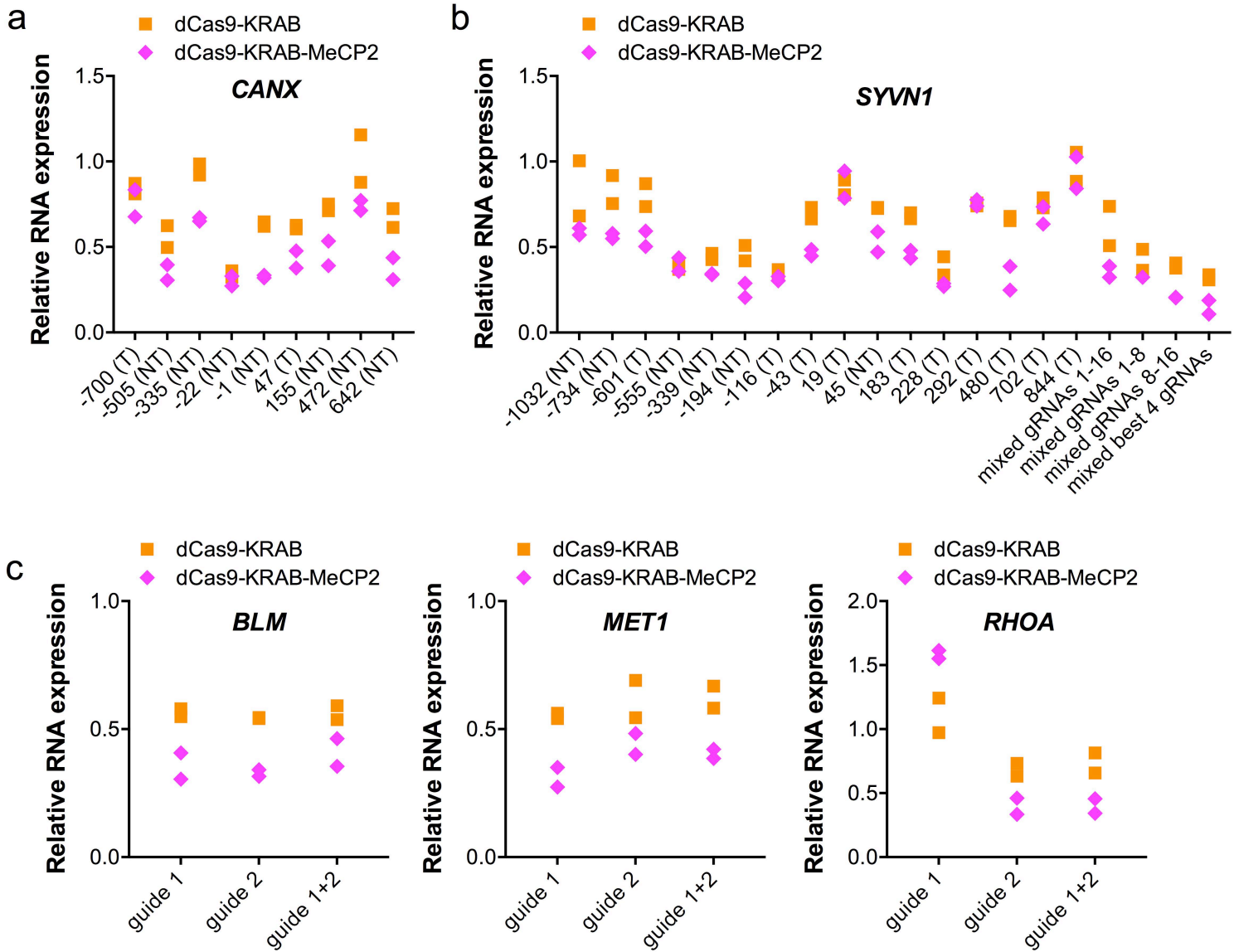
a
dCas9-KRAB
dCas9-KRAB-MeCP2
CANX
Relative RNA expression
1.5
1.0
0.5
0.0
-700 (T)
-505 (NT)
-335 (NT)
-22 (NT)
-1 (NT)
47 (T)
155 (NT)
472 (NT)
642 (NT)
b
dCas9-KRAB
dCas9-KRAB-MeCP2
SYVN1
Relative RNA expression
1.5
1.0
0.5
0.0
-1032 (NT)
-734 (NT)
-601 (T)
-555 (NT)
-339 (NT)
-194 (NT)
-116 (T)
-43 (T)
19 (T)
45 (NT)
183 (T)
228 (T)
292 (T)
480 (T)
702 (T)
844 (T)
mixed gRNAs 1-16
mixed gRNAs 1-8
mixed gRNAs 8-16
mixed best 4 gRNAs
c
dCas9-KRAB
dCas9-KRAB-MeCP2
BLM
Relative RNA expression
1.0
0.5
0.0
guide 1
guide 2
guide 1+2
dCas9-KRAB
dCas9-KRAB-MeCP2
MET1
Relative RNA expression
1.0
0.5
0.0
guide 1
guide 2
guide 1+2
dCas9-KRAB
dCas9-KRAB-MeCP2
RHOA
Relative RNA expression
2.0
1.5
1.0
0.5
0.0
guide 1
guide 2
guide 1+2

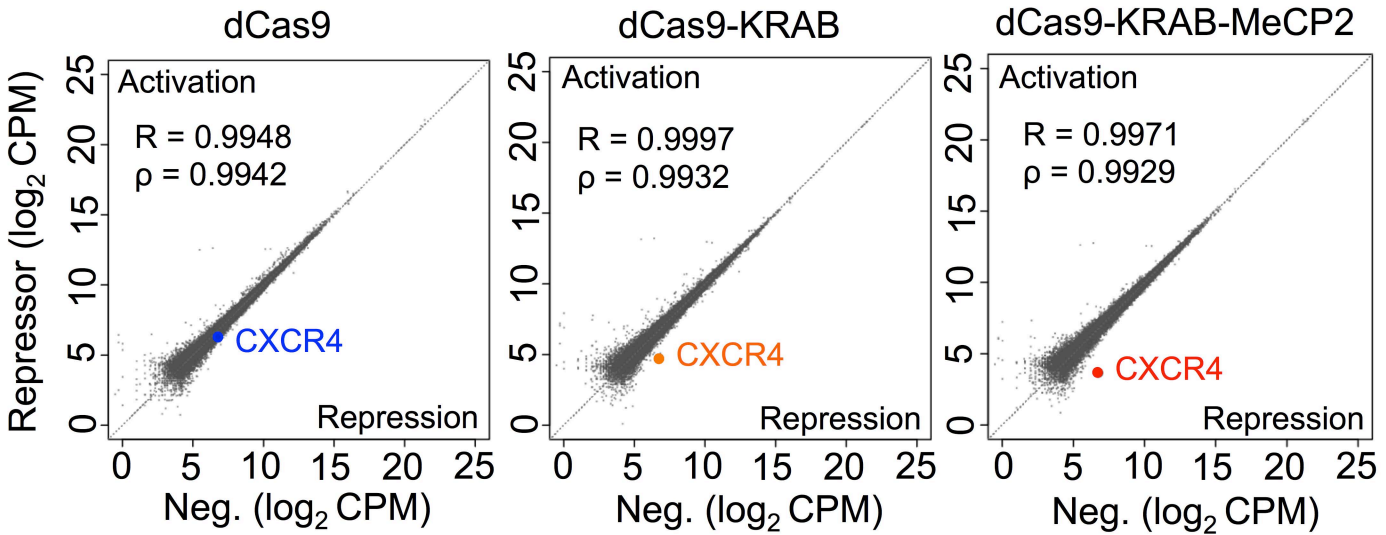
dCas9
dCas9-KRAB
dCas9-KRAB-MeCP2
Activation
Repression
R = 0.9948
ρ = 0.9942
R = 0.9997
ρ = 0.9932
R = 0.9971
ρ = 0.9929
CXCR4
Repressor (log2 CPM)
Neg. (log2 CPM)
0
5
10
15
20
25

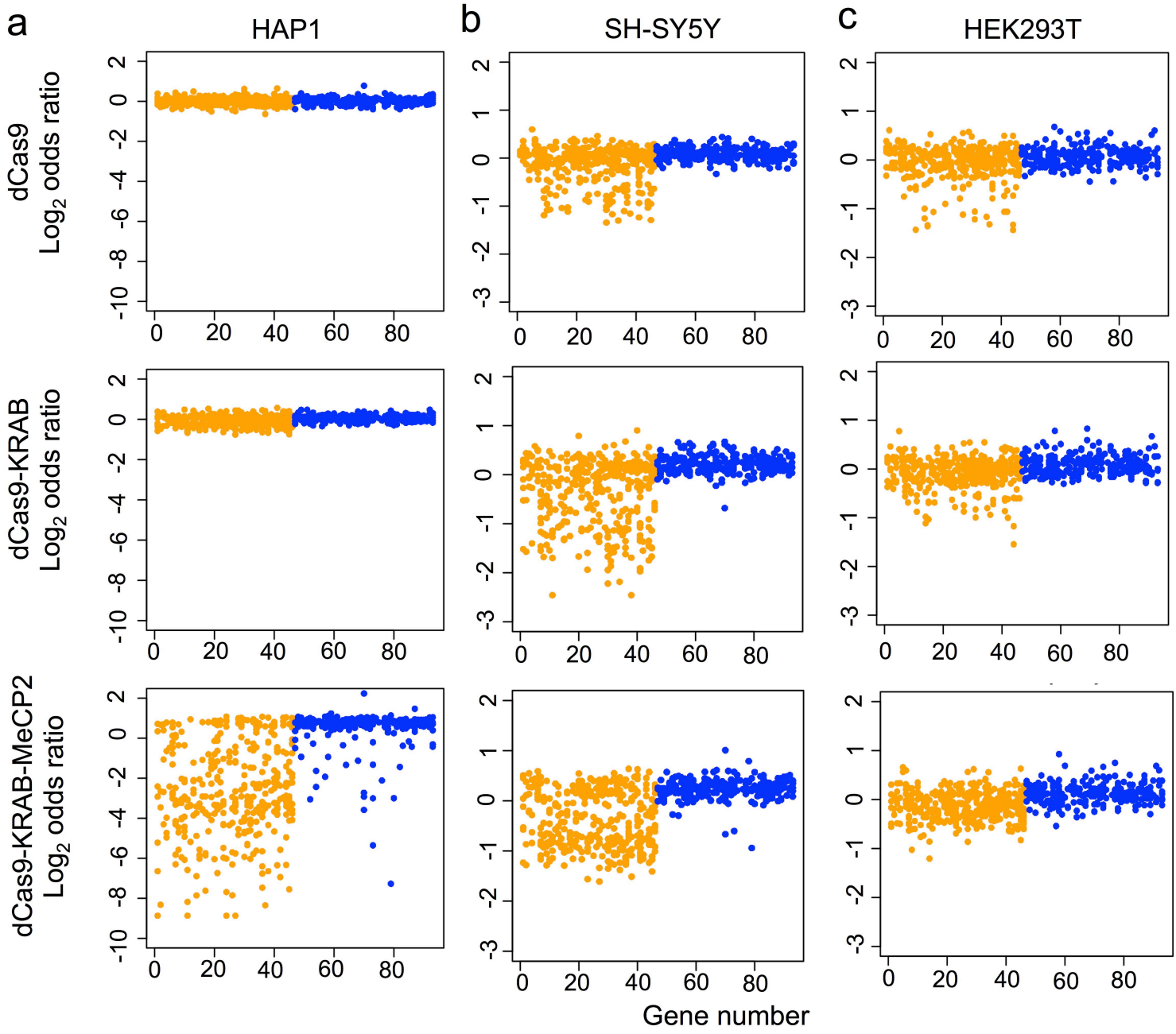
a
b
c
HAP1
SH-SY5Y
HEK293T
dCas9
Log2 odds ratio
dCas9-KRAB
Log2 odds ratio
dCas9-KRAB-MeCP2
Log2 odds ratio
Gene number

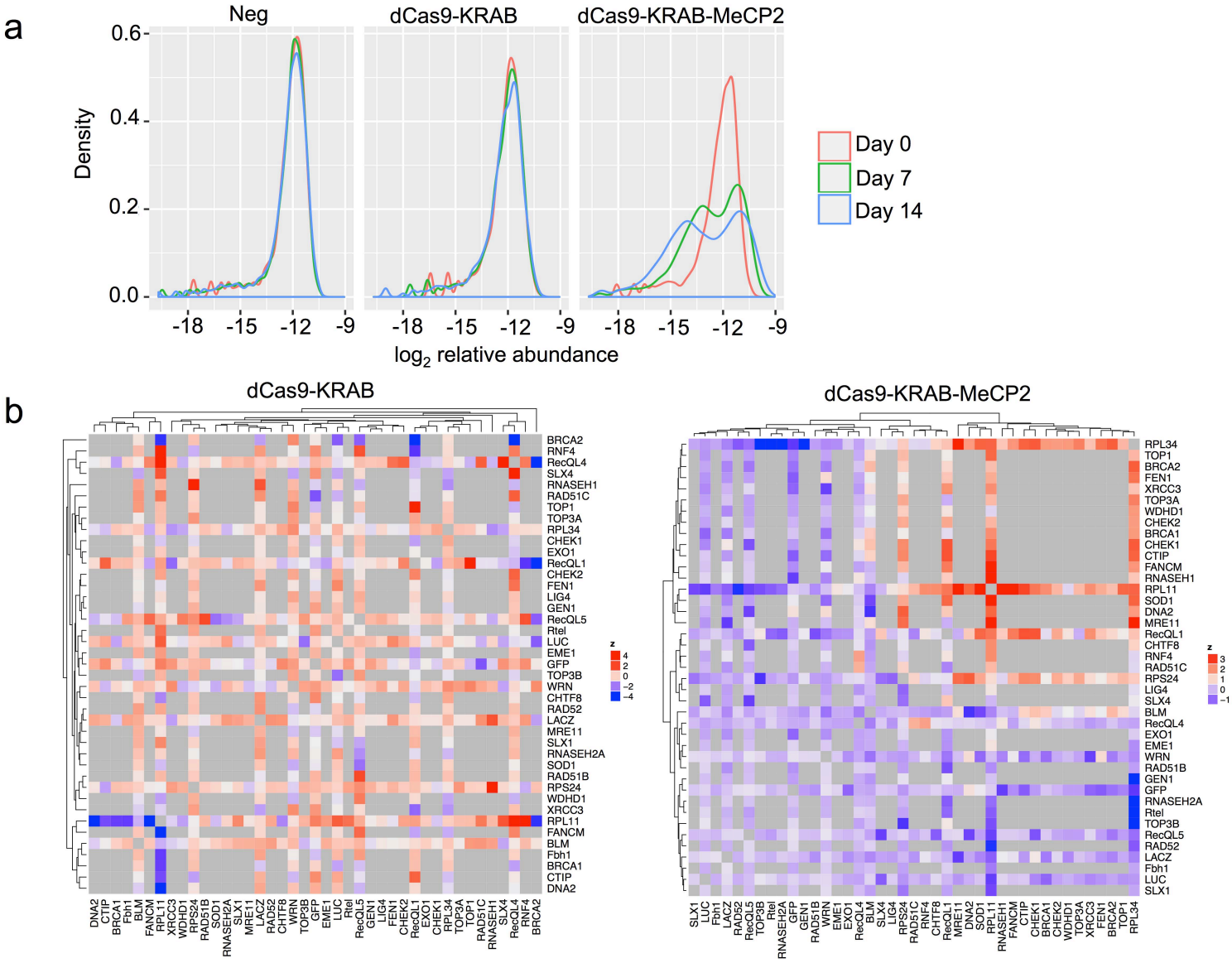
a
Neg
dCas9-KRAB
dCas9-KRAB-MeCP2
Density
0.6
0.4
0.2
0.0
-18
-15
-12
-9
log2 relative abundance
Day 0
Day 7
Day 14
b
dCas9-KRAB
dCas9-KRAB-MeCP2
z

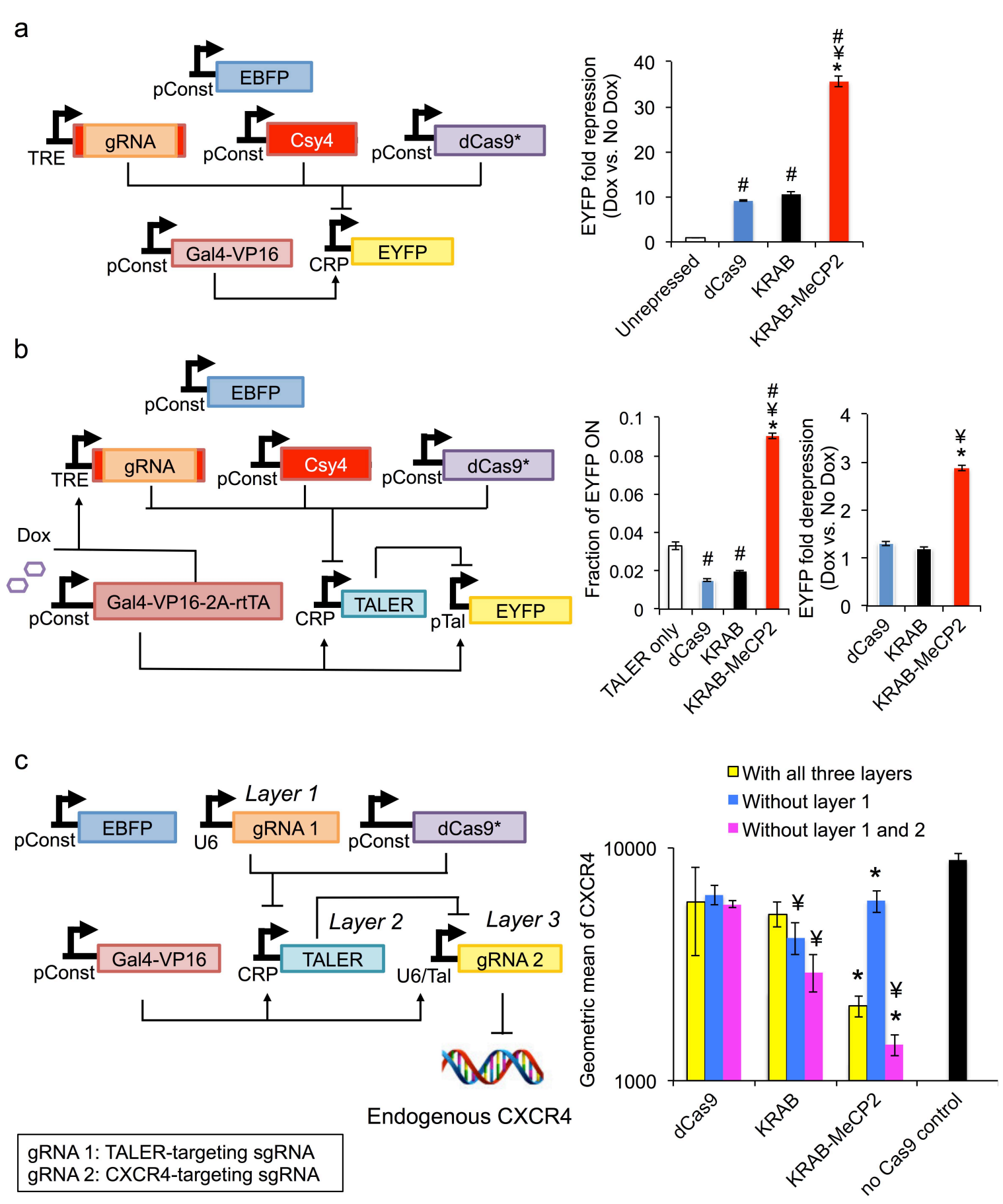
a
pConst
EBFP
TRE
gRNA
pConst
Csy4
pConst
dCas9*
pConst
Gal4-VP16
CRP
EYFP
EYFP fold repression
(Dox vs. No Dox)
40
30
20
10
0
#
#
#¥*
Unrepressed
dCas9
KRAB
KRAB-MeCP2
b
pConst
EBFP
TRE
gRNA
pConst
Csy4
pConst
dCas9*
Dox
pConst
Gal4-VP16-2A-rtTA
CRP
TALER
pTal
EYFP
Fraction of EYFP ON
0.1
0.08
0.06
0.04
0.02
0
#
#
#¥*
TALER only
dCas9
KRAB
KRAB-MeCP2
EYFP fold derepression
(Dox vs. No Dox)
4
3
2
1
0
¥*
dCas9
KRAB
KRAB-MeCP2
c
pConst
EBFP
Layer 1
U6
gRNA 1
pConst
dCas9*
Layer 2
Layer 3
pConst
Gal4-VP16
CRP
TALER
U6/Tal
gRNA 2
Endogenous CXCR4
With all three layers
Without layer 1
Without layer 1 and 2
Geometric mean of CXCR4
10000
1000
¥
¥
*
*
¥
*
dCas9
KRAB
KRAB-MeCP2
no Cas9 control
gRNA 1: TALER-targeting sgRNA
gRNA 2: CXCR4-targeting sgRNA

An enhanced CRISPR repressor for targeted mammalian gene regulation

Nan Cher Yeo[1,2,†], Alejandro Chavez[3,†,*], Alissa Lance-Byrne[1], Yingleong Chan[1,2,Φ], David Menn[4,Φ], Denitsa Milanova[1,2,Φ], Chih-Chung Kuo[5,6,Φ], Xiaoge Guo[1,2], Sumana Sharma[7], Angela Tung[1], Ryan J. Cecchi[1], Marcelle Tuttle[1], Swechchha Pradhan[4], Elaine T Lim[1,2], Noah Davidsohn[1,2], Mo R. Ebrahimkhani[4,8], James J. Collins[1,9,10,11,11], Nathan E. Lewis[5,6,13], Samira Kiani[4,*], and George M. Church[1,2,*]

[1]Wyss Institute for Biologically Inspired Engineering, Harvard University, Cambridge, Massachusetts, USA.
[2]Department of Genetics, Harvard Medical School, Boston, Massachusetts, USA.
[3]Department of Pathology and Cell Biology, Columbia University College of Physicians and Surgeons, New York, New York, USA
[4]School of Biological and Health Systems Engineering, Ira. A Fulton Schools of Engineering, Arizona State University, Tempe, Arizona, USA.
[5]Department of Bioengineering, University of California, San Diego, USA.
[6]Novo Nordisk Foundation Center for Biosustainability at the University of California, San Diego, USA.
[7]Cell Surface Signalling Laboratory, Wellcome Trust Sanger Institute, Cambridge CB101SA, United Kingdom.
[8]Division of Gastroenterology and Hematology, Mayo Clinic College of Medicine and Science, Phoenix, Arizona, USA.
[9]Institute for Medical Engineering & Science, Massachusetts Institute of Technology, Cambridge, Massachusetts, USA.
[10]Synthetic Biology Center, Massachusetts Institute of Technology, Cambridge, Massachusetts, USA.
[11]Department of Biological Engineering, Massachusetts Institute of Technology, Cambridge, Massachusetts, USA.
[12]Broad Institute of MIT and Harvard, Cambridge, Massachusetts, USA.
[13]Department of Pediatrics, University of California, San Diego, USA

[†]Co-first authors
[Φ]These authors contributed equally to the manuscript

[*]Correspondence can be addressed to:
Alejandro Chavez
E-mail: ac4304@cumc.columbia.edu

Samira Kiani
E-mail: samira.Kiani@asu.edu

George M. Church
E-mail: gchurch@genetics.med.harvard.edu

This document contains:
Supplementary Figure 1-15
Supplementary Table 1-13
Supplementary Note 1-5

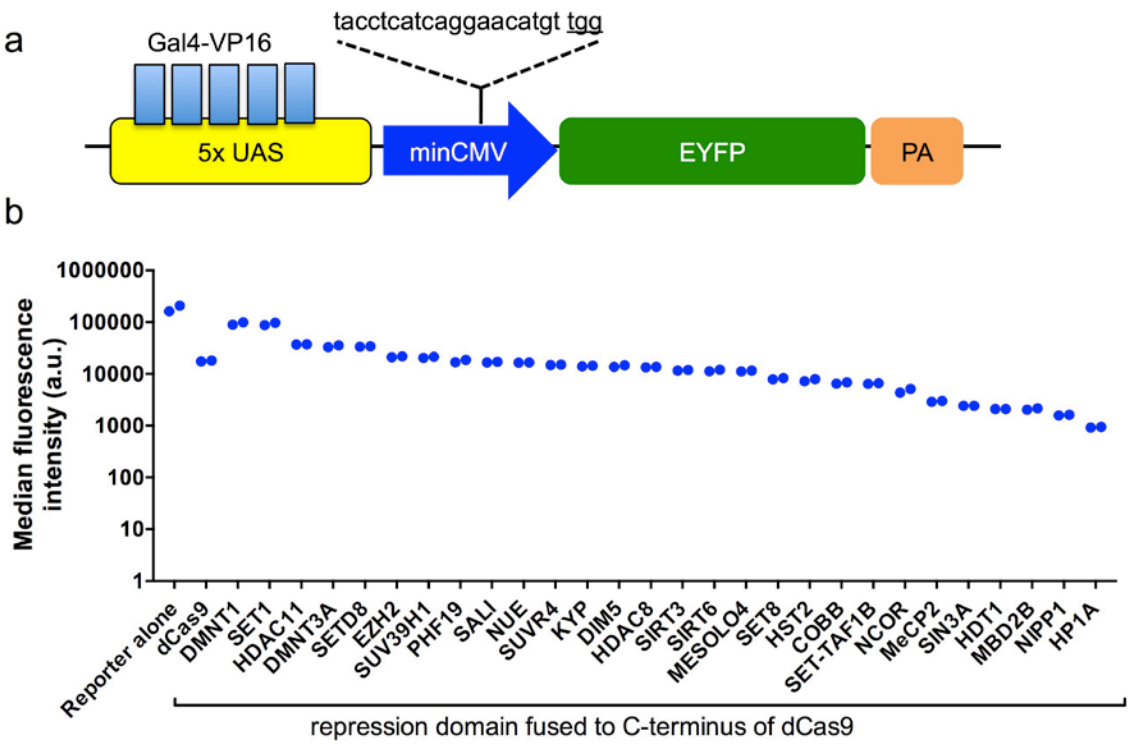

Supplementary Figure 1 Targeted screen to identify repression domains that function with dCas9. (a) Schematic of the EYFP fluorescent reporter construct used in the targeted screen. A protospacer sequence followed by TGG PAM is placed within the minimal CMV (minCMV) promoter upstream of the EYFP reporter gene. Transcription of the EYFP reporter is driven upon binding of a GAL4-VP16 protein to the UAS sequences present upstream of the minCMV promoter. (b) The fluorescent reporter and sgRNA were co-transfected with the indicated repressors into HEK293T cells. At 2 days post-transfection, EYFP fluorescence levels were measured to quantify the amount of repression from the various dCas9 fusion proteins. The name of the protein from which the transcriptional regulatory domain was isolated is listed on the x-axis. All domains were fused to the C-terminus of the dCas9 protein. KRAB and the six top-performing domains were used for subsequent engineering. n=2 biologically independent samples (cell cultures).

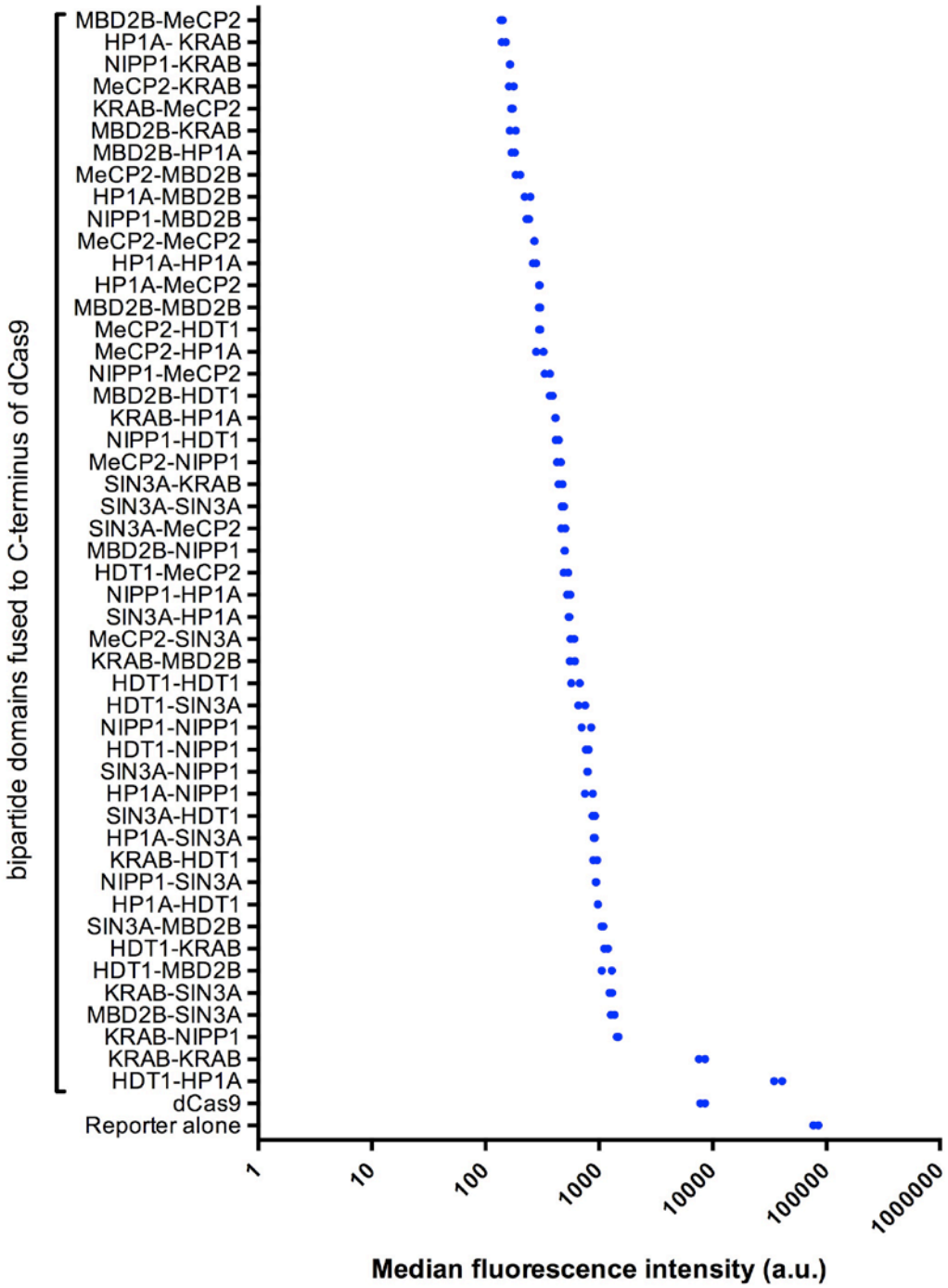

Supplementary Figure 2 Reporter screen of 49 dCas9 bipartite repressors. A series of all pairwise repeating and non-repeating bipartite repressors were generated using KRAB and the six top-performing domains identified from the initial screen (MeCP2, SIN3A, HDT1, MBD2B, NIPP1, and HP1a). Each repressor was tested using the same fluorescent reporter assay as in Supplementary Figure 1. n=2 biologically independent samples (cell cultures).

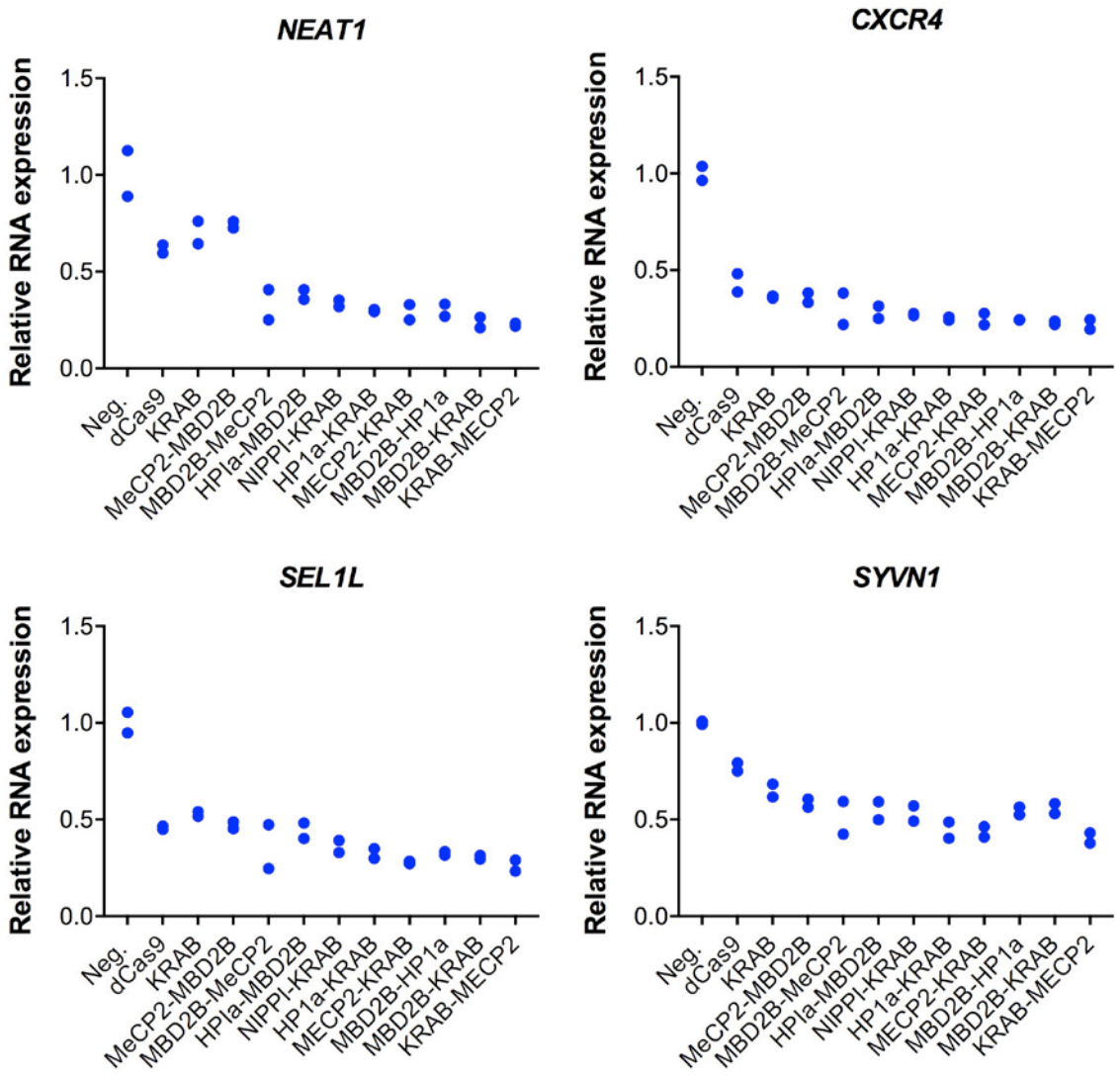

Supplementary Figure 3 Repression of endogenous genes using top bipartite fusions. HEK293T cells were co-transfected with gRNAs against the indicated four genes simultaneously with the labeled repressors. Samples were collected for RNA extraction at 4 days post-transfection. The expression levels of targeted genes were measured by RT-qPCR. n=2 biologically independent samples (cell cultures).

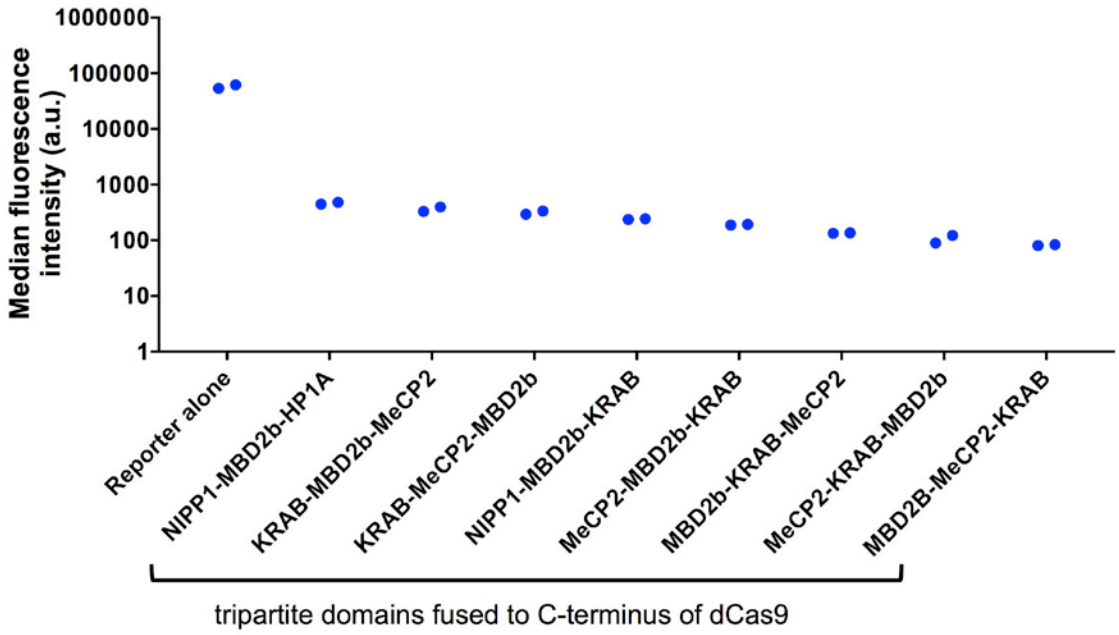

Supplementary Figure 4 Reporter screen of 8 dCas9 tripartite repressors. A series of rationally designed tripartite repressors were generated based on the top-performing bipartite repression domains. Each repressor was tested using the same fluorescent reporter assay as in Supplementary Figure 1. n=2 biologically independent samples (cell cultures).

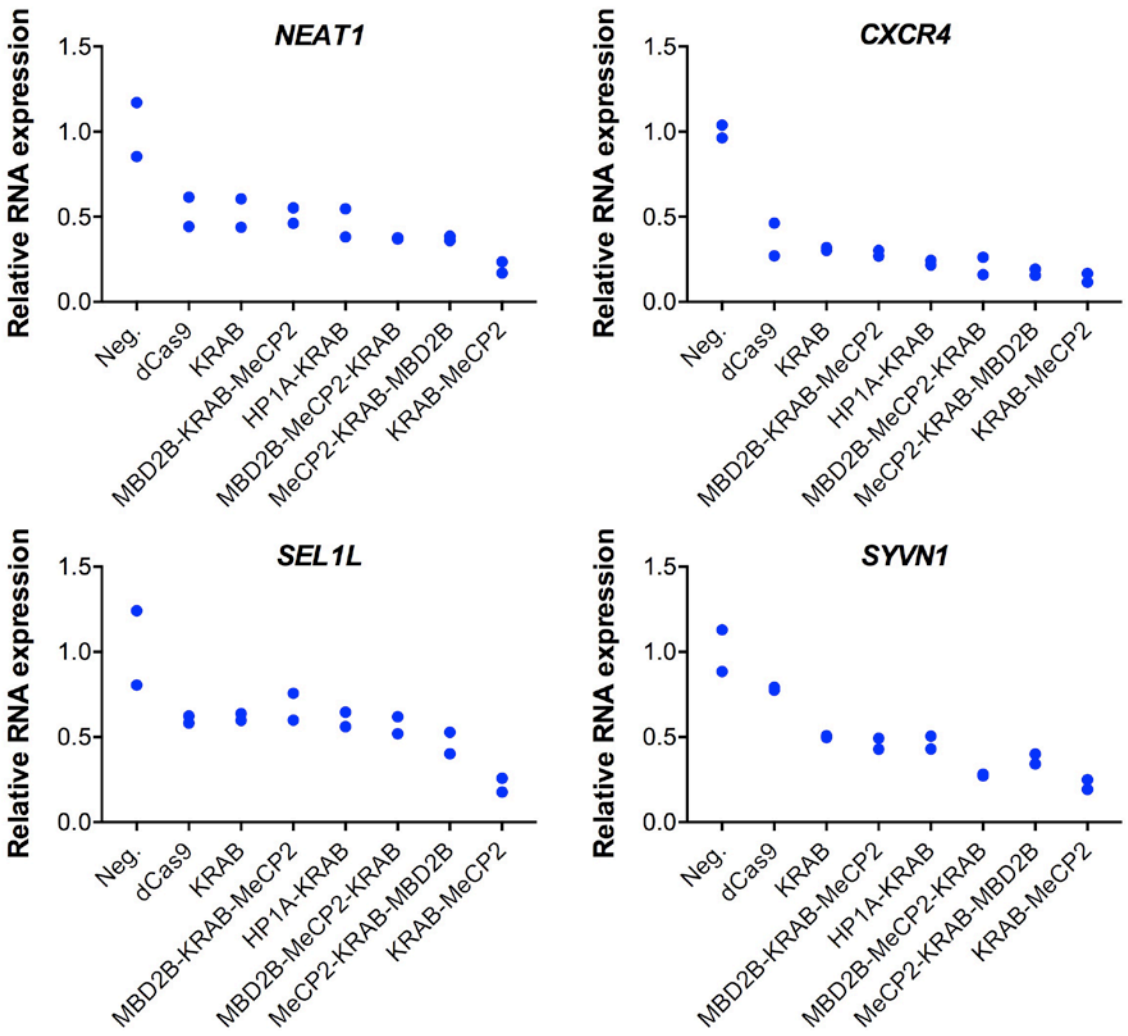

Supplementary Figure 5 Repression of endogenous genes using top tripartite fusions as compared to the bipartite KRAB-MeCP2 repressor. The three best performing tripartite repressors based on the reporter screen were selected and tested against a series of endogenous loci, along with HP1A-KRAB and KRAB-MeCP2. RNA levels of the four indicated genes from a multiplexed repression experiment were measured using RT-qPCR. n=2 biologically independent samples (cell cultures).

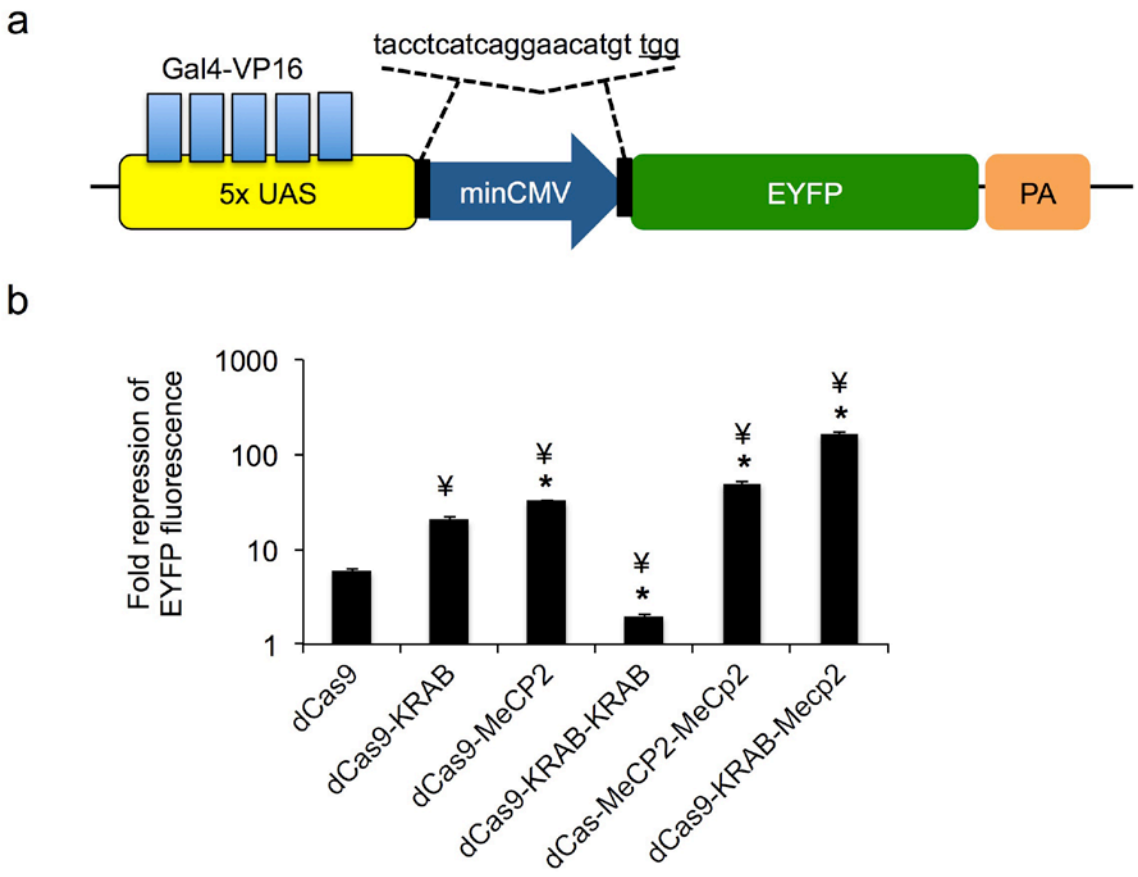

Supplementary Figure 6 Reporter screening of different dCas9 fusion proteins consisting KRAB or MeCP2. (a) Schematic of CRP repression device. dCas9 repressors coupled with a U6-driven gRNA regulate EYFP output through binding two targets sites within the CRP promoter. (b) dCas9-KRAB-MeCP2 outperformed either KRAB or MeCP2 either as single or double fusions to dCas9 when paired with sgRNA in repressing EYFP output. Data are presented as mean ± s.e.m. n=3 biologically independent samples (cell cultures). One-sided Student's T-test was used for statistical comparison. ¥ indicates $p< 0.05$ vs. dCas9, * indicates $p< 0.05$ vs. dCas9-KRAB.

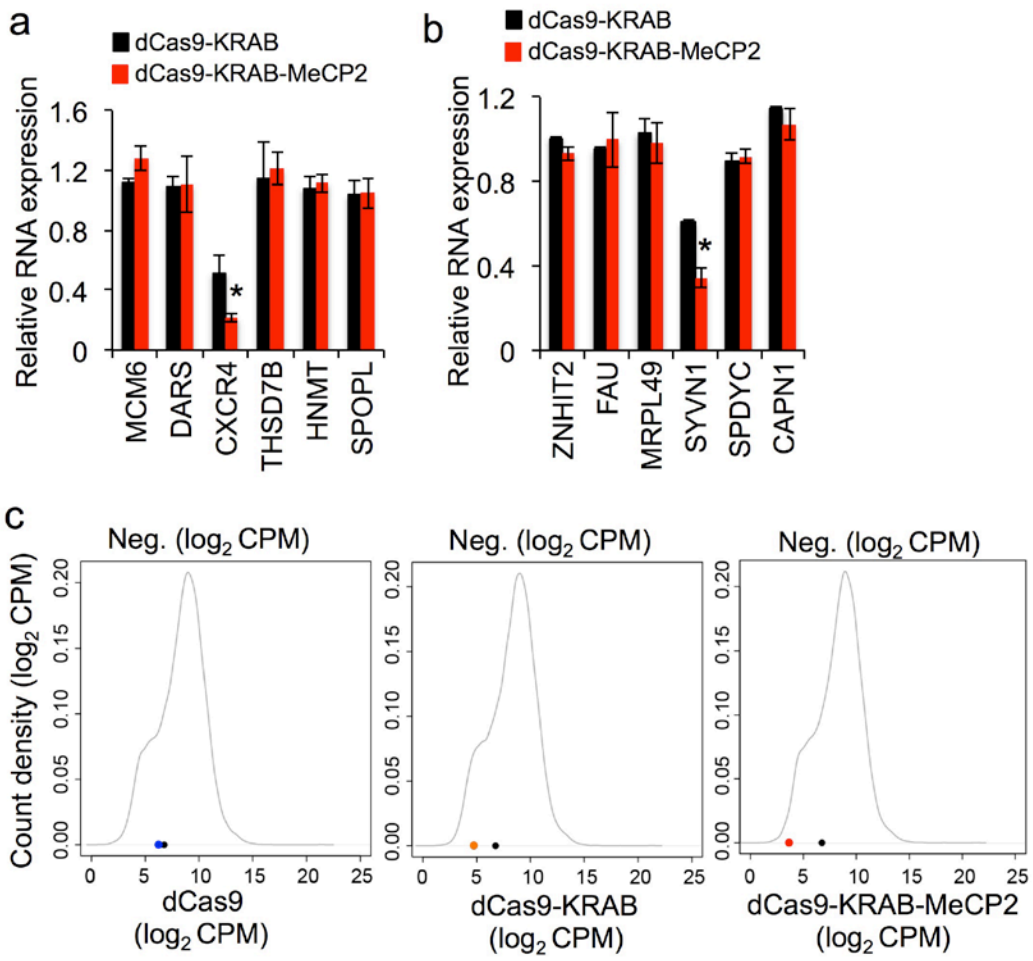

Supplementary Figure 7 dCas9-KRAB-MeCP2-mediated repression is highly specific in human cells. (a) HEK293T cells were transfected with a gRNA targeting the *CXCR4* gene along with the indicated dCas9 repressor. Expression of the target gene *CXCR4* and several nearest neighboring genes, including *MCM6, DARS, THSD7B, HNMT,* and *SPOPL*, were examined. These genes are located at approximately -274, -208, 651, 1849, and 2387 kb, respectively, away from *CXCR4*. (b) Expression of the target gene *SYVN1* and several nearest neighboring genes, including *ZNHIT2, FAU, MRPL49, SPDYC,* and *CAPN1*, were examined. These genes are located at approximately -10, -6, -5, 42, and 53 kb, respectively, away from *SYVN1*. For a-b, data are shown as mean ± s.e.m. n=4 biologically independent samples (cell cultures). One-sided Student T-test was used to perform statistical comparison. * p< 0.05 v.s. dCas9-KRAB. (c) RNA-seq analysis of HEK293T cells transfected with gRNA targeting *CXCR4* along with dCas9, dCas9-KRAB or dCas9-KRAB-MeCP2. Shown are density plots indicating the fold changes in gene expression from different groups. *CXCR4* expression is indicated with blue, orange, or red dot and control is indicated with a black dot. n=2 biologically independent samples (cell cultures).

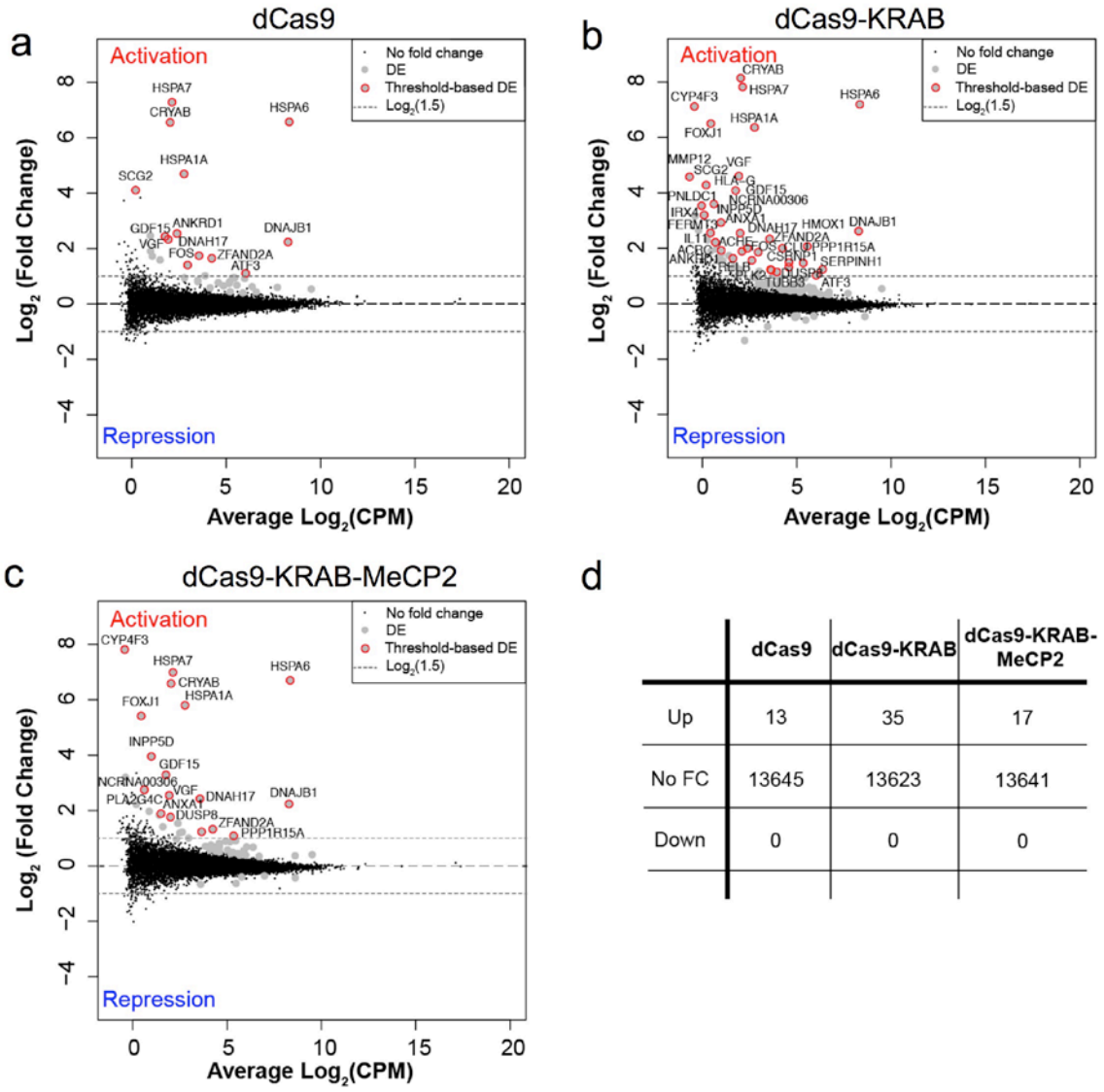

	dCas9	dCas9-KRAB	dCas9-KRAB-MeCP2
Up	13	35	17
No FC	13645	13623	13641
Down	0	0	0

Supplementary Figure 8 Differentially expressed (DE) genes in RNA-seq experiment. (a-c) Shown are $\log_2$ fold change (FC) versus average $\log_2$ count per millions (CPM) for dCas9, dCas9-KRAB and dCas9-KRAB-MeCP2 relative to the negative control. Genes with no fold change are marked in black, DE genes are marked in grey, and DE genes above $\log_2$ FC of 1.5 threshold are marked in red. Positive $\log_2$ FC represents transcriptional activation while negative values indicate repression. (d) Shown is a summary of the number of DE genes showing up- or down-regulation with $\log_2$ FC >1.5 in different groups. (Methods associated with this figure are described in **Supplementary Note 2**)

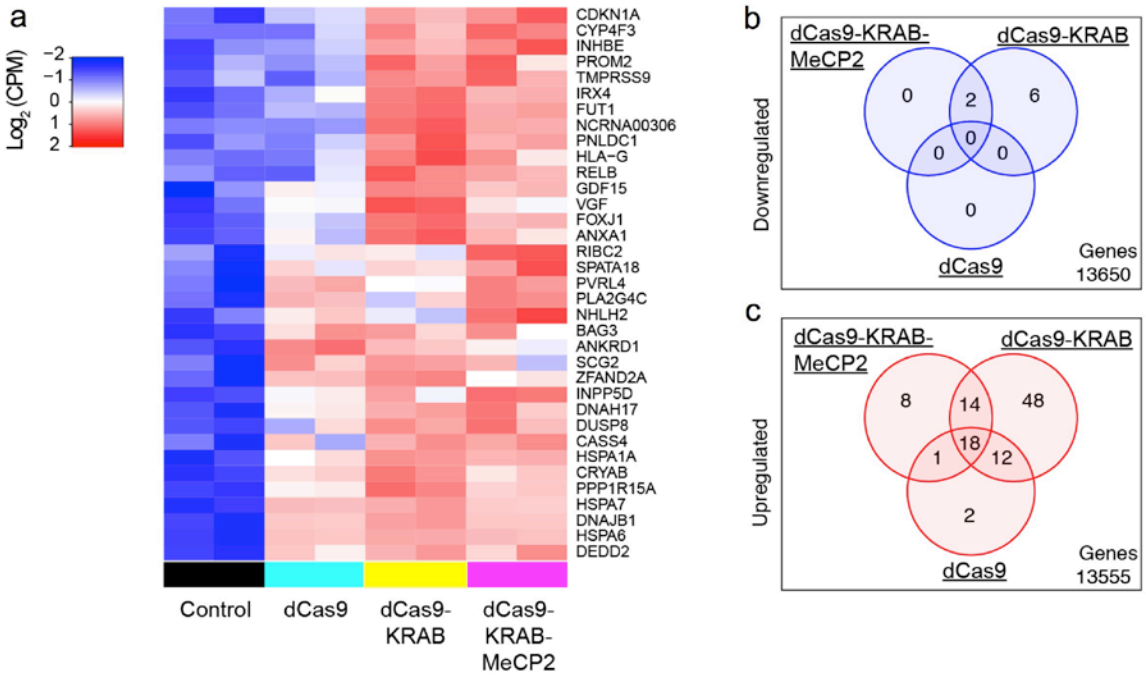

Supplementary Figure 9 Cluster analysis of the top 35 DE genes in negative control, dCas9, dCas9-KRAB, and dCas9-KRAB-MeCP2 groups. (a) Clustering of genes with correlated expression provides insights into the biological effects of repressor's activity. Heatmap representing distances between each gene pair is calculated based on Euclidean distance, $(1\text{-}R)^2/2$ where R represents the Pearson's correlation of two genes. A scale key bar of normalized $\log_2$ CPM shows large negative (colored in blue) and positive (colored in red) correlations. Genes with large positive correlations correspond to small Euclidean distances and cluster together. (b-c) Shown are Venn diagrams comparing transcriptome-wide downregulated or upregulated genes among the different repressors. (Methods associated with this figure are described in **Supplementary Note 2**)

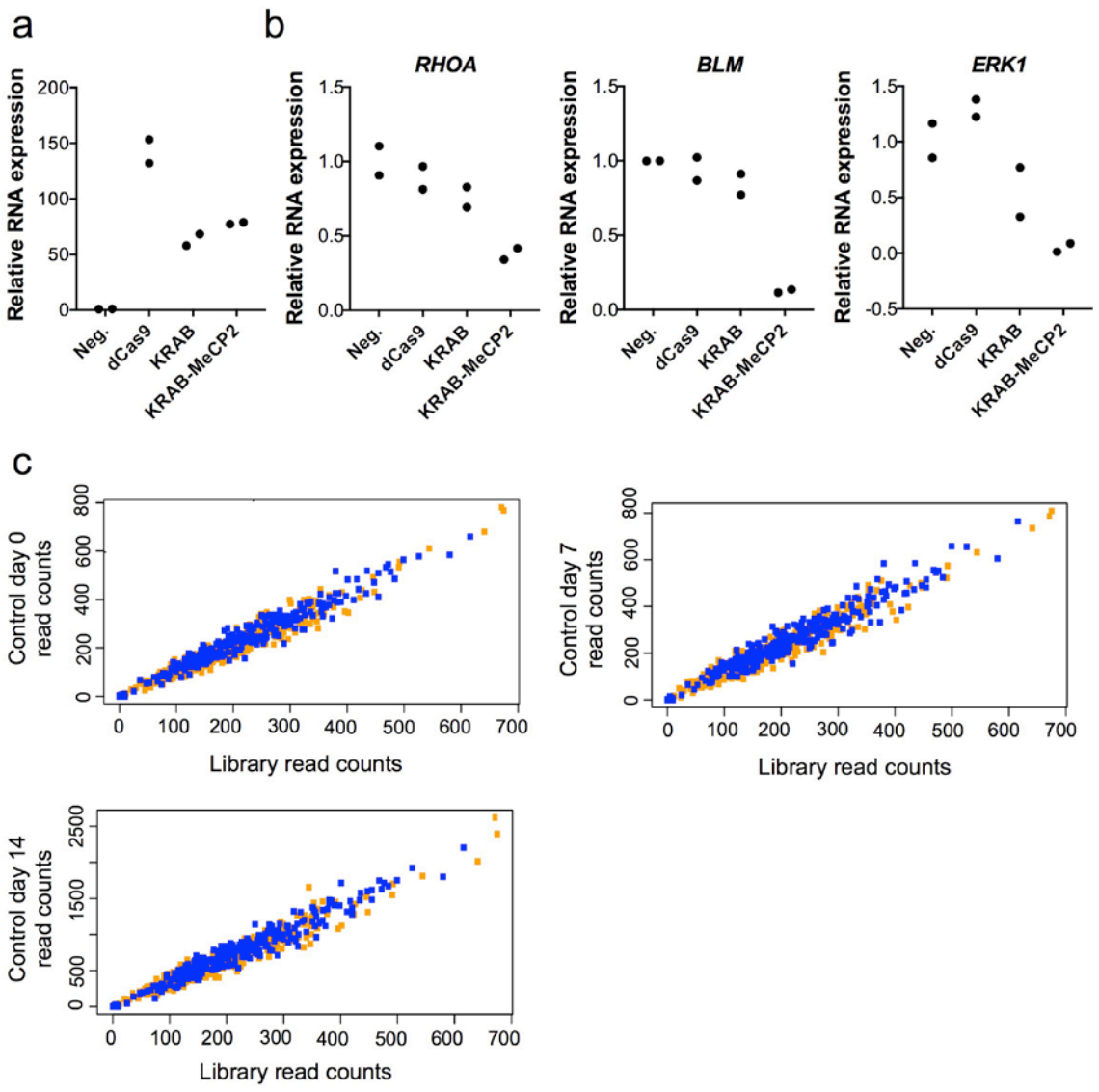

Supplementary Figure 10 HAP1 cells stably expressing dCas9 repressors. (a) Shown is the expression level of dCas9 repressors in the different stable cell lines. n=2 biologically independent samples (cell cultures). (b) Stable cells were transduced with lentiviruses containing a gRNA targeting the indicated genes. dCas9-KRAB-MeCP2-containing cell line induced stronger suppression of most target genes. For a-b, n=2 biologically independent samples (cell cultures). (c) Shown are distributions of sgRNA constructs transduced into HAP1 wild-type cells over time. The sgRNA counts remained similar to that of the initial DNA library used to generate lentivirus. Blue squares represent non-essential gene-targeting constructs and orange squares represent essential gene-targeting constructs.

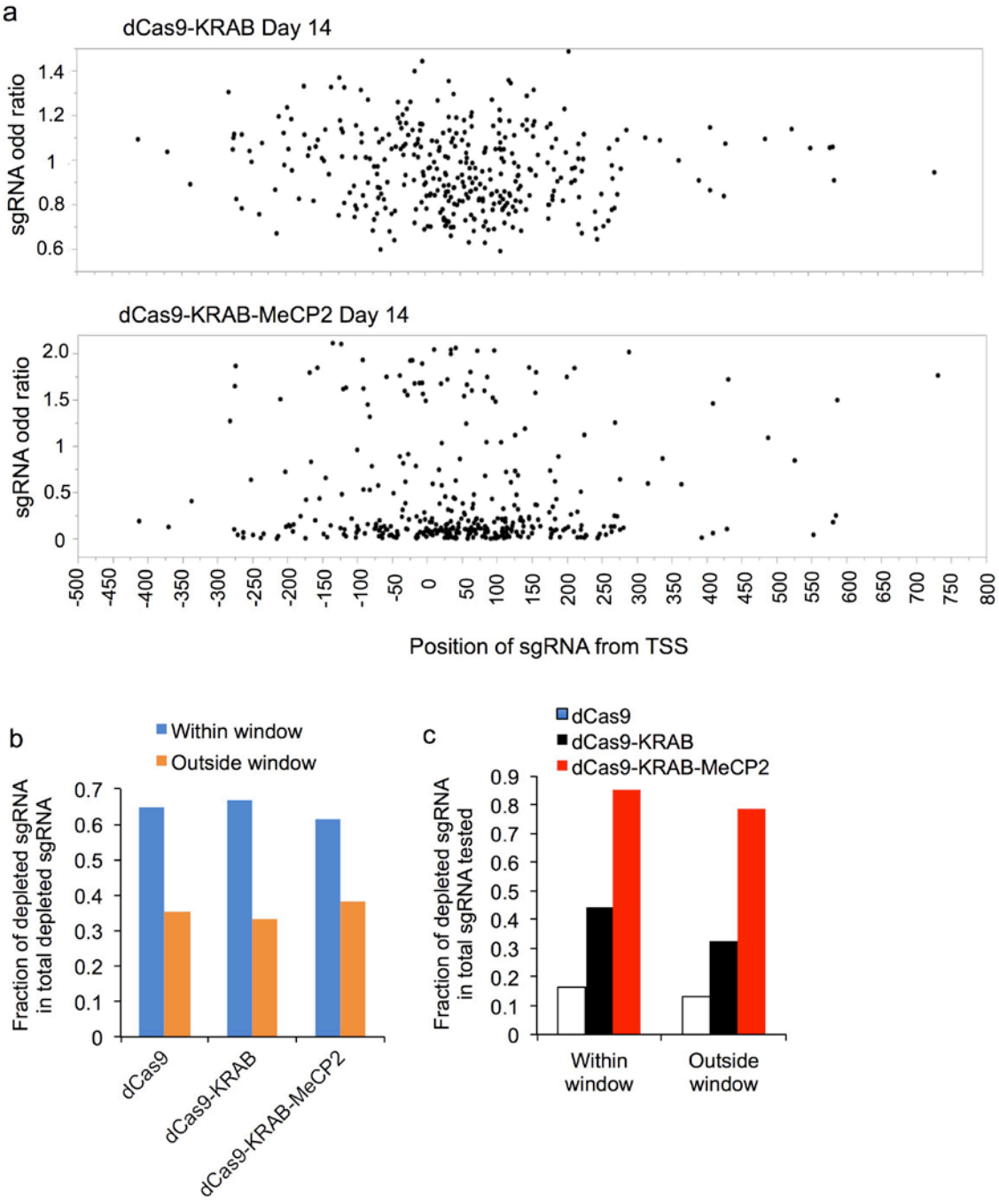
a
dCas9-KRAB Day 14
sgRNA odd ratio
1.4
1.2
1
0.8
0.6
dCas9-KRAB-MeCP2 Day 14
sgRNA odd ratio
2.0
1.5
1
0.5
0
-500 -450 -400 -350 -300 -250 -200 -150 -100 -50 0 50 100 150 200 250 300 350 400 450 500 550 600 650 700 750 800
Position of sgRNA from TSS
b
Within window
Outside window
Fraction of depleted sgRNA in total depleted sgRNA
0.7
0.6
0.5
0.4
0.3
0.2
0.1
0
dCas9
dCas9-KRAB
dCas9-KRAB-MeCP2
c
dCas9
dCas9-KRAB
dCas9-KRAB-MeCP2
Fraction of depleted sgRNA in total sgRNA tested
0.9
0.8
0.7
0.6
0.5
0.4
0.3
0.2
0.1
0
Within window
Outside window

Supplementary Figure 11 dCas9-KRAB-MeCP2 outperformed dCas9-KRAB regardless of targeting position. (a) Using the data from our pooled library screens, we plot sgRNA odd ratio (<1 indicates depletion) as a function of position from the transcription start site (TSS) for 370 essential gene-targeting sgRNAs. Shown are results from HAP1 cells using dCas9-KRAB or dCas9-KRAB-MeCP2 in the screen at day 14. (b) Of the total sgRNAs depleted by each repressor, we quantified the fraction of significantly depleted sgRNAs within or outside of the optimal window. sgRNAs located within the optimal targeting window showed a higher likelihood of being depleted as compared to sgRNAs positioned outside of the window across all repressors. (c) Of the total sgRNAs tested within or outside of the previously defined targeting window (-50bp to +200 bp from TSS), we quantified the fraction of significantly depleted sgRNAs when combined with the different repressors. dCas9-KRAB-MeCP2 showed the highest performance regardless of sgRNA targeting window. Similar results were observed in SH-SY5Y and HEK293T screens (figures not shown). See **Supplementary Table 7** for a summary of the data in all three cell lines.

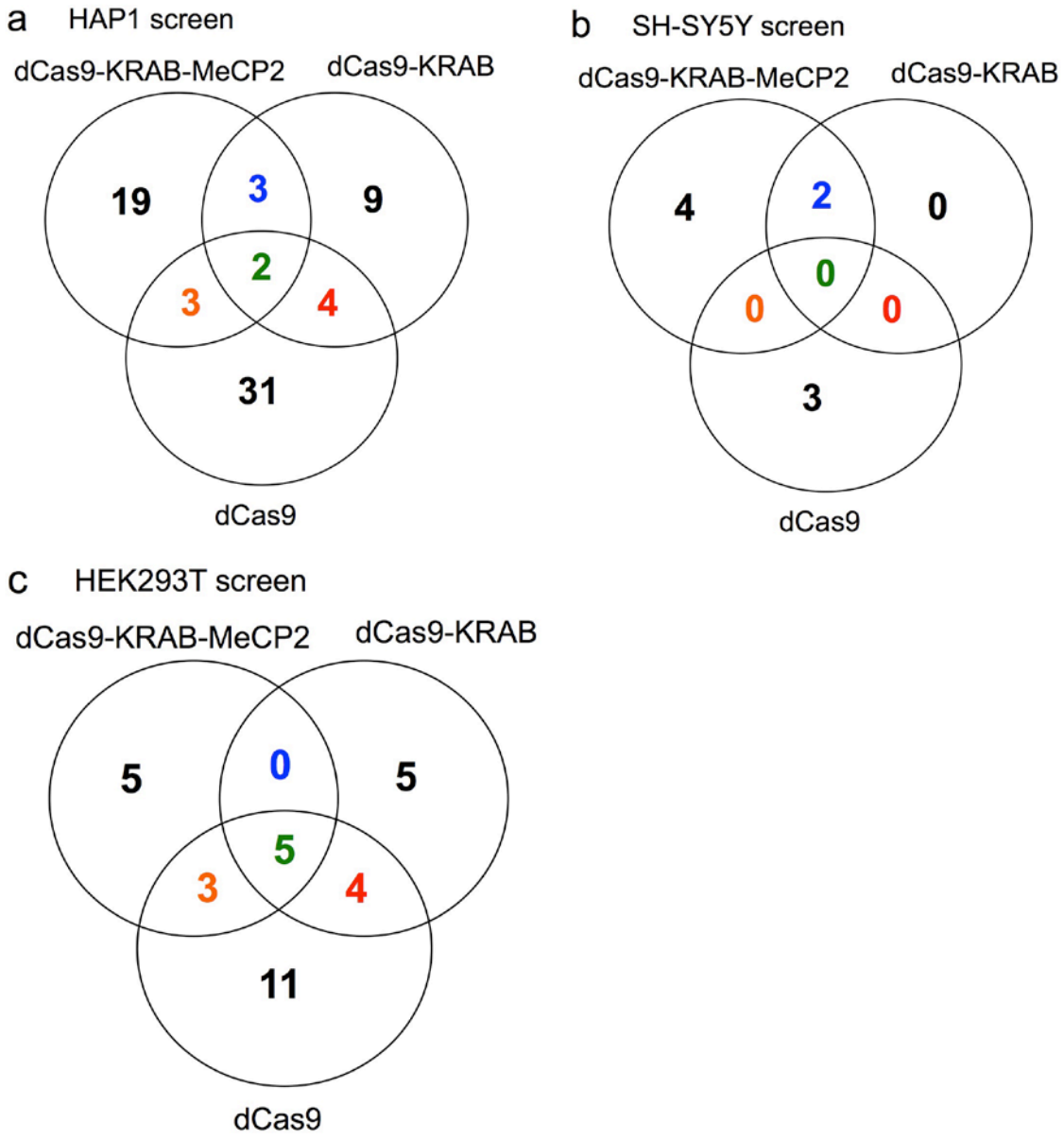

Supplementary Figure 12 Overlap of non-essential (NE) gene-targeting sgRNAs showing depletion in (a) HAP1, (b) SH-SY5Y, and (c) HEK293T cells. Venn diagrams show the numbers of NE-targeting sgRNAs exhibiting depletion that are unique to a repressor or common among repressors. (a) In HAP1 cells, PLA2G2E-19, sgRNA with the strongest depletion score, was depleted by both dCas9-KRAB-MeCP2 and dCas9-KRAB. Other top depleted sgRNAs seen in KRAB-MeCP2 screen, including HTR3D-6, LHX5-8, MRGPRD-2, and POU4F2-15, are also common to dCas9-KRAB or dCas9. (b) In SH-SY5Y screen, the top two NE-targeting sgRNAs, NPHS2-7 and PLA2G2E-19, seen with dCas9-KRAB-MeCP2 were also depleted with dCas9-KRAB. (c) Overlap of NE-targeting sgRNAs observed in HEK293T was shown. See **Supplementary Data 5** for a full list of NE guides exhibiting depletion when combined with different repressors.

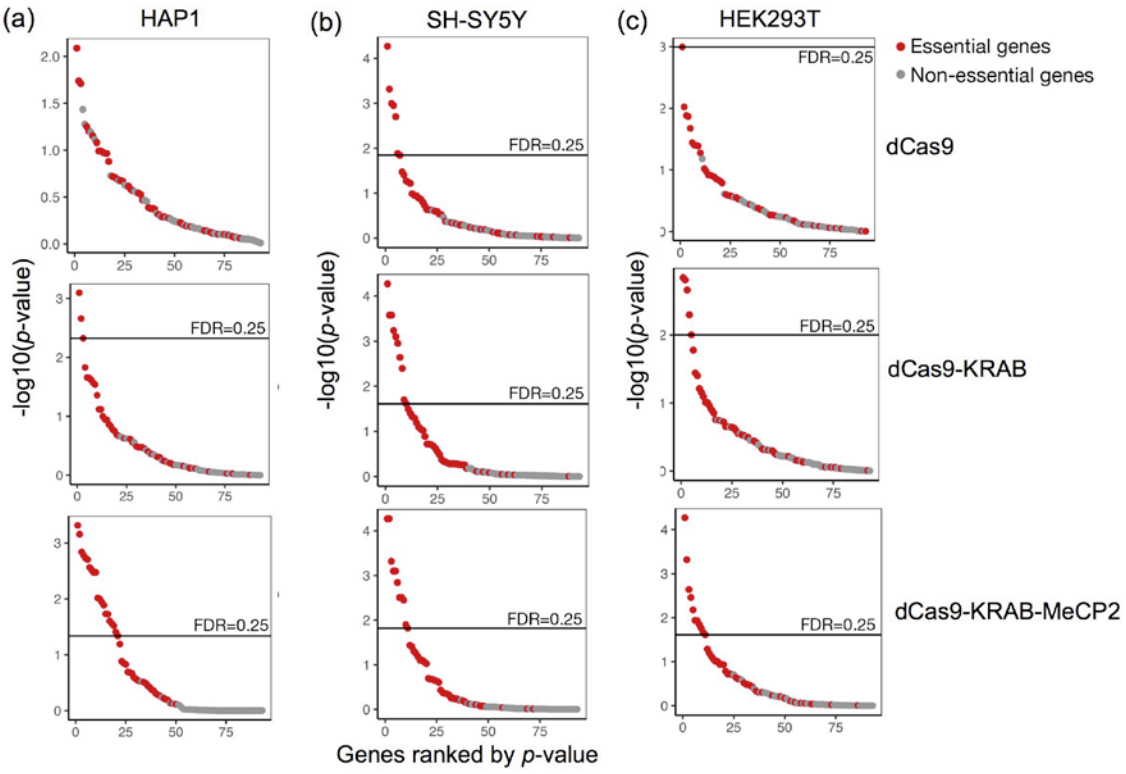

Supplementary Figure 13 Performance of different dCas9 repressors in pooled essentiality screens. Shown are rank-ordered genes identified from sgRNA enrichment analysis performed using MAGeCK analysis pipeline in (a) HAP1 (day 14), (b) SH-SY5Y (day 14), and (c) HEK293T (day 14) with the indicated repressors. Genes were plotted according to the *p*-values obtained from MAGeCK and marked the FDR threshold at 0.25 (25%). The genes are colored by essentiality (red indicates essential genes and gray indicates non-essential genes). The horizontal lines indicate the FDR threshold and where there is no line indicates no genes were identified at the given threshold.

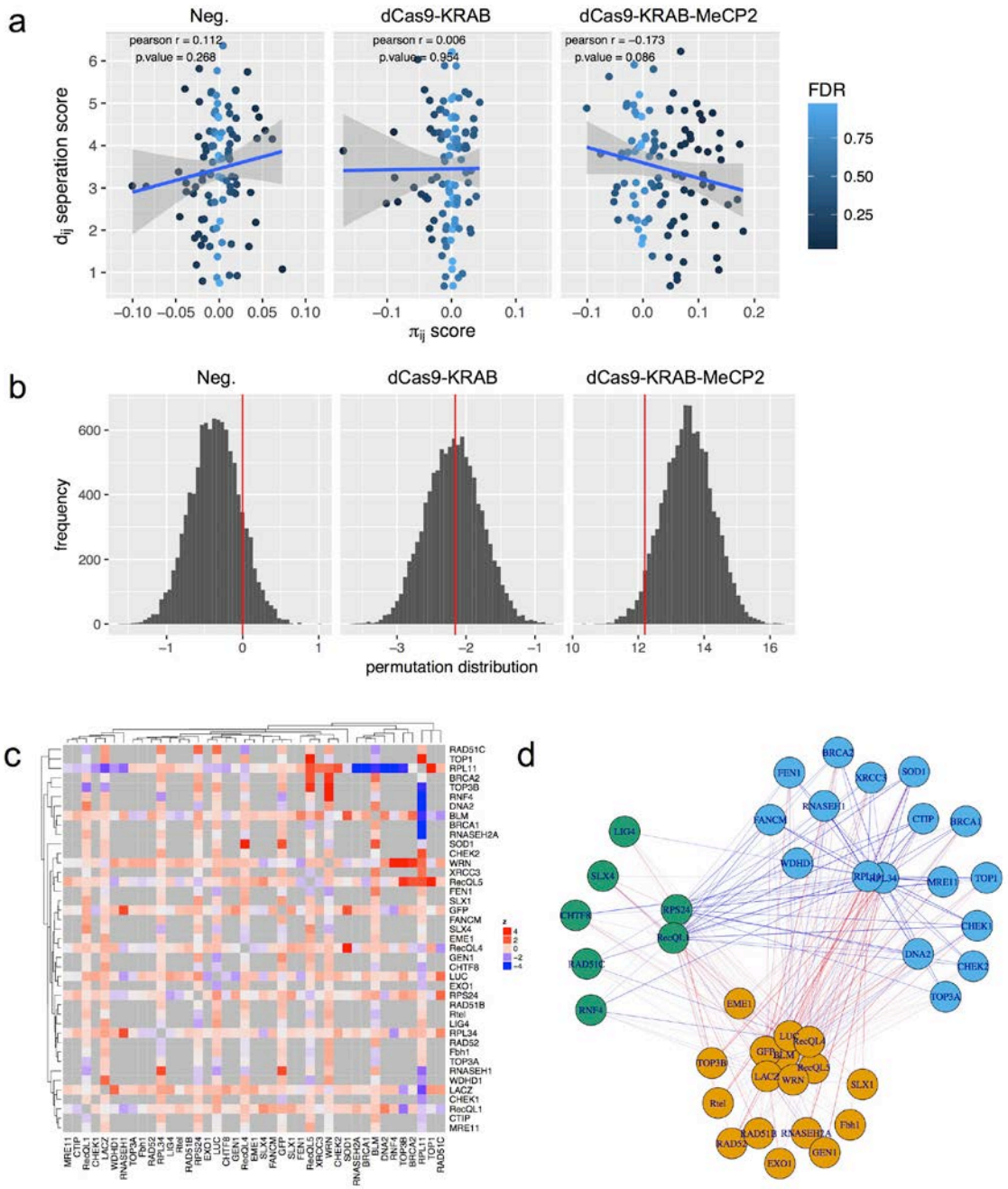
a
Neg.
dCas9-KRAB
dCas9-KRAB-MeCP2
pearson r = 0.112
p.value = 0.268
pearson r = 0.006
p.value = 0.954
pearson r = −0.173
p.value = 0.086
d_{ij} seperation score
π_{ij} score
FDR
0.75
0.50
0.25
b
Neg.
dCas9-KRAB
dCas9-KRAB-MeCP2
frequency
permutation distribution
c
d

Supplementary Figure 14 Genetic interactions captured through dCas9-KRAB-MeCP2. (a) Proteins that are in the same complex are expected to have positive genetic interactions, while pair of proteins in parallel pathways are expected to show a negative genetic interaction and be more distant from each other in a protein complex network. The negative control (Neg.) and dCas9-KRAB samples failed to capture this expected behavior, and their pi-scores (quantifying genetic interactions) were smaller in general. However, the dCas9-KRAB-MeCP2 samples demonstrated a wider range of pi-scores, and these were moderately consistent with the expected behavior. Specifically, gene pairs that were more closely connected in the protein complex network tended to show more positive genetic interactions. (b) A permutation test was used to assess the significance of this correlation. Specifically, the genetic interaction scores and protein complex network distances were multiplied for each gene pair, and then all such scores were summed across all genetic interactions. This was repeated 10000 times after randomizing the gene identifiers. Only the dCas9-KRAB-MeCP2 showed a significant trend. (permutation *p*-value: 0.8654, 0.53, and 0.041 for Neg., dCas9-KRAB, and dCas9-KRAB-MeCP2, respectively) (c) The hierarchical clustered heatmap of genetic interactions for negative control (wild-type HAP1 without repressor). (d) Resulting network diagram derived from dCas9-KRAB-MeCP2 screening data.

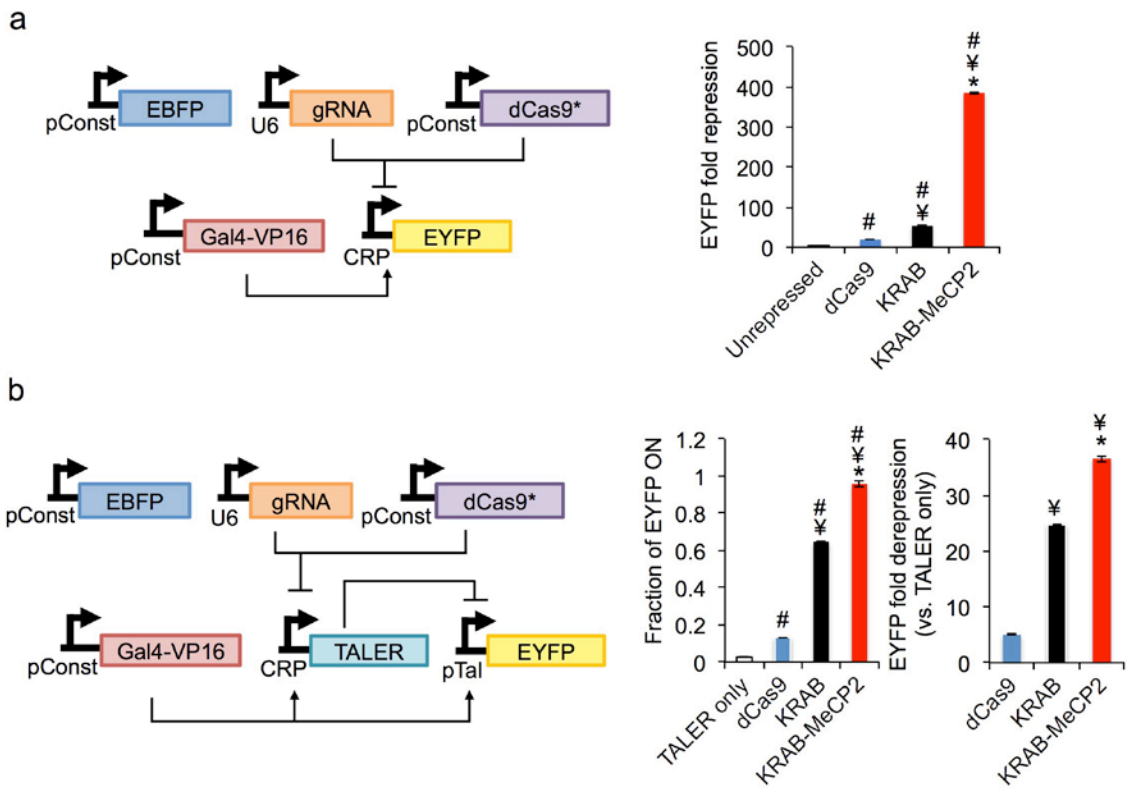

Supplementary Figure 15 Superiority of dCas9-Krab-MeCP2 in regulating synthetic circuits. (a) When paired with dCas9-KRAB-MeCP2, gRNA expressed from a U6 promoter shows improved repression of EYFP over those paired with dCas9 or dCas9-KRAB. (b) In a two-tier repressor cascade comprised of a gRNA repressing a TALER which in turn inhibits EYFP expression, dCas9-KRAB-MeCP2 improves the transfer of information. While dCas9 and dCas9-KRAB repressors propagate some of the signal through the circuit, dCas9-KRAB-MeCP2 increases signal fidelity, making the full circuit indistinguishable from an unrepressed EYFP. For a-b, n=4 biologically independent samples (cell cultures). Data are shown as mean ± s.e.m. One-sided Student T-test was used to perform statistical comparison. # $p < 0.05$ vs. unrepressed or TALER only control, ¥ $p < 0.05$ v.s. dCas9, and * $p < 0.05$ v.s. dCas9-KRAB.

Supplementary Table 1 Sequences of dCas9-Krab and dCas9-KRAB-MeCP2

>dCas9-KRAB

Labels: dCas9; SV40 nucleus localization signal (NLS); KRAB; glycine serine-rich linker (bold); stop codon (italic)

ATGGACAAGAAGTACTCCATTGGGCTCGCTATCGGCACAAACAGCGTCGGCTGGGCCGTCA
TTACGGACGAGTACAAGGTGCCGAGCAAAAAATTCAAAGTTCTGGGCAATACCGATCGCCA
CAGCATAAAGAAGAACCTCATTGGCGCCCTCCTGTTCGACTCCGGGGAGACGGCCGAAGC
CACGCGGCTCAAAAGAACAGCACGGCGCAGATATACCCGCAGAAAGAATCGGATCTGCTAC
CTGCAGGAGATCTTTAGTAATGAGATGGCTAAGGTGGATGACTCTTTCTTCCATAGGCTGGA
GGAGTCCTTTTTGGTGGAGGAGGATAAAAAGCACGAGCGCCACCCAATCTTTGGCAATATC
GTGGACGAGGTGGCGTACCATGAAAAGTACCCAACCATATATCATCTGAGGAAGAAGCTTG
TAGACAGTACTGATAAGGCTGACTTGCGGTTGATCTATCTCGCGCTGGCGCATATGATCAAA
TTTCGGGGACACTTCCTCATCGAGGGGGACCTGAACCCAGACAACAGCGATGTCGAtAAACT
CTTTATCCAACTGGTTCAGACTTACAATCAGCTTTTCGAAGAGAACCCGATCAACGCATCCG
GAGTTGACGCCAAAGCAATCCTGAGCGCTAGGCTGTCCAAATCCCGGCGGCTCGAAAACCT
CATCGCACAGCTCCCTGGGGAGAAGAAGAACGGCCTGTTTGGTAATCTTATCGCCCTGTCA
CTCGGGCTGACCCCCAACTTTAAATCTAACTTCGACCTGGCCGAAGATGCCAAGCTTCAACT
GAGCAAAGACACCTACGATGATGATCTCGACAATCTGCTGGCCCAGATCGGCGACCAGTAC
GCAGACCTTTTTTTGGCGGCAAAGAACCTGTCAGACGCCATTCTGCTGAGTGATATTCTGCG
AGTGAACACGGAGATCACCAAAGCTCCGCTGAGCGCTAGTATGATCAAGCGCTATGATGAG
CACCACCAAGACTTGACTTTGCTGAAGGCCCTTGTCAGACAGCAACTGCCTGAGAAGTACAA
GGAAATTTTCTTCGATCAGTCTAAAAATGGCTACGCCGGATACATTGACGGCGGAGCAAGCC
AGGAGGAATTTTACAAATTTATTAAGCCCATCTTGGAAAAAATGGACGGCACCGAGGAGCTG
CTGGTAAAGCTTAACAGAGAAGATCTGTTGCGCAAACAGCGCACTTTCGACAATGGAAGCAT
CCCCCACCAGATTCACCTGGGCGAACTGCACGCTATCCTCAGGCGGCAAGAGGATTTCTAC
CCCTTTTTGAAAGATAACAGGGAAAAGATTGAGAAAATCCTCACATTTCGGATACCCTACTAT
GTAGGCCCCCTCGCCCGGGGAAATTCCAGATTCGCGTGGATGACTCGCAAATCAGAAGAGA
CCATCACTCCCTGGAACTTCGAGGAAGTCGTGGATAAGGGGGCCTCTGCCCAGTCCTTCAT
CGAAAGGATGACTAACTTTGATAAAAATCTGCCTAACGAAAAGGTGCTTCCTAAACACTCTCT
GCTGTACGAGTACTTCACAGTTTATAACGAGCTCACCAAGGTCAAATACGTCACAGAAGGGA
TGAGAAAGCCAGCATTCCTGTCTGGAGAGCAGAAGAAAGCTATCGTGGACCTCCTCTTCAA
GACGAACCGGAAAGTTACCGTGAAACAGCTCAAAGAAGACTATTTCAAAAAGATTGAATGTT
TCGACTCTGTTGAAATCAGCGGAGTGGAGGATCGCTTCAACGCATCCCTGGGAACGTATCA
CGATCTCCTGAAAATCATTAAAGACAAGGACTTCCTGGACAATGAGGAGAACGAGGACATTC
TTGAGGACATTGTCCTCACCCTTACGTTGTTTGAAGATAGGGAGATGATTGAAGAACGCTTG
AAAACTTACGCTCATCTCTTCGACGACAAAGTCATGAAACAGCTCAAGAGGCGCCGATATAC
AGGATGGGGGCGGCTGTCAAGAAAACTGATCAATGGGATCCGAGACAAGCAGAGTGGAAA
GACAATCCTGGATTTTCTTAAGTCCGATGGATTTGCCAACCGGAACTTCATGCAGTTGATCC
ATGATGACTCTCTCACCTTTAAGGAGGACATCCAGAAAGCACAAGTTTCTGGCCAGGGGGA
CAGTCTTCACGAGCACATCGCTAATCTTGCAGGTAGCCCAGCTATCAAAAAGGGAATACTGC
AGACCGTTAAGGTCGTGGATGAACTCGTCAAAGTAATGGGAAGGCATAAGCCCGAGAATAT
CGTTATCGAGATGGCCCGAGAGAACCAAACTACCCAGAAGGGACAGAAGAACAGTAGGGAA
AGGATGAAGAGGATTGAAGAGGGTATAAAAGAACTGGGGTCCCAAATCCTTAAGGAACACC
CAGTTGAAAACACCCAGCTTCAGAATGAGAAGCTCTACCTGTACTACCTGCAGAACGGCAG
GGACATGTACGTGGATCAGGAACTGGACATCAATCGGCTCTCCGACTACGACGTGGCTGCT
ATCGTGCCCCAGTCTTTTCTCAAAGATGATTCTATTGATAATAAAGTGTTGACAAGATCCGAT
AAAgcTAGAGGGAAGAGTGATAACGTCCCCTCAGAAGAAGTTGTCAAGAAAATGAAAAATTAT
TGGCGGCAGCTGCTGAACGCCAAACTGATCACACAACGGAAGTTCGATAATCTGACTAAGG
CTGAACGAGGTGGCCTGTCTGAGTTGGATAAAGCCGGCTTCATCAAAAGGCAGCTTGTTGA
GACACGCCAGATCACCAAGCACGTGGCCCAAATTCTCGATTCACGCATGAACACCAAGTAC
GATGAAAATGACAAACTGATTCGAGAGGTGAAAGTTATTACTCTGAAGTCTAAGCTGGTCTC
AGATTTCAGAAAGGACTTTCAGTTTTATAAGGTGAGAGAGATCAACAATTACCACCATGCGC
ATGATGCCTACCTGAATGCAGTGGTAGGCACTGCACTTATCAAAAAATATCCCAAGCTTGAA

TCTGAATTTGTTTACGGAGACTATAAAGTGTACGATGTTAGGAAAATGATCGCAAAGTCTGAG
CAGGAAATAGGCAAGGCCACCGCTAAGTACTTCTTTTACAGCAATATTATGAATTTTTTCAAG
ACCGAGATTACACTGGCCAATGGAGAGATTCGGAAGCGACCACTTATCGAAACAAACGGAG
AAACAGGAGAAATCGTGTGGGACAAGGGTAGGGATTTCGCGACAGTCCGGAAGGTCCTGTC
CATGCCGCAGGTGAACATCGTTAAAAAGACCGAAGTACAGACCGGAGGCTTCTCCAAGGAA
AGTATCCTCCCGAAAAGGAACAGCGACAAGCTGATCGCACGCAAAAAAGATTGGGACCCCA
AGAAATACGGCGGATTCGATTCTCCTACAGTCGCTTACAGTGTACTGGTTGTGGCCAAAGTG
GAGAAAGGGAAGTCTAAAAAACTCAAAAGCGTCAAGGAACTGCTGGGCATCACAATCATGG
AGCGATCAAGCTTCGAAAAAAACCCCATCGACTTTCTCGAGGCGAAAGGATATAAAGAGGTC
AAAAAAGACCTCATCATTAAGCTTCCCAAGTACTCTCTCTTTGAGCTTGAAAACGGCCGGAA
ACGAATGCTCGCTAGTGCGGGCGAGCTGCAGAAAGGTAACGAGCTGGCACTGCCCTCTAAA
TACGTTAATTTCTTGTATCTGGCCAGCCACTATGAAAAGCTCAAAGGGTCTCCCGAAGATAAT
GAGCAGAAGCAGCTGTTCGTGGAACAACACAAACACTACCTTGATGAGATCATCGAGCAAAT
AAGCGAATTCTCCAAAAGAGTGATCCTCGCCGACGCTAACCTCGATAAGGTGCTTTCTGCTT
ACAATAAGCACAGGGATAAGCCCATCAGGGAGCAGGCAGAAAACATTATCCACTTGTTTACT
CTGACCAACTTGGGCGCGCCTGCAGCCTTCAAGTACTTCGACACCACCATAGACAGAAAGC
GGTACACCTCTACAAAGGAGGTCCTGGACGCCACACTGATTCATCAGTCAATTACGGGGCT
CTATGAAACAAGAATCGACCTCTCTCAGCTCGGTGGAGACAGCAGGGCTGACCCCAAGAAG
AAGAGGAAGGTG**AGTGGTGGAGGAAGTGGCGGGTCAGGGTCG**ATGGACGCGAAATCACTT
ACGGCATGGTCGAGAACACTGGTTACGTTCAAGGACGTGTTTGTGGACTTTACACGTGAGG
AGTGGAAATTGCTGGATACTGCGCAACAAATTGTGTATCGAAATGTCATGCTTGAGAATTAC
AAGAACCTCGTCAGTCTCGGATACCAGTTGACGAAACCGGATGTGATCCTTAGGCTCGAAAA
GGGGGAAGAACCTTGGCTGGTA*TAG*

>dCas9-KRAB-MeCP2

Labels: dCas9; SV40 nucleus localization signal (NLS); KRAB; TRD domain of MeCP2; glycine serine-rich linker (bold); stop codon (italic)

ATGGACAAGAAGTACTCCATTGGGCTCGCTATCGGCACAAACAGCGTCGGCTGGGCCGTCA
TTACGGACGAGTACAAGGTGCCGAGCAAAAAATTCAAAGTTCTGGGCAATACCGATCGCCA
CAGCATAAAGAAGAACCTCATTGGCGCCCTCCTGTTCGACTCCGGGGAGACGGCCGAAGC
CACGCGGCTCAAAAGAACAGCACGGCGCAGATATACCCGCAGAAAGAATCGGATCTGCTAC
CTGCAGGAGATCTTTAGTAATGAGATGGCTAAGGTGGATGACTCTTTCTTCCATAGGCTGGA
GGAGTCCTTTTTGGTGGAGGAGGATAAAAAGCACGAGCGCCACCCAATCTTTGGCAATATC
GTGGACGAGGTGGCGTACCATGAAAAGTACCCAACCATATATCATCTGAGGAAGAAGCTTG
TAGACAGTACTGATAAGGCTGACTTGCGGTTGATCTATCTCGCGCTGGCGCATATGATCAAA
TTTCGGGGACACTTCCTCATCGAGGGGGACCTGAACCCAGACAACAGCGATGTCGAtAAACT
CTTTATCCAACTGGTTCAGACTTACAATCAGCTTTTCGAAGAGAACCCGATCAACGCATCCG
GAGTTGACGCCAAAGCAATCCTGAGCGCTAGGCTGTCCAAATCCCGGCGGCTCGAAAACCT
CATCGCACAGCTCCCTGGGGAGAAGAAGAACGGCCTGTTTGGTAATCTTATCGCCCTGTCA
CTCGGGCTGACCCCCAACTTTAAATCTAACTTCGACCTGGCCGAAGATGCCAAGCTTCAACT
GAGCAAAGACACCTACGATGATGATCTCGACAATCTGCTGGCCCAGATCGGCGACCAGTAC
GCAGACCTTTTTTTGGCGGCAAAGAACCTGTCAGACGCCATTCTGCTGAGTGATATTCTGCG
AGTGAACACGGAGATCACCAAAGCTCCGCTGAGCGCTAGTATGATCAAGCGCTATGATGAG
CACCACCAAGACTTGACTTTGCTGAAGGCCCTTGTCAGACAGCAACTGCCTGAGAAGTACAA
GGAAATTTTCTTCGATCAGTCTAAAAATGGCTACGCCGGATACATTGACGGCGGAGCAAGCC
AGGAGGAATTTTACAAATTTATTAAGCCCATCTTGGAAAAAATGGACGGCACCGAGGAGCTG
CTGGTAAAGCTTAACAGAGAAGATCTGTTGCGCAAACAGCGCACTTTCGACAATGGAAGCAT
CCCCCACCAGATTCACCTGGGCGAACTGCACGCTATCCTCAGGCGGCAAGAGGATTTCTAC
CCCTTTTTGAAAGATAACAGGGAAAAGATTGAGAAAATCCTCACATTTCGGATACCCTACTAT
GTAGGCCCCCTCGCCCGGGGAAATTCCAGATTCGCGTGGATGACTCGCAAATCAGAAGAGA

CCATCACTCCCTGGAACTTCGAGGAAGTCGTGGATAAGGGGGCCTCTGCCCAGTCCTTCAT
CGAAAGGATGACTAACTTTGATAAAAATCTGCCTAACGAAAAGGTGCTTCCTAAACACTCTCT
GCTGTACGAGTACTTCACAGTTTATAACGAGCTCACCAAGGTCAAATACGTCACAGAAGGGA
TGAGAAAGCCAGCATTCCTGTCTGGAGAGCAGAAGAAAGCTATCGTGGACCTCCTCTTCAA
GACGAACCGGAAAGTTACCGTGAAACAGCTCAAAGAAGACTATTTCAAAAAGATTGAATGTT
TCGACTCTGTTGAAATCAGCGGAGTGGAGGATCGCTTCAACGCATCCCTGGGAACGTATCA
CGATCTCCTGAAAATCATTAAAGACAAGGACTTCCTGGACAATGAGGAGAACGAGGACATTC
TTGAGGACATTGTCCTCACCCTTACGTTGTTTGAAGATAGGGAGATGATTGAAGAACGCTTG
AAAACTTACGCTCATCTCTTCGACGACAAAGTCATGAAACAGCTCAAGAGGCGCCGATATAC
AGGATGGGGGCGGCTGTCAAGAAAACTGATCAATGGGATCCGAGACAAGCAGAGTGGAAA
GACAATCCTGGATTTTCTTAAGTCCGATGGATTTGCCAACCGGAACTTCATGCAGTTGATCC
ATGATGACTCTCTCACCTTTAAGGAGGACATCCAGAAAGCACAAGTTTCTGGCCAGGGGGA
CAGTCTTCACGAGCACATCGCTAATCTTGCAGGTAGCCCAGCTATCAAAAAGGGAATACTGC
AGACCGTTAAGGTCGTGGATGAACTCGTCAAAGTAATGGGAAGGCATAAGCCCGAGAATAT
CGTTATCGAGATGGCCCGAGAGAACCAAACTACCCAGAAGGGACAGAAGAACAGTAGGGAA
AGGATGAAGAGGATTGAAGAGGGTATAAAAGAACTGGGGTCCCAAATCCTTAAGGAACACC
CAGTTGAAAACACCCAGCTTCAGAATGAGAAGCTCTACCTGTACTACCTGCAGAACGGCAG
GGACATGTACGTGGATCAGGAACTGGACATCAATCGGCTCTCCGACTACGACGTGGCTGCT
ATCGTGCCCCAGTCTTTTCTCAAAGATGATTCTATTGATAATAAAGTGTTGACAAGATCCGAT
AAAgcTAGAGGGAAGAGTGATAACGTCCCCTCAGAAGAAGTTGTCAAGAAAATGAAAAATTAT
TGGCGGCAGCTGCTGAACGCCAAACTGATCACACAACGGAAGTTCGATAATCTGACTAAGG
CTGAACGAGGTGGCCTGTCTGAGTTGGATAAAGCCGGCTTCATCAAAAGGCAGCTTGTTGA
GACACGCCAGATCACCAAGCACGTGGCCCAAATTCTCGATTCACGCATGAACACCAAGTAC
GATGAAAATGACAAACTGATTCGAGAGGTGAAAGTTATTACTCTGAAGTCTAAGCTGGTCTC
AGATTTCAGAAAGGACTTTCAGTTTTATAAGGTGAGAGAGATCAACAATTACCACCATGCGC
ATGATGCCTACCTGAATGCAGTGGTAGGCACTGCACTTATCAAAAAATATCCCAAGCTTGAA
TCTGAATTTGTTTACGGAGACTATAAAGTGTACGATGTTAGGAAAATGATCGCAAAGTCTGAG
CAGGAAATAGGCAAGGCCACCGCTAAGTACTTCTTTTACAGCAATATTATGAATTTTTTCAAG
ACCGAGATTACACTGGCCAATGGAGAGATTCGGAAGCGACCACTTATCGAAACAAACGGAG
AAACAGGAGAAATCGTGTGGGACAAGGGTAGGGATTTCGCGACAGTCCGGAAGGTCCTGTC
CATGCCGCAGGTGAACATCGTTAAAAAGACCGAAGTACAGACCGGAGGCTTCTCCAAGGAA
AGTATCCTCCCGAAAAGGAACAGCGACAAGCTGATCGCACGCAAAAAAGATTGGGACCCCA
AGAAATACGGCGGATTCGATTCTCCTACAGTCGCTTACAGTGTACTGGTTGTGGCCAAAGTG
GAGAAAGGGAAGTCTAAAAAACTCAAAAGCGTCAAGGAACTGCTGGGCATCACAATCATGG
AGCGATCAAGCTTCGAAAAAAACCCCATCGACTTTCTCGAGGCGAAAGGATATAAAGAGGTC
AAAAAAGACCTCATCATTAAGCTTCCCAAGTACTCTCTCTTTGAGCTTGAAAACGGCCGGAA
ACGAATGCTCGCTAGTGCGGGCGAGCTGCAGAAAGGTAACGAGCTGGCACTGCCCTCTAAA
TACGTTAATTTCTTGTATCTGGCCAGCCACTATGAAAAGCTCAAAGGGTCTCCCGAAGATAAT
GAGCAGAAGCAGCTGTTCGTGGAACAACACAAACACTACCTTGATGAGATCATCGAGCAAAT
AAGCGAATTCTCCAAAAGAGTGATCCTCGCCGACGCTAACCTCGATAAGGTGCTTTCTGCTT
ACAATAAGCACAGGGATAAGCCCATCAGGGAGCAGGCAGAAAACATTATCCACTTGTTTACT
CTGACCAACTTGGGCGCGCCTGCAGCCTTCAAGTACTTCGACACCACCATAGACAGAAAGC
GGTACACCTCTACAAAGGAGGTCCTGGACGCCACACTGATTCATCAGTCAATTACGGGGCT
CTATGAAACAAGAATCGACCTCTCTCAGCTCGGTGGAGACAGCAGGGCTGACCCCAAGAAG
AAGAGGAAGGTGAGTGGTGGAGGAAGTGGCGGGTCAGGGTCGATGGACGCGAAATCACTT
ACGGCATGGTCGAGAACACTGGTTACGTTCAAGGACGTGTTTGTGGACTTTACACGTGAGG
AGTGGAAATTGCTGGATACTGCGCAACAAATTGTGTATCGAAATGTCATGCTTGAGAATTAC
AAGAACCTCGTCAGTCTCGGATACCAGTTGACGAAACCGGATGTGATCCTTAGGCTCGAAAA
GGGGGAAGAACCTTGGCTGGTATCGGGAGGTGGTTCGGGTGGCTCTGGATCAAGCCCAAA
GAAGAAACGGAAGGTGGAAGCCTCAGTGCAGGTGAAAAGGGTGCTGGAAAAATCCCCCGG
CAAACTCCTCGTGAAGATGCCCTTCCAGGCTTCCCCTGGCGGAAAAGGTGAAGGGGGTGG
CGCAACCACATCTGCCCAGGTCATGGTCATCAAGCGACCTGGAAGGAAAAGAAAGGCCGAG
GCTGACCCTCAGGCCATTCCAAAGAAACGGGGACGCAAGCCAGGGTCCGTGGTCGCAGCT
GCAGCAGCTGAGGCTAAGAAAAAGGCAGTGAAGGAAAGCTCCATCCGCAGTGTGCAGGAG
ACTGTCCTGCCCATCAAGAAGAGGAAGACTAGGGAGACCGTGTCCATCGAGGTCAAAGAAG
TGGTCAAGCCCCTGCTCGTGTCCACCCTGGGCGAAAAATCTGGAAAGGGGCTCAAAACATG

CAAGTCACCTGGACGGAAAAGCAAGGAGTCTAGTCCAAAGGGGCGCTCAAGCTCCGCTTCT
AGTCCCCCTAAAAAGGAACACCATCACCATCACCATCACGCCGAGTCTCCTAAGGCTCCTAT
GCCACTGCTCCCACCACCTCCACCACCTGAGCCACAGTCAAGCGAAGACCCCATCAGCCCA
CCCGAGCCTCAGGATCTGTCCTCTAGTATTTGCAAAGAGGAAAAGATGCCCAGAGCAGGCA
GCCTGGAGAGTGATGGCTGTCCAAAAGAACCCGCCAAGACCCAGCCTATGGTGGCAGCCG
CTGCAACTACCACCACAACCACAACTACCACAGTGGCCGAAAAATACAAGCATCGCGGCGA
GGGCGAACGAAAGGACATTGTGTCAAGCTCCATGCCCAGACCTAACCGGGAGGAACCAGT
CGATAGTAGGACACCCGTGACTGAGAGAGTCTCA*TAG*

Supplementary Table 2 A list of differentially expressed (DE) genes with log_2 FC above 1.5 threshold in RNA-seq experiment. (Note that all of these genes have positive log_2 FC, which corresponds to increased transcriptional activity).

dCas9				
	Log_2FC	**Log_2CPM**	**P-Value**	**FDR**
HSPA6[1]	6.57	8.3400	2.00E-25	2.74E-21
DNAJB1[1]	2.24	8.2800	6.09E-23	4.16E-19
HSPA7[1]	7.28	2.1290	9.68E-16	4.41E-12
HSPA1A[1]	4.69	2.7660	4.75E-13	1.62E-09
CRYAB[1]	6.55	2.0320	4.09E-12	1.12E-08
ANKRD1[2]	2.54	2.3950	4.02E-11	9.16E-08
ZFAND2A[1]	1.65	4.2370	3.74E-10	7.29E-07
ATF3[2]	1.11	6.0300	2.30E-07	3.93E-04
DNAH17[1]	1.74	3.5590	2.92E-07	4.44E-04
SCG2	4.11	0.1960	1.35E-05	1.75E-02
VGF[1]	2.33	1.9290	1.41E-05	1.75E-02
FOS[2]	1.41	2.9560	1.65E-05	1.88E-02
GDF15[1]	2.43	1.7580	2.68E-05	2.82E-02
dCas9-KRAB				
	Log_2FC	**Log_2CPM**	**P-Value**	**FDR**
HSPA6[1]	7.19	8.3398	2.26E-26	2.65E-22
DNAJB1[1]	2.62	8.2801	3.88E-26	2.65E-22
HSPA1A[1]	6.36	2.7657	8.82E-21	4.02E-17
HMOX1	2.07	5.5632	1.31E-20	4.48E-17
CRYAB[1]	8.14	2.0315	2.86E-18	7.82E-15
HSPA7[1]	7.82	2.1293	5.79E-18	1.32E-14
VGF[1]	4.6	1.9288	4.29E-16	8.37E-13
ZFAND2A[1]	2	4.2367	6.13E-14	1.05E-10
PPP1R15A[3]	1.47	5.3442	2.88E-12	4.36E-09
GDF15[1]	4.08	1.7576	6.69E-12	9.13E-09
DNAH17[1]	2.34	3.5595	2.04E-11	2.53E-08
CLU	1.49	4.588	6.38E-11	7.26E-08
SERPINH1	1.24	6.3749	1.08E-10	1.14E-07
FOXJ1[3]	6.5	0.4447	1.47E-10	1.43E-07
ANXA1	2.55	1.9991	1.02E-09	9.33E-07
FOS[2]	1.86	2.9564	3.62E-09	3.09E-06
NCRNA00306	3.6	0.6114	1.87E-08	1.50E-05
CSRNP1	1.32	4.5789	2.82E-08	2.14E-05
ANKRD1[2]	2	2.3946	1.28E-07	9.22E-05

ACHE	1.89	2.0935	2.28E-06	1.56E-03
SCG2	4.28	0.1963	4.42E-06	2.75E-03
ATF3[2]	1.02	6.0304	4.42E-06	2.75E-03
HLA-G	3.54	-0.0433	5.02E-06	2.98E-03
INPP5D[3]	2.93	0.983	5.69E-06	3.24E-03
RELB	1.56	2.6216	6.66E-06	3.64E-03
PNLDC1	3.2	0.0906	8.19E-06	4.15E-03
CYP4F3	7.12	-0.4274	8.21E-06	4.15E-03
MMP12	4.58	-0.6846	9.52E-06	4.64E-03
TUBB3	1.15	3.9455	1.39E-05	6.53E-03
PLK2	1.23	3.6057	1.52E-05	6.92E-03
IRX4	2.55	0.425	2.43E-05	1.07E-02
DUSP8	1.22	3.6476	3.69E-05	1.57E-02
FERMT3	2.22	0.6882	5.66E-05	2.34E-02
ACRC	1.63	1.6191	7.17E-05	2.88E-02
IL11	1.92	0.9971	9.89E-05	3.86E-02
dCas9-KRAB-MeCP2				
	Log_2FC	**Log_2CPM**	**P-Value**	**FDR**
HSPA6[1]	6.7	8.34	1.27E-25	1.73E-21
DNAJB1[1]	2.24	8.28	6.26E-23	4.28E-19
HSPA1A[1]	5.8	2.766	4.26E-18	1.94E-14
HSPA7[1]	6.99	2.129	2.26E-14	7.71E-11
CRYAB[1]	6.59	2.032	4.73E-12	1.29E-08
DNAH17[1]	2.43	3.559	8.96E-12	2.04E-08
INPP5D[3]	3.96	0.983	1.65E-09	3.23E-06
GDF15[1]	3.29	1.758	2.00E-08	3.41E-05
CYP4F3	7.81	-0.427	3.40E-07	5.16E-04
FOXJ1[3]	5.41	0.445	4.53E-07	6.19E-04
ZFAND2A[1]	1.33	4.237	1.24E-06	1.54E-03
PPP1R15A[3]	1.09	5.344	1.46E-06	1.66E-03
VGF[1]	2.55	1.929	2.43E-06	2.56E-03
NCRNA00306	2.75	0.611	2.56E-05	2.50E-02
DUSP8[3]	1.23	3.648	3.32E-05	2.92E-02
PLA2G4C	1.89	1.495	3.55E-05	2.92E-02
ANXA1	1.76	1.999	3.64E-05	2.92E-02

Note: [1] indicates genes common to all three repressor groups, [2] indicates common genes between dCas9 and dCas9-KRAB, and [3] indicates common genes between dCas9-KRAB and dCas9-KRAB-MeCP2. FC = fold-change, CPM = counts per million, FDR = false discovery rate. n=2 biologically independent samples. For DE analyses, see **Supplementary Note 2**.

Supplementary Table 3. A list of down-regulated genes identified in RNA-seq experiment. Note that all of these genes have log_2 FC below 1.5 threshold.

dCas9-KRAB				
	Log_2FC	**Log_2CPM**	**P-Value**	**FDR**
EIF5B[1]	-0.59	5.4743	6.88E-07	2.54E-04
TMEM44	-1.329	2.2374	5.03E-06	1.37E-03
HNRNPA2B1[1]	-0.463	8.6101	1.72E-05	3.86E-03
HNRNPD	-0.451	5.9149	2.69E-05	5.74E-03
HIST1H2AE	-0.822	3.4547	4.20E-05	8.44E-03
TAF15	-0.497	4.9187	1.88E-04	3.02E-02
NFXL1	-0.444	5.0202	2.40E-04	3.62E-02
ODZ3	-0.452	4.8766	2.44E-04	3.62E-02
dCas9-KRAB-MeCP2				
	Log_2FC	**Log_2CPM**	**P-Value**	**FDR**
EIF5B[1]	-0.63	5.474	2.87E-07	1.87E-04
HNRNPA2B1[1]	-0.427	8.61	5.75E-05	1.96E-02
LRRFIP1	-0.398	5.767	1.54E-04	4.34E-02
PRPF19	-0.359	6.983	1.55E-04	4.34E-02
RNU6ATAC	-0.662	3.595	1.67E-04	4.36E-02

Note: [1] indicates genes down-regulated in both dCas9-KRAB and dCas9-KRAB-MeCP2 groups. None of the down-regulated genes showed a near sequence match to the *CXCR4* targeting sgRNA. No downregulated genes were observed in the dCas9 group. FC = fold-change, CPM = counts per million, FDR = false discovery rate. n=2 biologically independent samples. For DE analyses, see **Supplementary Note 2**.

Supplementary Table 4 Mean fold changes of all essential gene-targeting sgRNAs and *p*-values for statistical comparison between essential and non-essential guides in HAP1 lethality screen.

Experiment	Mean essential guides log_2 OR	P-value[#]
dCas9_day0	-0.008	0.1329
dCas9_day7	0.001	0.669
dCas9_day14	-0.001	0.6289
dCas9-KRAB_day0	-0.015	0.005708
dCas9-KRAB _day7	-0.056	1.83E-07
dCas9-KRAB _day14	-0.081	5.41E-19
dCas9-KRAB-MeCP2_day0	0.031	0.9996
dCas9-KRAB-MeCP2_day7*	-2.358	4.87E-78
dCas9-KRAB-MeCP2_day14**	-2.586	3.52E-80

[#] p-value is derived from one-tailed Welch T-test comparing the log_2 OR of the essential guides versus the log_2 OR of the non-essential guides. See **Supplementary Note 3** for detailed analysis and statistical test.

* Log_2 Odds-ratio (log_2 OR) that was -Infinity, i.e. complete depletion, were replaced by the least finite OR for day 7, i.e. -7.607176

** log_2 Odds-ratio (log_2 OR) that were -Infinity, i.e. complete depletion, were replaced by the least finite OR for day 14, i.e. -8.867043

Supplementary Table 5 Mean fold changes of all essential gene-targeting sgRNAs and *p*-values for statistical comparison between essential and non-essential guides in SH-SY5Y lethality screen.

Experiment	mean essential guides log2 OR	P-value[#]
dCas9_day0	-0.0517	0.0009321
dCas9_day7	-0.10179	9.92E-16
dCas9_day14	-0.12011	3.76E-20
dCas9_day22	-0.149066	1.31E-23
dCas9-KRAB_day0	-0.1341297	3.79E-22
dCas9-KRAB _day7	-0.3476919	4.72E-37
dCas9-KRAB _day14	-0.3733395	2.16E-44
dCas9-KRAB _day22	-0.386887	2.24E-52
dCas9-KRAB-MeCP2_day0	-0.1937839	5.27E-26
dCas9-KRAB-MeCP2_day7	-0.4740388	2.55E-55
dCas9-KRAB-MeCP2_day14	-0.3774654	1.19E-63
dCas9-KRAB-MeCP2_day22	-0.525382	3.08E-70

[#] p-value is derived from one-tailed Welch T-test comparing the $\log_2$ OR of the essential guides versus the $\log_2$ OR of the non-essential guides. See **Supplementary Note 3** for detailed analysis and statistical test.

Supplementary Table 6 Mean fold changes of all essential gene-targeting sgRNAs and *p*-values for statistical comparison between essential and non-essential guides in HEK293T lethality screen.

Experiment	mean essential guides log2 OR	P-value[#]
dCas9_day0	0.003201572	0.12
dCas9_day7	-0.03381157	1.18E-06
dCas9_day14	-0.05741197	2.43E-08
dCas9-KRAB_day0	-0.07741853	0.02
dCas9-KRAB _day7	-0.06196394	1.53E-14
dCas9-KRAB _day14	-0.007220968	4.15E-15
dCas9-KRAB-MeCP2_day0	-0.03050618	2.34E-06
dCas9-KRAB-MeCP2_day7	-0.120637	7.67E-38
dCas9-KRAB-MeCP2_day14	-0.1226212	4.63E-34

[#] p-value is derived from one-tailed Welch T-test comparing the $\log_2$ OR of the essential guides versus the $\log_2$ OR of the non-essential guides. See **Supplementary Note 3** for detailed analysis and statistical test.

Supplementary Table 7. Shown is the total number of sgRNAs showing depletion within or outside of the optimal targeting window previously defined for repression. Data was based on our pooled essentiality screens where 370 essential gene-targeting sgRNAs were tested.

a. Summary of depleted sgRNAs in HAP1 cells at day 14

Targeting window	Total number of essential sgRNAs	Number of significantly depleted sgRNAs with dCas9	Number of significantly depleted sgRNAs with dCas9-KRAB	Number of significantly depleted sgRNAs with dCas9-KRAB-MeCP2
Within -50 to +200bp from TSS	213	35	94	181
Outside -50 to +200bp from TSS	144	19	47	113

b. Summary of depleted sgRNAs in SH-SY5Y cells at day 22

Targeting window	Total number of essential sgRNAs	Number of significantly depleted sgRNAs with dCas9	Number of significantly depleted sgRNAs with dCas9-KRAB	Number of significantly depleted sgRNAs with dCas9-KRAB-MeCP2
Within -50 to +200bp from TSS	213	75	117	149
Outside -50 to +200bp from TSS	144	27	58	77

c. Summary of depleted sgRNAs in 293T cells at day 14

Targeting window	Total number of essential sgRNAs	Number of significantly depleted sgRNAs with dCas9	Number of significantly depleted sgRNAs with dCas9-KRAB	Number of significantly depleted sgRNAs with dCas9-KRAB-MeCP2
Within -50 to +200bp from TSS	213	50	64	84
Outside -50 to +200bp from TSS	144	26	29	49

Supplementary Table 8 Sequence of oligos used to construct dual guide RNA library

Target genes	Sequence of oligos used for cloning	Note
BLM	[TTTTCGTCTCTCACCG] AGGAAACGGAAGAACCCGAG [gttttagagctatgctgaaaagca]	first spacer BLM_1
WRN	[TTTTCGTCTCTCACCG] CCGGCTTGTACTCGGCAGCG [gttttagagctatgctgaaaagca]	first spacer WRN_1
RECQL1	[TTTTCGTCTCTCACCG] GCTGAACGGACCGACCCGGA [gttttagagctatgctgaaaagca]	first spacer RecQL1_1
RECQL4	[TTTTCGTCTCTCACCG] TCGCTGGACGATCGCAAGCG [gttttagagctatgctgaaaagca]	first spacer RecQL4_1
RECQL5	[TTTTCGTCTCTCACCG] CGACGGATATAAGATTGCGT [gttttagagctatgctgaaaagca]	first spacer RecQL5_1
BLM	[TTTTCGTCTCTCACCG] CCTCGCACGCAGACTCCTAG [gttttagagctatgctgaaaagca]	first spacer BLM_2
WRN	[TTTTCGTCTCTCACCG] CTAGCACTATAGATACCCCG [gttttagagctatgctgaaaagca]	first spacer WRN_2
RECQL1	[TTTTCGTCTCTCACCG] GAGATCGGAGAGTCGGACAC [gttttagagctatgctgaaaagca]	first spacer RecQL1_2
RECQL4	[TTTTCGTCTCTCACCG] TGGAGCGGCTGCGGGACGTG [gttttagagctatgctgaaaagca]	first spacer RecQL4_2
RECQL5	[TTTTCGTCTCTCACCG] TGAGTTGGGGTTGTGTATAG [gttttagagctatgctgaaaagca]	first spacer RecQL5_2
BLM	[TTTTCGTCTCTCACCG] CCGCTAGGAGTCTGCGTGCG [gttttagagctatgctgaaaagca]	first spacer BLM_3
WRN	[TTTTCGTCTCTCACCG] GATGTGTACTGTGTGCGCCG [gttttagagctatgctgaaaagca]	first spacer WRN_3
RECQL1	[TTTTCGTCTCTCACCG] AAGATTTTACTCCCGAGTAG [gttttagagctatgctgaaaagca]	first spacer RecQL1_3
RECQL4	[TTTTCGTCTCTCACCG] CTGGACGATCGCAAGCGCGG [gttttagagctatgctgaaaagca]	first spacer RecQL4_3
RECQL5	[TTTTCGTCTCTCACCG] TTTAATTCTTGGGCGGACCA [gttttagagctatgctgaaaagca]	first spacer RecQL5_3
GFP	[TTTTCGTCTCTCACCG] CAAGTTCAGCGTGTCCGGCG [gttttagagctatgctgaaaagca]	first spacer GFP_1
LACZ	[TTTTCGTCTCTCACCG] AGGTAGCAGAGCGGGTAAAC	first spacer LACZ_1

	[gttttagagctatgctgaaaagca]	
LUC	[TTTTCGTCTCTCACCG] AACGCCTTGATTGACAAGGA [gttttagagctatgctgaaaagca]	first spacer LUC_1
RPL34 (ESSENTIAL GENE)	[TTTTCGTCTCTCACCG] TGGTGAGCTGTGGCTACTCA [gttttagagctatgctgaaaagca]	first spacer RPL34_1
RPL11 (ESSENTIAL GENE)	[TTTTCGTCTCTCACCG] TCTCTTCCTGCTCTCCATCA [gttttagagctatgctgaaaagca]	first spacer RPL11_1
RPS24 (ESSENTIAL GENE)	[TTTTCGTCTCTCACCG] CCATCATGGTGAGTCTCCCT [gttttagagctatgctgaaaagca]	first spacer RPS24_1
GFP	[TTTTCGTCTCTCACCG] CAGCTCGATGCGGTTCACCA [gttttagagctatgctgaaaagca]	first spacer GFP_2
LACZ	[TTTTCGTCTCTCACCG] TTTGTGGACGAAGTACCGAA [gttttagagctatgctgaaaagca]	first spacer LACZ_2
LUC	[TTTTCGTCTCTCACCG] ACAACTTTACCGACCGCGCC [gttttagagctatgctgaaaagca]	first spacer LUC_2
RPL34 (ESSENTIAL GENE)	[TTTTCGTCTCTCACCG] CTCCTCGGATGGCAGCCGAT [gttttagagctatgctgaaaagca]	first spacer RPL34_2
RPL11 (ESSENTIAL GENE)	[TTTTCGTCTCTCACCG] CCAGCTACTCACCGCCATGA [gttttagagctatgctgaaaagca]	first spacer RPL11_2
RPS24 (ESSENTIAL GENE)	[TTTTCGTCTCTCACCG] TCCGTGCGCGTTGATATGAT [gttttagagctatgctgaaaagca]	first spacer RPS24_2
GFP	[TTTTCGTCTCTCACCG] CATGCCGAGAGTGATCCCGG [gttttagagctatgctgaaaagca]	first spacer GFP_3
LACZ	[TTTTCGTCTCTCACCG] AGGGCGGCTTCGTCTGGGAC [gttttagagctatgctgaaaagca]	first spacer LACZ_3
LUC	[TTTTCGTCTCTCACCG] AGCTATTCTGATTACACCCG [gttttagagctatgctgaaaagca]	first spacer LUC_3
RPL34 (ESSENTIAL GENE)	[TTTTCGTCTCTCACCG] GAATGCAGCAAAGTCCCGGG [gttttagagctatgctgaaaagca]	first spacer RPL34_3
RPL11 (ESSENTIAL GENE)	[TTTTCGTCTCTCACCG] CGGCCTGCCATGGATGGCGA [gttttagagctatgctgaaaagca]	first spacer RPL11_3
RPS24 (ESSENTIAL GENE)	[TTTTCGTCTCTCACCG] CCGCGTATCCGAGCCATCCG [gttttagagctatgctgaaaagca]	first spacer RPS24_3
BLM	[TTTTCGTCTCTAAAC] CTCGGGTTCTTCCGTTTCCT[cggtgACCCAGGCGGCGCACAAG]	second spacer BLM_1
WRN	[TTTTCGTCTCTAAAC] CGCTGCCGAGTACAAGCCGG[cggtgACCCAGGCGGCGCACAAG]	second spacer WRN_1

RECQL1	[TTTTCGTCTCTAAAC] TCCGGGTCGGTCCGTTCAGC[cggtgACCCAGGCG GCGCACAAG]	second spacer RecQL1_1
RECQL4	[TTTTCGTCTCTAAAC] CGCTTGCGATCGTCCAGCGA[cggtgACCCAGGCG GCGCACAAG]	second spacer RecQL4_1
RECQL5	[TTTTCGTCTCTAAAC] ACGCAATCTTATATCCGTCG[cggtgACCCAGGCGG CGCACAAG]	second spacer RecQL5_1
CHEK1	[TTTTCGTCTCTAAAC] CCTGGTACCATTCCTCCACC[cggtgACCCAGGCGG CGCACAAG]	second spacer CHEK1_1
CHEK2	[TTTTCGTCTCTAAAC] CCTGGAGCCGCACACTCTCC[cggtgACCCAGGCG GCGCACAAG]	second spacer CHEK2_1
SLX4	[TTTTCGTCTCTAAAC] CCCGGGTGCCGACTCCCAGC[cggtgACCCAGGCG GCGCACAAG]	second spacer SLX4_1
DNA2	[TTTTCGTCTCTAAAC] CCGGTTCCGCTGTCTTTTCT[cggtgACCCAGGCGG CGCACAAG]	second spacer DNA2_1
EME1	[TTTTCGTCTCTAAAC] CTATCAGGAGATCTACTTCC[cggtgACCCAGGCGG CGCACAAG]	second spacer EME1_1
GEN1	[TTTTCGTCTCTAAAC] CTCGGCTTTCCCTTGCCGGC[cggtgACCCAGGCG GCGCACAAG]	second spacer GEN1_1
RNF4	[TTTTCGTCTCTAAAC] ACTTCCGCTTCGGAGGCCTC[cggtgACCCAGGCG GCGCACAAG]	second spacer RNF4_1
SLX1	[TTTTCGTCTCTAAAC] GTCGGCGAGCGCGTACCATT[cggtgACCCAGGCG GCGCACAAG]	second spacer SLX1_1
TOP3A	[TTTTCGTCTCTAAAC] CCTCAGCACCGAATCCAGTA[cggtgACCCAGGCG GCGCACAAG]	Second spacer TOP3A_1
TOP3B	[TTTTCGTCTCTAAAC] CTATTTCCGGGTCCAGCCGC[cggtgACCCAGGCG GCGCACAAG]	second spacer TOP3B_1
WDHD1	[TTTTCGTCTCTAAAC] CAGTGGCGGAGGCTCGGTCA[cggtgACCCAGGCG GCGCACAAG]	second spacer WDHD1_1
CHTF8	[TTTTCGTCTCTAAAC] CGCGGCCAACGGGCGACAAC[cggtgACCCAGGCG GCGCACAAG]	second spacer CHTF8_1
SOD1	[TTTTCGTCTCTAAAC] CGTCTCCGCGACTACTTTAT[cggtgACCCAGGCGG CGCACAAG]	second spacer SOD1_1
GFP	[TTTTCGTCTCTAAAC] CGCCGGACACGCTGAACTTG[cggtgACCCAGGCG GCGCACAAG]	second spacer GFP_1
LACZ	[TTTTCGTCTCTAAAC] GTTTACCCGCTCTGCTACCT[cggtgACCCAGGCGG CGCACAAG]	second spacer LACZ_1

LUC	[TTTTCGTCTCTAAAC] TCCTTGTCAATCAAGGCGTT[cggtgACCCAGGCGGCGCACAAG]	second spacer LUC_1
RPL34 (ESSENTIAL GENE)	[TTTTCGTCTCTAAAC] TGAGTAGCCACAGCTCACCA[cggtgACCCAGGCGGCGCACAAG]	second spacer RPL34_1
RPL11 (ESSENTIAL GENE)	[TTTTCGTCTCTAAAC] TGATGGAGAGCAGGAAGAGA[cggtgACCCAGGCGGCGCACAAG]	second spacer RPL11_1
RPS24 (ESSENTIAL GENE)	[TTTTCGTCTCTAAAC] AGGGAGACTCACCATGATGG[cggtgACCCAGGCGGCGCACAAG]	second spacer RPS24_1
BLM	[TTTTCGTCTCTAAAC] CTAGGAGTCTGCGTGCGAGG[cggtgACCCAGGCGGCGCACAAG]	second spacer BLM_2
WRN	[TTTTCGTCTCTAAAC] CGGGGTATCTATAGTGCTAG[cggtgACCCAGGCGGCGCACAAG]	second spacer WRN_2
RECQL1	[TTTTCGTCTCTAAAC] GTGTCCGACTCTCCGATCTC[cggtgACCCAGGCGGCGCACAAG]	second spacer RecQL1_2
RECQL4	[TTTTCGTCTCTAAAC] CACGTCCCGCAGCCGCTCCA[cggtgACCCAGGCGGCGCACAAG]	second spacer RecQL4_2
RECQL5	[TTTTCGTCTCTAAAC] CTATACACAACCCCAACTCA[cggtgACCCAGGCGGCGCACAAG]	second spacer RecQL5_2
CHEK1	[TTTTCGTCTCTAAAC] TCCCTCACTAATCTAGACCC[cggtgACCCAGGCGGCGCACAAG]	second spacer CHEK1_2
CHEK2	[TTTTCGTCTCTAAAC] CTCTGCTGGCTGAGGCTGCG[cggtgACCCAGGCGGCGCACAAG]	second spacer CHEK2_2
SLX4	[TTTTCGTCTCTAAAC] CGGAGCCAGCGAGGGAGACG[cggtgACCCAGGCGGCGCACAAG]	second spacer SLX4_2
DNA2	[TTTTCGTCTCTAAAC] CTCCGCTCACAGCTCCGCCG[cggtgACCCAGGCGGCGCACAAG]	second spacer DNA2_2
EME1	[TTTTCGTCTCTAAAC] CCTGAACACCGCTCTGCAGA[cggtgACCCAGGCGGCGCACAAG]	second spacer EME1_2
GEN1	[TTTTCGTCTCTAAAC] CCCGTGCCTACCAGCTTCCC[cggtgACCCAGGCGGCGCACAAG]	second spacer GEN1_2
RNF4	[TTTTCGTCTCTAAAC] CGAGAAAGATGCCGCCGCCT[cggtgACCCAGGCGGCGCACAAG]	second spacer RNF4_2
SLX1	[TTTTCGTCTCTAAAC] CGGTACCGGGGCCGCGTCTA[cggtgACCCAGGCGGCGCACAAG]	second spacer SLX1_2
TOP3A	[TTTTCGTCTCTAAAC] CGCTTCGGTCACGTCCCCAC[cggtgACCCAGGCGGCGCACAAG]	second spacer TOP3A_2

TOP3B	[TTTTCGTCTCTAAAC] GAGCTGGATCCGCGGTGCGG[cggtgACCCAGGCG GCGCACAAG]	second spacer TOP3B_2
WDHD1	[TTTTCGTCTCTAAAC] CTAGGGCCCGTTCTCCGCAG[cggtgACCCAGGCG GCGCACAAG]	second spacer WDHD1_2
CHTF8	[TTTTCGTCTCTAAAC] CTCGGCTCGCCATTCTTCTC[cggtgACCCAGGCGG CGCACAAG]	second spacer CHTF8_2
SOD1	[TTTTCGTCTCTAAAC] TCGTCGCCATAACTCGCTAG[cggtgACCCAGGCGG CGCACAAG]	second spacer SOD1_2
GFP	[TTTTCGTCTCTAAAC] TGGTGAACCGCATCGAGCTG[cggtgACCCAGGCG GCGCACAAG]	second spacer GFP_2
LACZ	[TTTTCGTCTCTAAAC] TTCGGTACTTCGTCCACAAA[cggtgACCCAGGCGG CGCACAAG]	second spacer LACZ_2
LUC	[TTTTCGTCTCTAAAC] GGCGCGGTCGGTAAAGTTGT[cggtgACCCAGGCG GCGCACAAG]	second spacer LUC_2
RPL34 (ESSENTIAL GENE)	[TTTTCGTCTCTAAAC] ATCGGCTGCCATCCGAGGAG[cggtgACCCAGGCG GCGCACAAG]	second spacer RPL34_2
RPL11 (ESSENTIAL GENE)	[TTTTCGTCTCTAAAC] TCATGGCGGTGAGTAGCTGG[cggtgACCCAGGCG GCGCACAAG]	second spacer RPL11_2
RPS24 (ESSENTIAL GENE)	[TTTTCGTCTCTAAAC] ATCATATCAACGCGCACGGA[cggtgACCCAGGCG GCGCACAAG]	second spacer RPS24_2
BLM	[TTTTCGTCTCTAAAC] CGCACGCAGACTCCTAGCGG[cggtgACCCAGGCG GCGCACAAG]	second spacer BLM_3
WRN	[TTTTCGTCTCTAAAC] CGGCGCACACAGTACACATC[cggtgACCCAGGCG GCGCACAAG]	second spacer WRN_3
RECQL1	[TTTTCGTCTCTAAAC] CTACTCGGGAGTAAAATCTT[cggtgACCCAGGCGG CGCACAAG]	second spacer RecQL1_3
RECQL4	[TTTTCGTCTCTAAAC] CCGCGCTTGCGATCGTCCAG[cggtgACCCAGGCG GCGCACAAG]	second spacer RecQL4_3
RECQL5	[TTTTCGTCTCTAAAC] TGGTCCGCCCAAGAATTAAA[cggtgACCCAGGCGG CGCACAAG]	second spacer RecQL5_3
CHEK1	[TTTTCGTCTCTAAAC] CTCTGAATGTCGGCGGCTCC[cggtgACCCAGGCG GCGCACAAG]	second spacer CHEK1_3
CHEK2	[TTTTCGTCTCTAAAC] CATATGACTCACCGCGTGAG[cggtgACCCAGGCG GCGCACAAG]	second spacer CHEK2_3
SLX4	[TTTTCGTCTCTAAAC] CCGCGGAGCATTGCCTGCGC[cggtgACCCAGGCG GCGCACAAG]	second spacer SLX4_3

DNA2	[TTTTCGTCTCTAAAC] CGCGTCCAGGATGGAGCAGC[cggtgACCCAGGCG GCGCACAAG]	second spacer DNA2_3
EME1	[TTTTCGTCTCTAAAC] CAGGCCTGCGACCGGGGACG[cggtgACCCAGGCG GCGCACAAG]	second spacer EME1_3
GEN1	[TTTTCGTCTCTAAAC] CCGAGTCCGGTCACTGCGGA[cggtgACCCAGGCG GCGCACAAG]	second spacer GEN1_3
RNF4	[TTTTCGTCTCTAAAC] CGCAGCGCGGCTCCCCCAAG[cggtgACCCAGGCG GCGCACAAG]	second spacer RNF4_3
SLX1	[TTTTCGTCTCTAAAC] TACTAAGGCGTACGTCAACG[cggtgACCCAGGCG GCGCACAAG]	second spacer SLX1_3
TOP3A	[TTTTCGTCTCTAAAC] CACAGCGACCTGGAACTACA[cggtgACCCAGGCG GCGCACAAG]	second spacer TOP3A_3
TOP3B	[TTTTCGTCTCTAAAC] CCCCGGGAACAAGGACCGGA[cggtgACCCAGGCG GCGCACAAG]	second spacer TOP3B_3
WDHD1	[TTTTCGTCTCTAAAC] GAGTGGGGACTCACCCGGGT[cggtgACCCAGGCG GCGCACAAG]	second spacer WDHD1_3
CHTF8	[TTTTCGTCTCTAAAC] CCAATCCCGGCTCGGCCCTC[cggtgACCCAGGCG GCGCACAAG]	second spacer CHTF8_3
SOD1	[TTTTCGTCTCTAAAC] TTCAGCACGCACACGGCCTT[cggtgACCCAGGCG GCGCACAAG]	second spacer SOD1_3
GFP	[TTTTCGTCTCTAAAC] CCGGGATCACTCTCGGCATG[cggtgACCCAGGCG GCGCACAAG]	second spacer GFP_3
LACZ	[TTTTCGTCTCTAAAC] GTCCCAGACGAAGCCGCCCT[cggtgACCCAGGCG GCGCACAAG]	second spacer LACZ_3
LUC	[TTTTCGTCTCTAAAC] CGGGTGTAATCAGAATAGCT[cggtgACCCAGGCGG CGCACAAG]	second spacer LUC_3
RPL34 (ESSENTIAL GENE)	[TTTTCGTCTCTAAAC] CCCGGGACTTTGCTGCATTC[cggtgACCCAGGCG GCGCACAAG]	second spacer RPL34_3
RPL11 (ESSENTIAL GENE)	[TTTTCGTCTCTAAAC] TCGCCATCCATGGCAGGCCG[cggtgACCCAGGCG GCGCACAAG]	second spacer RPL11_3
RPS24 (ESSENTIAL GENE)	[TTTTCGTCTCTAAAC] CGGATGGCTCGGATACGCGG[cggtgACCCAGGCG GCGCACAAG]	second spacer RPS24_3
TOP1	[TTTTCGTCTCTAAAC] AAGTTCGCATTTGGGCTCAC[cggtgACCCAGGCGG CGCACAAG]	second spacer TOP1_1
FEN1	[TTTTCGTCTCTAAAC] CCGGGAGCGACGGGGTCCGC[cggtgACCCAGGC GGCGCACAAG]	second spacer FEN1_1

EXO1	[TTTTCGTCTCTAAAC] TTCGCGCGCTGTGTAGGCAA[cggtgACCCAGGCG GCGCACAAG]	second spacer EXO1_1
RNASEH1	[TTTTCGTCTCTAAAC] CGCCGGTGACGGAAGTGCGG[cggtgACCCAGGCG GCGCACAAG]	second spacer RNASEH1_1
LIG4	[TTTTCGTCTCTAAAC] CCGGTCTGTTGCCCCACAGA[cggtgACCCAGGCG GCGCACAAG]	second spacer LIG4_1
BRCA1	[TTTTCGTCTCTAAAC] TCTGTCAGCTTCGGAAATCC[cggtgACCCAGGCGG CGCACAAG]	second spacer BRCA1_1
MRE11	[TTTTCGTCTCTAAAC] CGGGAGAGAACGGCGTCCGT[cggtgACCCAGGCG GCGCACAAG]	second spacer MRE11_1
CTIP	[TTTTCGTCTCTAAAC] CCGAGATTGCCTCGGGATTC[cggtgACCCAGGCG GCGCACAAG]	second spacer CTIP_1
RNASEH2A	[TTTTCGTCTCTAAAC] CATCGACGCCCAGGACGCAA[cggtgACCCAGGCG GCGCACAAG]	second spacer RNASEH2A_1
RAD51B	[TTTTCGTCTCTAAAC] CCTTAAGACTCGGGATCGTC[cggtgACCCAGGCG GCGCACAAG]	second spacer RAD51B_1
XRCC3	[TTTTCGTCTCTAAAC] CCCGCGGGTTCCGCACTCCT[cggtgACCCAGGCG GCGCACAAG]	second spacer XRCC3_1
RAD51C	[TTTTCGTCTCTAAAC] CCGAGCTTAGCAAAGGTAAC[cggtgACCCAGGCG GCGCACAAG]	second spacer RAD51C_1
BRCA2	[TTTTCGTCTCTAAAC] CCTAGTTTCAGAAGCTCGCG[cggtgACCCAGGCG GCGCACAAG]	second spacer BRCA2_1
RAD52	[TTTTCGTCTCTAAAC] TCTTGTTACTCCCTAGCAGT[cggtgACCCAGGCGG CGCACAAG]	second spacer RAD52_1
RTEL	[TTTTCGTCTCTAAAC] CGGCGAACCTTCCAGAACCG[cggtgACCCAGGCG GCGCACAAG]	second spacer Rtel_1
FBH1	[TTTTCGTCTCTAAAC] CGTCTGCGGCCTCACGCACT[cggtgACCCAGGCG GCGCACAAG]	second spacer Fbh1_1
FANCM	[TTTTCGTCTCTAAAC] CTACGGTTCCGATCCCCATC[cggtgACCCAGGCGG CGCACAAG]	second spacer FANCM_1
TOP1	[TTTTCGTCTCTAAAC] CCGCTTACCTGCGCCTCCTC[cggtgACCCAGGCG GCGCACAAG]	second spacer TOP1_2
FEN1	[TTTTCGTCTCTAAAC] CCCGCCGCTAAGCTGAGAAG[cggtgACCCAGGCG GCGCACAAG]	second spacer FEN1_2
EXO1	[TTTTCGTCTCTAAAC] GTGTTCTGCGTTGCCGGCCG[cggtgACCCAGGCG GCGCACAAG]	second spacer EXO1_2

RNASEH1	[TTTTCGTCTCTAAAC] CCGGCGCTCAACACCGCACT[cggtgACCCAGGCG GCGCACAAG]	second spacer RNASEH1_2
LIG4	[TTTTCGTCTCTAAAC] GCGTGCTTGAGCCCGGTGAC[cggtgACCCAGGCG GCGCACAAG]	second spacer LIG4_2
BRCA1	[TTTTCGTCTCTAAAC] TCCAGGAAGTCTCAGCGAGC[cggtgACCCAGGCG GCGCACAAG]	second spacer BRCA1_2
MRE11	[TTTTCGTCTCTAAAC] TGGGTCGCGATTGTGGGGCT[cggtgACCCAGGCG GCGCACAAG]	second spacer MRE11_2
CTIP	[TTTTCGTCTCTAAAC] CCGAGTGTAGCCCGGGCCCG[cggtgACCCAGGCG GCGCACAAG]	second spacer CTIP_2
RNASEH2A	[TTTTCGTCTCTAAAC] CGGGCACAGGCGAACTCAGG[cggtgACCCAGGCG GCGCACAAG]	second spacer RNASEH2A_2
RAD51B	[TTTTCGTCTCTAAAC] CCAATATCGAAACCCACGAG[cggtgACCCAGGCG GCGCACAAG]	second spacer RAD51B_2
XRCC3	[TTTTCGTCTCTAAAC] CGGGTTCCGCACTCCTCTTC[cggtgACCCAGGCG GCGCACAAG]	second spacer XRCC3_2
RAD51C	[TTTTCGTCTCTAAAC] CGCTGGGGCGTGCGGCGTGA[cggtgACCCAGGCG GCGCACAAG]	second spacer RAD51C_2
BRCA2	[TTTTCGTCTCTAAAC] CGGGTGTCTTTTGCGGCGGT[cggtgACCCAGGCG GCGCACAAG]	second spacer BRCA2_2
RAD52	[TTTTCGTCTCTAAAC] TTCATTTCTTGGACATCCGG[cggtgACCCAGGCGG CGCACAAG]	second spacer RAD52_2
RTEL	[TTTTCGTCTCTAAAC] TTGCTTTGTGCTCCCGGCGG[cggtgACCCAGGCG GCGCACAAG]	second spacer Rtel_2
FBH1	[TTTTCGTCTCTAAAC] CCGTGTGGAAAACTTAACCT[cggtgACCCAGGCGG CGCACAAG]	second spacer Fbh1_2
FANCM	[TTTTCGTCTCTAAAC] TCGGTGGTTGTCGGCCTAAT[cggtgACCCAGGCG GCGCACAAG]	second spacer FANCM_2
TOP1	[TTTTCGTCTCTAAAC] CACAGGCCGGTTCGCCGTCT[cggtgACCCAGGCG GCGCACAAG]	second spacer TOP1_3
FEN1	[TTTTCGTCTCTAAAC] CGAACCAAGCTTTAGCCGCC[cggtgACCCAGGCG GCGCACAAG]	second spacer FEN1_3
EXO1	[TTTTCGTCTCTAAAC] CTGGGCGGGGCCGCAAGGAA[cggtgACCCAGGCG GCGCACAAG]	second spacer EXO1_3
RNASEH1	[TTTTCGTCTCTAAAC] ACAGAGTCGCCTTGGCCGCC[cggtgACCCAGGCG GCGCACAAG]	second spacer RNASEH1_3

LIG4	[TTTTCGTCTCTAAAC] CACAGACTTCTCGCCGCCTG[cggtgACCCAGGCG GCGCACAAG]	second spacer LIG4_3
BRCA1	[TTTTCGTCTCTAAAC] CCCGTCAAAGAATACCCATC[cggtgACCCAGGCGG CGCACAAG]	second spacer BRCA1_3
MRE11	[TTTTCGTCTCTAAAC] CGGAATTCAGGTTTACGGCC[cggtgACCCAGGCG GCGCACAAG]	second spacer MRE11_3
CTIP	[TTTTCGTCTCTAAAC] CGGTGGGAAAGCCGACCCCT[cggtgACCCAGGCG GCGCACAAG]	second spacer CTIP_3
RNASEH2A	[TTTTCGTCTCTAAAC] AGACCCGCTCCTGCAGTATT[cggtgACCCAGGCGG CGCACAAG]	second spacer RNASEH2A_3
RAD51B	[TTTTCGTCTCTAAAC] CACAACGGCACCCCACATGA[cggtgACCCAGGCG GCGCACAAG]	second spacer RAD51B_3
XRCC3	[TTTTCGTCTCTAAAC] CGGGTCTCCATTGCCCGAGC[cggtgACCCAGGCG GCGCACAAG]	second spacer XRCC3_3
RAD51C	[TTTTCGTCTCTAAAC] CTGCATTTCAAAGCGGAACG[cggtgACCCAGGCG GCGCACAAG]	second spacer RAD51C_3
BRCA2	[TTTTCGTCTCTAAAC] CGCCGGTCACAAATCTGTCC[cggtgACCCAGGCG GCGCACAAG]	second spacer BRCA2_3
RAD52	[TTTTCGTCTCTAAAC] CCGGGGTGGTTCTAGCCGTG[cggtgACCCAGGCG GCGCACAAG]	second spacer RAD52_3
RTEL	[TTTTCGTCTCTAAAC] TCGACTGGAGTCGGTTGAGT[cggtgACCCAGGCG GCGCACAAG]	second spacer Rtel_3
FBH1	[TTTTCGTCTCTAAAC] CAGTGCGTGAGGCCGCAGAC[cggtgACCCAGGCG GCGCACAAG]	second spacer Fbh1_3
FANCM	[TTTTCGTCTCTAAAC] CACGTCTGAAAAAGCGTTCT[cggtgACCCAGGCGG CGCACAAG]	second spacer FANCM_3

Note: Sequences in bracket '[ ]' are homologous to guide expression vector. First spacer represents oligo sequence cloned into the first guide position, while second spacer represents oligo sequence cloned into the second guide position in the vector.

Supplementary Table 9 Sequence of sgRNAs used in the studies

Target gene	sgRNA sequence
EYFP reporter[1]	TACCTCATCAGGAACATGT
NEAT1 sgRNA1	GCGACAGGGAGGGATGCGCGCC
NEAT1 sgRNA2	GCGCGCCTGGGTGTAGTTGT
NEAT1 sgRNA3	GAAGTGGCTAGCTCAGGGCTTC
CXCR4	CAGGTAGCAAAGTGACGCCGA
SEL1L sgRNA1	GCAGGAAGAGCAGCGGCGAGG
SEL1L sgRNA2	GGGGGCGGATACTGACCCG
SEL1L sgRNA3[2]	GATACTGACCCGAGGACGCCG
ARPC2 sgRNA1[2]	TGTCGGTGAAGCGGCAGTGG
ARPC2 sgRNA2	CAGGCGGGTTCAGGCTTCGG
ERK1 sgRNA1[2]	GGGAGCCCCGTAGAACCGAG
ERK1 sgRNA2	CACCGCCCTCCTCCCCACGG
BRCA1 sgRNA1	GGATTTCCGAAGCTGACAGA
BRCA1 sgRNA2[2]	GCTCGCTGAGACTTCCTGGA
BLM sgRNA1	AGGAAACGGAAGAACCCGAG
BLM sgRNA2	CCTCGCACGCAGACTCCTAG
MET1 sgRNA1	TGAGCAGATGCGGAGCCGAG
MET1 sgRNA2	ACTGGTTCCTGGGCACCGAA
RHOA sgRNA1	AGTTCCCGTGATGCCCCACG
RHOA sgRNA2	GCGCGCCTCCGAGTGCCCAG
CHK2 sgRNA1	GGAGAGTGTGCGGCTCCAGG
CHK2 sgRNA2	CGCAGCCTCAGCCAGCAGAG
CHK1 sgRNA1	GGTGGAGGAATGGTACCAGG
CHK1 sgRNA2[2]	GGGTCTAGATTAGTGAGGGA
CANX_-700*	TGAAGTGAGATTAGGTGTCA
CANX_-335*	GTTGGGTTGGAACGCCCCGA
CANX_-505*	GGTTCTGCTCACGCCCGTAG
CANX_-22*	GCTCGCTCGCGCGGCAGCGG
CANX_-1[2]*	GGCCGAGGCCTCTTGGTTCTG
CANX_47*	GCGCCGCAGTAAAGAGAGAGG
CANX_155*	TCGGGCCTGTGAGGACCTCG
CANX_263*	CGACGCGCCCGCCGTGAGCG
CANX_472*	GAGTAACTGGGTAAAAGTAT
CANX_642*	ACCAGAAGGAGAACACGCAG
SYVN1_-1032[3,4]*	GGAAAACGCAAGGCACAAAG
SYVN1_-734[3,4]*	AACGTTCCCGGAGGCCAGCC
SYVN1_-601[3,4]*	ACCTTTGCTGGCCTATAGAA
SYVN1_-555[3,4,6]*	AACTTATCGCAACCAATCAG
SYVN1_-339[3,4,6]*	CAGGTGGTACAGCCCGCAAG

SYVN1_-194[3,4]*	ATTACCTTCCGACCACCTCT
SYVN1_-116[3,4,6]*	CCTACGTGGGCCCATAGCAA
SYVN1_-43[3,4]*	ACACCTCACTTCCGGCGGCG
SYVN1_19[3,5]*	CCGCTCAATCCGCGCGACTG
SYVN1_45[3,5]*	GGCGCTGGGTTCCTGGTGAGT
SYVN1_183[3,5]*	GCACCGGCGTCTGAGGTCTC
SYVN1_228[2,3,5,6]*	GTTGCGGGCGTCGCAGGCA
SYVN1_292[3,5]*	GAGAGCAGCAGCGGGACGGG
SYVN1_480[3,5]*	TGAGAGCAGCCAAGGCACAG
SYVN1_702[3,5]*	TAAGTGATCACACTGACGCA
SYVN1_844[3,5]*	TCGTGCTGTGCAAAATAGCC

1: Guide RNA targeting EYFP reporter in the reporter screen assay
2: Guide RNA used in single gene targeting experiments
3: Guide RNA used in ‘mixed gRNAs 1-16’ group shown in Figure 2b and Supplementary Figure 8
4: Guide RNA used in ‘mixed gRNAs 1-8’ group shown in Figure 2b and Supplementary Figure 8
5: Guide RNA used in ‘mixed gRNAs 8-16’ group shown in Figure 2b and Supplementary Figure 8
6: Guide RNA used in ‘mixed best 4 gRNAs’ group shown in Figure 2b and Supplementary Figure 8
*: The numerical number indicates the position of spacer relative to transcription start site of the target gene.

Supplementary Table 10 Sequences of all qPCR primers in the studies.

Target gene	Forward qPCR primer sequence	Reverse qPCR primer sequence
NEAT1	GTGGCTGTTGGAGTCGGTAT	ATTCACTCCCCACCCTCTCT
CXCR4	ACTACACCGAGGAAATGGGCT	CCCACAATGCCAGTTAAGAAGA
SEL1L	GAGGGGGAAAGTGTCACAGA	GGTCAAAGCTGGTTTCCGTA
SYVN	ACCAGCATCCCTAGCTCAGA	TCCTCAGGCATCTCCTCTGT
ARPC2	CTGGAGGTGAACAACCGCAT	GACCCCATCGAAATCTGCAAA
ERK1	ATGTCATCGGCATCCGAGAC	GGATCTGGTAGAGGAAGTAGCA
BRCA1	CTCAAGGAACCAGGGATGAA	GCTGTAATGAGCTGGCATGA
BLM	CAGACTCCGAAGGAAGTTGTATG	TTTGGGGTGGTGTAACAAATGAT
MET1	AGCAATGGGGAGTGTAAAGAGG	CCCAGTCTTGTACTCAGCAAC
RHOA	GGAAAGCAGGTAGAGTTGGCT	GGCTGTCGATGGAAAAACACAT
CHK1	ATATGAAGCGTGCCGTAGACT	TGCCTATGTCTGGCTCTATTCTG
CHK2	GCGCCTGAAGTTCTTGTTTC	CGTAAAACGTGCCTTTGGAT
CANX	GATCCAGACGCAGAGAAACC	CATCCAGGAGCTGACTCACA
TERC	CCCTAACTGAGAAGGGCGTA	GCTCTAGAATGAACGGTGGAA
XIST	AGGTCAGGCAGAGGAAGTCA	CTGCCTCCCGATACAACAAT
ACTB	CATGTACGTTGCTATCCAGGC	CTCCTTAATGTCACGCACGAT
CAS9	GAGTTGACGCCAAAGCAATC	TACCAAACAGGCCGTTCTTC

Supplementary Table 11 Sequence of sgRNA2-7SK template

sgRNA1 tail; 7SK promoter
gttttagagctatgctgaaaagcatagcaagttaaaataaggcagtgatttttaatccagtccgtacacaacttgaaaaagtgcgcaccg attcggtgctttttttCCTACGCACCTCGTCGAACCCTCACTGCAGTATTTAGCATGCCCCACCCATCT GCAAGGCATTCTGGATAGTGTCAAAACAGCCGGAAATCAAGTCCGTTTATCTCAAACTTTAG CATTTTGGGAATAAATGATATTTGCTATGCTGGTTAAATTAGATTTTAGTTAAATTTCCTGCTG AAGCTCTAGTACGATAAGTAACTTGACCTAAGTGTAAAGTTGAGATTTCCTTCAGGTTTATAT AGCTTGTGCGCCGCCTGGGTcaccg

Supplementary Table 12 Sequence of PCR primers for next generation sequencing

PCR 1 primers	Sequence
Forward primer (lethality screen)	**CTTTCCCTACACGACGCTCTTCCGATCT** NNNNNNCCCTTGGAGAAAAGCCTTGTTT
Reverse primer (lethality screen)	**GGAGTTCAGACGTGTGCTCTTCCGATCT**TGTACA AGAAAGCTGGGTCTAG
Forward primer (epistasis screen)	**CTTTCCCTACACGACGCTCTTCCGATCT** NNNNNNCTTGTGGAAAGGACGAAACACC
Reverse primer (epistasis screen)	**GGAGTTCAGACGTGTGCTCTTCCGATCT**CATTTG TCTCGAGGTCGAGAATTC

Sequences in bold are adaptor sequence for next generation sequencing.

Supplementary Table 13 PCR cycling conditions to amplify libraries for next generation sequencing

PCR 1

Step	Temperature	Duration
Step 1	95 °C	8 min
Step 2	95 °C	30 sec
Step 3	60 °C	30 sec
Step 4	72 °C	30 sec# / 1 min*
Repeat step 2-4 for a total a 25-30 cycles		
Step 5	72 °C	2 min

extension time for lethality screen library; * extension time for epistasis screen library

PCR 2

Step	Temperature	Duration
Step 1	95	3 min
Step 2	95	10 sec
Step 3	55	20 sec
Step 4	72	30 sec
Repeat step 2-4 for a total a 5-10 cycles		

Supplementary Note 1 Interpretation of pi scores. A positive pi-score suggests that the fitness effect of the gene pair knockdown is less than expected from individual knockdowns (e.g., loss of two proteins in a pathway or complex), while a negative pi-score means that the fitness effect was more pronounced than expected based on the individual fitness effects from single-gene knockdowns (e.g., synthetic lethal effects).

Supplementary Note 2 This section describes the strategy used to identify and analyze genes with differential expression (DE) in our RNA-seq experiments. Related results are **Supplementary Figure 10-11** and **Supplementary Table 2**.

To analyze raw reads from RNA-sequencing experiments and profile whole transcriptome activity induced by dCas9, dCas9-KRAB and dCAS9-KRAB-MeCP2 repressors, we implemented edgeR quasi-likelihood (edgeR-quasi) pipeline for DE. EdgeR-quasi uses negative binomial generalized linear model[1] with F-tests[2], and holds advantages over other methods as it provides speed and reliable error rate control. For the DE analyses, we utilize edgeR-quasi and limma-voom pipelines for two independent biological replicates of dCas9, dCas9-KRAB and dCAS9-KRAB-MeCP2 repressors. The sample size of n=2 in each repressor group is reasonable due to the low biological variability characteristic of cell culture experiments. Our analysis involves importing of raw counts, filtering of lowly expressed counts, normalization due to library size bias, DE, and clustering testing.

First, we tested DE between each repressor group relative to a control group (delivered sgRNA only) using the edgeR QL functions set to *robust=TRUE* in *glmQLFit* to reduce the number of false positives from genes with extreme dispersions (very low and very high). In **Supplementary Figure 10a-c**, we plot these results on two axes - $\log_2$ fold change (FC) versus averaged $\log_2$ counts per million (CPM), where positive $\log_2$ FC indicates upregulated genes while negative $\log_2$ FC represent downregulated genes relative to the negative control. DE genes at FDR of 5% and corrected using Benjamini-Hochberg method are shown in grey, whereas genes with no significant fold change are shown in black. *glmQLFTest* function identifies all DE only based on statistical significance including genes with small fold changes. To remove such bias, we apply the TREAT method[3] which leverages a negative binomial framework using the edgeR's *glmTrea*t function, and simultaneously tests for significance and differential fold change at a cutoff of $\log_2$ FC > 1.5. This method is more stringent as it requires larger p-values for calling genes and leads to fewer detected genes. It therefore provides better specificity in recognizing genes with true biological function. The resulting genes are plotted in red on **Supplementary Figure 10a-c** and summarized in the table on **Supplementary Figure 10d**. The identity of these genes are listed in **Supplementary Table 2**. The application of log fold change cutoff of 1.5 results in no downregulated genes, and significantly reduces the number of upregulated genes.

We display expression patterns of transcriptional changes by plotting the top 35 genes with DE in the control, dCas9, dCas9-KRAB and dCas9-KRAB-MeCP2 groups. Clustering of genes with correlated expression provides insights into the biological effects of repressor's activity. To display relative changes in genes across the four groups, we performed scaling such that each gene has a mean of zero and standard deviation of 1. The displayed gene clusters are based on Euclidean distance, $(1\text{-}R)^2/2$ between each gene pair where R is the Pearson's correlation of the two genes. A scale bar key of normalized Log_2 CPM represents large negative (colored blue) and positive (colored red) correlations. Genes with large positive correlations correspond to small Euclidean distances and cluster together (**Supplementary Figure 11a**).

Lastly, we examine activated and repressed genes across all three repressor groups (all normalized to the negative control) by applying the limma-voom workflow. We performed linear modelling in limma, and used *lmFit* and *contrasts.fit* functions followed by empirical Bayes model, *eBayes*. This workflow removes variance-associated dependencies on the mean. In **Supplementary Figure 11b-c**, we plot genes on Venn diagrams for downregulation and upregulation where we define significance at 5% p-value with no log fold change cutoff as a less stringent method for examining transcriptome-wide transcriptional offsets for the different repressors. Based on these results, dCas9-KRAB repressor shows the largest clusters of activated genes followed by dCas9-KRAB-MeCP2, and dCas9.

Supplemental Note 3 This section describes the methods and bioinformatics analyses we used to interpret the repressor screens in HAP1, SH-SY5Y and 293T cell lines. Related results are **Supplementary Table 4-6** and **Supplementary Data 2-4**.

Alignment of sequencing reads to reference contig

The sequencing reads were aligned to a reference contig sequence (NNNNNNcccttggagaaaagccttgtttNNNNNNNNNNNNNNNNNNNNgtttaagagctaga aatagcaagtttaaataaggctagtccgttatcaacttgaaaaagtggcaccgagtcggtgctttttttctagaccca gctttcttgtacaaaaaaaagaattcctgcagccccgataaaataaaag) using the alignment software BWA-MEM (version 0.7.8)[4]. We used samtools (version 1.2) to extract aligned sequences that have a mapping quality score >= 30[5]. The 20-nucleotide variable sequence was then match to the 20-nucleotide sgRNA library with 683 guide sequences. Sequences that do not match any of the 683 guide sequences were discarded from the analysis.

Analysis of the repressor sgRNA library

We first sequenced the sgRNA library to determine the distribution of the guide sequences. A total 129,362 sequences map to a guide sequence within the library of 683 guides. However, 53 of the guides were severely underrepresented, i.e. less than 50 reads mapped to the guide (< 0.04%) and

they were removed from all further analysis.

Comparing the guide sequences for all the conditions

For all the conditions, we compared the mapped guides against the corresponding control experiment. The control experiment for all the conditions is the experiment performed without any repressor, i.e. without dCas9, dCas9-KRAB or dCas9-KRAB-MeCP2. For each guide, we compared its frequency for the condition against its frequency for the control. This is done by calculating the odds-ratio (OR) for each guide using the formula,

$$OR_i = \frac{\frac{test_i}{testTotal}}{\frac{control_i}{controlTotal}}$$

where $test_i$ is the number of reads that map to guide *i* for the test condition and $control_i$ is the number of reads that map to guide *i* for the control while *testTotal* and *controlTotal* are the total number of reads for the test condition and control, respectively. If the guide is enriched in the test condition, the OR would be > 1 while if the guide is depleted, the OR would be < 1 (**Supplementary Data 2-4** list the OR and p-value of each tested guide).

Determining if the essential guides are depleted

Out of the 630 guides from the library, 370 target essential genes (essential guides) while the remaining 260 target non-essential genes. To determine if the essential guides were significantly depleted, we performed a 1-tailed Welch T-test between the $\log_2$ OR of the essential guides versus the $\log_2$ OR of the non-essential guides (**Supplementary Table 4-6**). Also, for the dCas9-KRAB-MeCP2 for HAP1 day 7 and day 14, there were a number of guides that were completely depleted, ie. they had 0 reads for the test condition. This presents a problem as the $\log_2$ OR for those guides would be -∞.To allow for the T-test, we replaced the log2 OR for those guides to the minimal finite $\log_2$ OR for that condition, which is -7.61 for day 7 and -8.87 for day 14.

Supplementary Note 4 This section describes detailed methods used to analyze the repressor-dual gRNA screen. The analysis was performed using an adapted version of a published workflow for computing genetic interactions using a combinatorial CRISPR-Cas9 knockouts[6] as follows.

Read alignment

Pair-end reads were first aligned to the sequence immediately upstream and downstream of the 20 bp protospacers, thus allowing us to extract protospacer sequences from each read. The protospacer sequences were then aligned to expected sequences, allowing for 3 mismatches (3< ½ * min(hamming(g_i, g_j) for all i, j). To ensure the robustness of the mapping, constructs with fewer than 5

reads mapped will be excluded from downstream analysis. Only when both reads in a pair were matched with a designed construct sequence was the pair considered for downstream scoring.

Quantification of fitness and gRNA fitness and gRNA–gRNA interactions

We modeled the cell population change over the 14 day duration of the screen using an assumption of exponential growth[6]. For each synthesized construct, we estimated the relative abundance (x_c) of the sub-population of cells harboring the construct. We did this by using the count of the reads that aligned to the designed construct.

$$x_c(t) = a_c + f_c t - log_2 \sum_c 2^{a_c + f_c t}$$

In which a_c denotes the initial abundance of the construct at day 0, f_c is the fitness of the cells with the construct. Since each gene is targeted by at least 3 gRNAs, gene-gene fitness $f_{g_i g_j}$ are calculated by collapsing f_c from all dual gRNA constructs targeting the same gene pairs.

We quantified genetic interactions as the difference between summation of single gene fitnesses and the double gene fitness, as follows:

$f_{g_i g_j} = f_{g_i} + f_{g_j} + \pi_{g_i g_j}$

Single gene fitnesses f_{g_i}, f_{g_j} were obtained by fitting of above equations to the screen data. The residual of the fit, $\pi_{g_i g_j}$, denotes the genetic interaction score (i.e., pi-score) for a gene pair $g_i\, g_j$. Note that theoretically f_{g_i}, f_{g_j} can be more easily obtained by measuring the fitness of the constructs that contain a negative control gene (lacZ, GFP and luc). We noticed that the negative controls lacZ and luc seemed neutral to cell fitness when a regression model was used to estimate the single gene fitnesses f_{g_i} from the fitness of all constructs $f_{g_i g_j}$ in which f_{g_i} participates, as previously done[6]. Interestingly, GFP gRNAs, expected to serve as a third negative control, showed positive fitness, suggesting that the used GFP targeting guide may be hitting an off-target sequence within the mammalian genome that when mutated causes a fitness benefit. **Supplementary Data 7** lists the genetic interactions uncovered in our screen.

Validation of genetic interaction screens by examining the topology of protein complex network and genetic interactions

We first filtered out gene-pairs that show zero interaction ($\{g_i g_j \; \forall \; |\pi_{ij}| > 0\}$), and the shortest path was computed for the remaining gene-pairs. The shortest paths between gene pairs were computed based on a network of experimentally characterized protein complexes[7] The number of intermediate genes that connect the gene pair as determined by the protein complex network is treated as the distance between the two genes ($d_{g_i g_j}$). $d_{g_i g_j}$ values are subsequently multiplied by the genetic interaction score π_{ij} derived from the 3 repression screens for gene-pair $g_i g_j$ to get the enrichment score $ES_{ij} = d_{g_i g_j} \cdot \pi_{ij}$. The overall enrichment score can then be calculated by the summing all enrichment

scores ($ES_{\text{overall}} = \sum_{i,j} \hat{} ES_{ij}$). Permutation tests are performed by shuffling the genetic interaction scores and repeating the above steps for a total of 10000 permutations. As valid screen should have a smaller $ES_{overall}$ compared to a non-valid one, left-tailed p values are reported.

Supplementary Note 5 This section describes detailed materials and methods used to perform circuit experiments.

Cell culture

Transfections were performed on HEK293ft cells using polyethylenemine (PEI). Cells were cultured in Debulcco's Modified Eagle Medium (DMEM), with 10% Fetal Bovine Serum (FBS), non-essential amino acids (NEAA), glutamine, sodium pyruvate, and penicillin/streptomycin. The day prior to transfection, cells were passaged and split into 24-well plates, then allowed to grow to 70-90% confluence. Mixes of DNA were used with a 2:1 PEI:DNA ratio to transfect the 90% confluent cells using standard transfection protocols. All conditions were transfected in quadruplicate. For inducible circuits, doxycycline was added to cultures to a concentration of 2000ng/uL. Media and inducers were changed daily post-transfection until flow cytometry was performed 72 hours later. In wells designated for control experiments, corresponding plasmid DNA under study was replaced by equal amount of empty DNA plasmid. 72 hours post-transfection, cells were collec-ted for flow cytometry assay.

Flow Cytometry and Data analysis

72 hours post-transfection, cells were trypsinized, washed with Hank's Balanced Salt Solution (HBSS) with 2% FBS, then resuspended in 200uL HBSS+FBS. Then flow cytometry was performed using a BD FACSCelesta flow cytometer. 200,000 events were collected, measuring forward scatter (FSC), side scatter (SSC), EBFP expression (BV421), and EYFP expression (BB515). Data were analyzed using FlowJo (FlowJo, LLC). For analysis, all data were compensated using single color and non-transfected controls. Cells were then gated by FSC and SSC to separate healthy, living cells from dead cells and debris. Living cells were further gated by EBFP; laser voltage was set in such a way as to make non-fluorescing cells express at 10^2 or lower, so the BV421 gate was set at 10^2 .

Cells with above 10^2 a.u of EBFP expression were considered transfected and were further analyzed by taking the geometric mean of the population's EYFP (BB515) expression. The geometric means of all samples were exported and further analyzed in Excel (Microsoft) or Prism (GraphPad Software). For single repression circuits, fold repression was calculated by dividing the average EYFP expression of the unrepressed samples by the EYFP of each of the four replicates. These four measures were then used to find average fold repression and standard error of the mean (s.e.m.).

For layered transcriptional repression circuits, fraction of maximum expression was calculated by dividing the average EYFP expression of the

unrepressed samples by the EYFP of each of the four replicates. These four measures were then used to find average fraction of maximum and standard deviation. For inducible layered transcriptional repression circuits, fold derepression was calculated by dividing the EYFP expression of each sample in the +Dox condition by the average EYFP expression of their No Dox counterpart. These four measures were then used to find the average fold derepression and s.e.m.

For transfections involving CXCR4 as the output, after supernatant was removed, cells in each well were labeled with 5 ul of CD184 (CXCR4) monoclonal antibody (eBioscienceTM) conjugated to PE and diluted (1:40) in HBSS without calcium and magnesium supplemented with 2% FBS and incubated at 4^{o}C for 30 minutes. Cells were then centrifuged and supernatant was removed. They were then resuspended in 7-AAD solution to exclude dead cells and subjected to FACS. Flow cytometry measurements were performed using BD FACSCelesta with the following settings: EBFP measured with 405 nm laser and a 450/40 filter, EYFP measured with 488 nm laser and a 530/30 filter, 7-AAD measured with a 488 nm laser and a 695/40 filter and CXCR4 measured with 561 nm laser and a 586/15 filter. At least 300,000 events were gathered from each well. Appropriate compensation controls were dedicated for each experiment. Untransfected and unstained cells were used as negative control. Similarly, untransfected cells stained only with CD184-PE antibody were used for CXCR4 control, cells transfected only with EBFP were used as BFP controls. Finally, a mixture of live and dead cells from untransfected wells were used as 7-AAD controls. Data from flow cytometry was analyzed using FlowJo software. Briefly, live cells (7-AAD negative population) were selected and then gated for EBFP expression >10^3 A.U. Geometric mean of PE fluorescence level was then calculated in this population.

Statistical analysis

Statistical comparison was performed using one-tailed Student's T-test with a *p*-value < 0.05 as the threshold for significance. In all synthetic reporter gene circuits, sample size (n) of 4 biologically independent samples (cell cultures) was used for statistical test. In the endogenous gene circuit, n of 3 biologically independent samples (cell cultures) was used for statistical test.

Plasmids

The plasmids used in each circuit, along with a brief description of their function, are as follows:

Circuit		1	2	3	4	5
Background Plasmids and dCas9	ND220	20	20	20	20	25
	114	20	20	20	20	20
	Csy4			50	50	
	dCas9 Variant	70	70	70	70	70
gRNA repression devices	3475	100	200			500
	LR2002			100	200	
	U6/Tal4-sgRNA-CXCR4					50
TALE repressor	473		50		50	50
Reporter	1341	20		20		
	ND252		20		20	
	Midi129					

- dCas9 Variants: CMV promoter driving dCas9, dCas9-KRAB, or dCas9-KRAB-MeCP2 expression.
- Background plasmids:
  1. ND220: CAG promoter driving EBFP expression. EBFP expression was used to gate transfected cells.
  2. 114: Hef1a promoter driving Gal4-VP16 and rtTA expression; the protein products are separated by a T2A amino acid sequence. The Gal4-VP16 activator binds upstream of the CRP promoter, driving its expression in the absence of a repressor. rtTA, when combined with Dox, binds upstream of the TRE promoter, driving its expression.
  3. Csy4: PGK promoter driving Csy4 expression. The Csy4 protein was used to cleave gRNAs in an mRNA transcript into functional gRNAs.
- Regulators in single repression circuits:
  1. 3475: U6 promoter driving gRNA expression.
  2. LR2002: TRE promoter driving gRNA expression 3’ to iRFP flanked by Csy4 target sites.
  3. U6/Tal14_CXCR4 gRNA: gRNA targeting endogenous CXCR4 locus under U6 promoter (repressed by TALER).
- Regulators in layered transcriptional repression circuits:
  1. 473: CRP promoter driving TALER expression.
- Reporters:
  1. 1341: CRP promoter driving EYFP expression.
  2. Midi129:CRP promoter driving EYFP expression, containing two gRNA target sites flanking the mini CMV.

ND252: pTal promoter driving EYFP expression.

Supplementary References:

1. McCarthy, D. J., Chen, Y, and Smyth, G. K. Differential Expression Analysis of Multifactor RNA-Seq Experiments with Respect to Biological Variation. *Nucleic Acids Research* **40**, 4288–97 (2012).

2. Lund, S. P., Nettleton, D, McCarthy, D. J., and Smyth, G. K. Detecting Differential Expression in RNA-Sequence Data Using Quasi-Likelihood with Shrunken Dispersion Estimates. *Statistical Applications in Genetics and Molecular Biology* **11**, Article 8 (2012).

3. McCarthy, D. J., and Smyth, G. K. Testing Significance Relative to a Fold-Change Threshold Is a TREAT. *Bioinformatics* **25**, 765–71 (2009).

4. Li, H. Aligning sequence reads, clone sequences and assembly contigs with BWA-MEM. *ArXiv13033997 Q-Bio* (2013).

5. Li, H. *et al.* The Sequence Alignment/Map format and SAMtools. *Bioinforma. Oxf. Engl.* **25,** 2078–2079 (2009).

6. Shen, JP *et al.* Combinatorial CRISPR-Cas9 screens for de novo mapping of genetic interactions. *Nat Methods.* **14,** 573-576 (2017).

7. Ruepp, A *et al.* CORUM: the comprehensive resource of mammalian protein complexes--2009. *Nucleic Acids Res.* **38** (Database issue), D497-501 (2010).

Supplementary Data 1 A list of differentially expressed genes considered significant at FDR < 0.05 in the RNA-seq experiment.
Supplementary Data 2 A list of all sgRNA sequences in single guide RNA library and their log2 odd ratios in HAP1 lethality screen.
Supplementary Data 3 A list of all sgRNA sequences in single guide RNA library and their log2 odd ratios in SH-SY5Y lethality screen.
Supplementary Data 4 A list of all sgRNA sequences in single guide RNA library and their log2 odd ratios in 293T lethality screen.
Supplementary Data 5 A list of non-essential gene-targeting sgRNAs that showed depletion in lethality screens.
Supplementary Data 6 Summary of rank-ordered genes identified from sgRNA enrichment analysis performed using MAGeCK software.
Supplementary Data 7 Genetic interactions captured through repressor screens.
Supplementary Data 8 DNA sequences and species origins of all protein domains used to construct the different repressors in this study.